SYNTHESIS AND BIOACTIVITIES OF NOVEL N^1-ACYLHYDRAZIDES

A Thesis Submitted to the College of

Graduate and Postdoctoral Studies

In Partial Fulfillment of the Requirements

For the Degree of Master of Science

In the College of Pharmacy and Nutrition

University of Saskatchewan

Saskatoon

By

Kinjal Murad Lakhani

PERMISSION TO USE

In presenting this thesis in partial fulfillment of the requirements for a postgraduate degree from the University of Saskatchewan, I agree that the libraries of this University may make it freely available for inspection. I further agree that permission for copying of this thesis/dissertation in any manner, in whole or in part, for scholarly purposes may be granted by the professor or professors who supervised my thesis/dissertation work or, in their absence, by the Head of the Department or the Dean of the College in which my thesis work was done. It is understood that any copying or publication or use of this thesis/dissertation or parts thereof for financial gain shall not be allowed without my written permission. It is also understood that due recognition shall be given to me and to the University of Saskatchewan in any scholarly use which may be made of any material in my thesis.

Requests for permission to copy or to make other uses of materials in this thesis in whole or part should be addressed to:

Head of the College of Pharmacy and Nutrition
University of Saskatchewan
Saskatoon, Saskatchewan S7N 5E5
Canada

OR

Dean
College of Graduate and Postdoctoral Studies
University of Saskatchewan
116 Thorvaldson Building, 110 Science Place
Saskatoon, Saskatchewan S7N 5C9
Canada

ABSTRACT

Curcumin, a herbal polyphenol, has demonstrated anticancer activity *in vitro* as well as *in vivo* but have limited clinical benefits due to low oral bioavailability. Structural modification such as truncation of the β-diketone moiety of curcumin led to the development of the 1,5-diaryl-3-oxo-1,4-pentadienyl pharmacophore and its importance in displaying antineoplastic properties has been demonstrated by our laboratory. In light of this concept, this thesis focuses on the design and development of novel 3,5-bis(benzylidene)-1-[3-(arylcarbonylaminoamino)-3-oxo-1-propyl]-4-piperidones **64a-g** having two pharmacophores, namely, the 1,5-diaryl-3-oxo-1,4-pentadienyl moiety which is believed to act at the primary binding site and N^1-acylhydrazides **60a-m** which are considered to be the auxiliary binders.

The biological screening reveals that the auxiliary binders **60m** (IC_{50} = 15.27 μM in HCT 116 cells) and **60l** (IC_{50} = 3.18 μM in MCF-7 cells) were the most potent cytotoxins in series **60**. The evaluation of druglike properties revealed that **64a** is the lead tumor-specific cytotoxin with an IC_{50} value of 1.38 μM against HCT 116 cells. When compared against colon CRL-1790 non-malignant cells, these cytotoxic agents (**60a**, **60m**, **63a** and **64a-g**) and **60j-l** showed greater selective toxicity towards colon HCT 116 cells and breast MCF-7 cells, respectively. (Tables 5.2, 5.3 and 5.5). The combinatorial study indicated that **60m** is a chemosensitizer towards HCT 116 cells to 3,5-bis(benzylidene)-4-piperidone **63a** and the reference drug 5-fluorouracil (Table 5.8, 6.2). When screened against various human oral carcinoma and normal cell lines, **63a** has shown potent cytotoxicity (CC_{50} < 0.46 μM) and **60a**, **60d** and **60l** showed moderate activity (CC_{50} in range of 46-47 μM) (Table 5.9). Four auxiliary binders **60a**, **60d**, **60h** and **60l** displayed excellent cytotoxicity in the range of 0.15-5.62 μM when screened against various adherent and non-adherent leukemic cells (Table 5.10). All four compounds displayed high cytotoxic potency and greater selectivity towards Ramos leukemic cells with **60h** being the most potent with an IC_{50} value of 0.15 μM and **60l** being highly selective with a selective index value greater than 90.

The cytotoxic effects of the auxiliary binder **60l** (in Ramos leukemic cells) and target compounds **64a**, **64e** and **64g** towards HCT 116 cells might be due to decreasing the mitochondrial membrane potential and a 2-4 fold increase in the reactive oxygen species levels (**60m**, **64a**, **64e** and **64g** in HCT 116 cells), as suggested by mechanistic investigations.

ACKNOWLEDGMENTS

I would like to thank my supervisors, Dr. Jonathan Dimmock and Dr. Rajendra Sharma, for their exceptional guidance and tremendous support during my program at the University of Saskatchewan. I also extend gratitude to my advisory committee (member Dr. David Sanders and chair Dr. David Blackburn) and the external examiner Dr. Jeremy Lee for examining and providing invaluable suggestions to revise this document.

I am grateful to our collaborators Drs. H. Sakagami at the Research Institute of Odontology, Meikai University School of Dentistry, Japan and M. Kawase at Matsuyama University, Japan (Table 5.9, page 77) and R. J. Aguilera at the University of Texas at El Paso, USA, (Table 5.10, page 78) for their support in the bioevaluations of the compounds. My deepest gratitude to Drs. Umashankar Das and Swagatika Das for their advice and guidance regarding all aspects of my project.

I appreciate the assistance from all the staff members of the College of Pharmacy and Nutrition including Claire, Erin, Jean, Dorota, Erling, Cathy as well as health sciences lab managers Vicki, Angela and Mark. I am thankful to my lab members and colleagues Dr. Sujit, Praveen, Muath, Raghu and Shujun for their support in learning some research analytical methods. The literature review and writing help by Erin Watson and Vicki Duncan are gratefully acknowledged.

I am grateful to the members of Ismaili community (in India and abroad) for financial support for my study at the U of S. I am also thankful to my work supervisors Chen Gwen (Library Services) and Monica Thurlbeck (Retail Services) for providing me an opportunity to get involved with the University community while earning to self-sustain.

I would like to thank my friends who made my journey in Saskatoon pleasant. Last but most importantly I would like to thank wholeheartedly my parents (Murad Lakhani and Ashraf Lakhani), my siblings (Arick and Reena) and my sister-in-law (Dr. Twinkle Narsagani) for their moral support. I am truly thankful to my husband Karim for his unconditional love, care and encouragement. I also extend my gratitude to my in-laws and the rest of my family.

DEDICATION

I would like to dedicate this thesis to:

My late grandparents and parents who always inspired me to believe in my dreams and their blessings made me stronger each day. My brother Arick and sister Reena whose love and care were of great encouragement during my studies. My heartfelt gratitude to my husband Karim Panjvani without his sacrifices and support nothing would have been possible.

TABLE OF CONTENTS

LIST OF TABLES

LIST OF FIGURES

LIST OF SCHEMES

LIST OF ABBREVIATIONS

mM	millimolar
µL	Microliter
µM	Micromolar
$\Delta\psi_m$	Mitochondrial membrane potential
5-FU	5-Fluorouracil
ABC	ATP-binding cassette
ADCC	Antibody dependent cell-mediated cytotoxicity
ADR	Adriamycin
ANOVA	Analysis of variance
ATCC	American type culture collection
ATP	Adenosine triphosphate
Avg	Average
Boc	tert-Butyloxycarbonyl functional group
BCNU	bis-chloroethylnitrosourea
BCRP	Breast cancer resistance protein
BSA	Bovine serum albumin
CCA	Cholangiocarcinoma
CCL-229	Colorectal adenocarcinoma
CCCP	Carbonyl cyanide 3-chlorophenylhydrazone
CEA	Carcinoembryonic antigen
CML	Chronic myeloid leukemia
COX-2	Cyclooxygenase 2
CRC	Colorectal cancer
CTCs	Circulating tumor cells
CRL-1790	Human normal colon epithelial cells
2,4-DNP	2,4-Dinitrophenol
DCF	2′,7′-Dichlorodihydrofluorescein
DCF-DA	2′,7′-Dichlorodihydrofluorescein diacetate
DMSO	Dimethyl sulfoxide
DMEM	Dulbecco’s modified eagle’s medium
DNA	Deoxyribonucleic acid
EGFR	Epidermal growth factor receptor

EMEM	Eagle's minimum essential medium
FDA	Food and drug administration
FGFs	Fibroblast growth factor
G_1 and G_2 phase	Growth phases in the cell cycle
GIST	Gastrointestinal stromal tumor
GSH	Glutathione reduced form
GSSG	Glutathione oxidized form
GST	Glutathione S-transferase
HepG2	Human hepatoma cancer cells
h	hour
HCC	Hepatocellular carcinoma
HCl	Hydrochloric acid
HCT-116	Human colon carcinoma cells
HGF	Human gingival fibroblasts
HER-2	Human epidermal growth factor receptor-2
HPC	Human pulp cells
HPLF	Human periodontal ligament fibroblasts
HSC	Human oral squamous cell carcinoma
HUVAC	Human umbilical vein endothelial cell
IC_{50}	Concentration at which growth is inhibited by 50 %
M phase	Mitotic phase in the cell-cycle
mCRC	Metastatic colorectal cancer
MCF-7	Human breast adenocarcinoma cells (estrogen and progesterone positive)
MDA-MB-231	Human breast adenocarcinoma cells (estrogen and progesterone negative)
MDR	Multidrug resistance
MDM2	Mouse double minute 2 homolog
mesna	Sodium salt of mercaptosulphonic acid
MetAP2	Methionine aminopeptidase 2
min	minute
MMP	Mitochondrial membrane potential
MMPs	Matrix metalloproteinases
MRP	Multiresistant protein
NADPH	Nicotinamide adenine dinucleotide phosphate reduced form
$NADP^+$	Nicotinamide adenine dinucleotide phosphate oxidized form
NCI	National Cancer Institute
NMR	Nuclear magnetic resonance

NSAIDs	Non-steroidal anti-inflammatory drugs
nPD-L1	Nuclear programmed death ligand 1
Nu	Nucleophile
PBS	Phosphate buffered saline
p53	Tumor suppressor gene
PARP	Poly (ADP-ribose) polymerase
P-gp	P-glycoprotein
QSAR	Quantitative structure-activity relationship
RNA	Ribonucleic acid
ROS	Reactive oxygen species
RPMI	Roswell Park Memorial Institute medium
RT	Room temperature
SAR	Structure-activity relationship
S phase	Synthesis phase in the cell-cycle
SD	Standard deviation
sec	seconds
SI	Selectivity Index
SRB	Sulforhodamine B
TCA	Trichloroacetic acid
TEA	Triethylamine
TGI	Total growth inhibition
TNBC	Triple negative breast cancer
TKIs	Tyrosine kinase inhibitors
TMRE	Tetramethylrhodamine ethyl ester
Tz	Cells fixed at time zero
US	United States
UV	Ultraviolet
VEGF	Vascular endothelial growth factor
WHO	World Health Organization

CHAPTER 1 : INTRODUCTION

1.1 Background

Although there have been many advances in the field of oncology over the years, cancer remains a major health issue globally. According to the WHO, 8.8 million deaths were due to cancer in 2015 and it became the second leading cause of mortality worldwide.[1] Cancer not only impacts the quality of life but also causes substantial economic burdens to society. Nearly US $113 billion was spent globally for cancer treatment in 2016 which is further expected to exceed US $147 billion worldwide by 2020.[2] In Canada, cancer is a life-threatening disease which is responsible for 30% of deaths in contrast to heart diseases (19.7%) and cerebrovascular diseases (5.3%).[3] Recent statistics from the Canadian Cancer Society suggest that approximately 50% of Canadians will be diagnosed with cancer and 2 out of 5 of them will die in 2017. It also indicates that the majority of cancer patients are over the age of 50 years which significantly lowers their life expectancy. The most common types of cancer among Canadians are lung, breast, colorectal and prostate cancer accounting for about 50% of the new cases. In Canada, colorectal cancer (CRC) is the third most commonly diagnosed cancer (excluding non-melanoma skin cancers) and based on the 2017 statistics, CRC accounts for 13% of all new cancer cases.[3]

1.2 Cancer

Cancer is a heterogeneous disease characterized by abnormal, uncontrolled cell multiplication. Cancer cells can either be localized resulting in a primary tumor formation or they can spread to other parts of the body through the blood or the lymphatic system by metastasis. The main factors for abnormal, uncontrolled multiplication include changes in growth factors/receptors, intracellular signaling pathways mainly controlling the cell cycle and apoptosis, telomerase expression and tumor-related angiogenesis.[4,5]

In simple terms, cancer can be classified into four main types which are carcinomas (cancer of different body organs), sarcomas (cancers of bones, cartilage, muscles and connective tissue), lymphomas (cancer of the lymphatic system) and leukemia (cancer of the blood). Various risk factors are linked to the prevalence of cancer. These include, but are not limited to alcohol use, smoking, unhealthy diet, physical inactivity and exposure to carcinogens (UV light, radiation, asbestos, arsenic) and chronic infections (Helicobacter pylori, human papillomavirus, hepatitis B

virus, hepatitis C virus, and Epstein-Barr virus).[1] Age is believed to be another factor contributing to cancer. Although the chances are higher in the elderly, children also have cancer. There is a significant reduction in cancer mortality rates if it is detected and treated in the early stages of development. Based on the type and progression of cancer, different treatment options are available such as surgery, radiation therapy, chemotherapy, immunotherapy and hormonal therapy. Amongst these options, surgery, and radiation therapy are used for localized treatment whereas chemotherapy can also be used for systemic treatment.

1.2.1 Chemotherapeutic agents

Cancer is the result of abnormal cell proliferation. Cell multiplication occurs in a cyclic fashion wherein reproduction of one cell results in two daughter cells and so on. In a cell cycle, there are four stages of cell division namely, G_1, S, G_2 and M phases. The G_1 and G_2 phases occur before the S and M phases, respectively. The synthesis of genetic material such as DNA occurs in the S phase. The M phase is responsible for mitotic cell division and cytokinesis.[6]

Different chemotherapeutic agents are classified as either cell-cycle specific or non-cell-cycle specific. Cell-cycle specific chemotherapeutic agents are active at a certain stage of the cell-cycle. Cell-cycle specific drugs act at one phase in the cell cycle such as antimetabolites which act at the synthesis phase. On the other hand, the antineoplastic alkylating agents are non-cell-cycle specific and act whether the cells are active or in the resting stage.[7] They can also be classified according to their mechanisms of action, their chemical structures and their relationship to other drugs. For example, anticancer drugs may be classified as alkylating agents (carmustine, busulfan), anti-metabolites (methotrexate, 5-fluorouracil), plant derivatives (vinca alkaloids, taxanes, camptothecin), cytotoxic antibiotics (doxorubicin), hormones (steroids such as estrogens and androgens) and miscellaneous agents (asparaginase).

Chemotherapy is given with the aims to either cure the cancer or to control the disease or as palliation to relieve symptoms when cancer is at an advanced stage. Most chemotherapeutic agents are effective during the logarithmic growth of tumors. However, with an increase in the size of a tumor, their efficacy decreases. This problem can be solved if the tumor is removed by surgery or radiation therapy is used along with chemotherapy. The success rate is highly dependent on the early detection of cancer and treatment with chemotherapy plus surgery or radiation.[7]

1.3 New paradigms in cancer treatment

Since the last decade, our perspective towards cancer and its treatment have changed considerably. Chemotherapy has been used for many years; however the problem of drug resistance and toxicity persists. The identification of various drug resistance proteins and their biochemical pathways have been successful with the help of various biomarkers *in vivo*. Recently, the concept of tailored drug therapy has come into the picture. Novel drugs have been designed and developed according to the genetic make-up of the individual. These therapeutics are designed with a "personalized" approach (right medication for the right person given at the right time with the right dose) instead of the traditional ones with "one size fits all".[8,9] Newer treatment options like biomarker-based patient segmentation and other diagnostic approaches have been added to the treatment regimen.

1.3.1 Cancer biomarkers

Genetic materials such as DNA and RNA, proteins, peptides, metabolites, and hormones are believed to be potential indicators of cancer. Moreover, biological processes such as apoptosis, angiogenesis or proliferation are also considered to be diagnostic markers. These biomarkers are specifically derived from neoplasms and isolated non-invasively and can be detected either in the circulatory fluids (blood, serum, plasma) or secretory fluids (urine, stools or sputum). The carcinoembryonic antigen (CEA) and epidermal growth factor receptor (EGFR) are cancer biomarkers used for monitoring and prediction of colorectal cancer.[9]

1.3.1.1 Circulating tumor cells (CTCs)

Circulating tumor cells were first noticed by an Australian pathologist in the late 18th century. He observed circulating cells in the autopsy of a metastatic tumor and concluded that these cells were isolated from a tumor network and became a part of the circulatory system. CTCs are considered as a "liquid biopsy" as they detach from the tumor and circulate either in the blood or the lymphatic system. CTCs are one of the unique emerging biomarkers gaining attention in recent years for the detection of neoplasms in patients. CellSearch® Test was clinically approved by the FDA in 2007 and is used for early prognosis in a patient.

When isolated, the phenotypic and genotypic properties of CTCs can provide a significant amount of information regarding the tumor cells propagation and metastasis biology. Their molecular characterization can serve as a predicative tool for drug resistance as a few multi-drug resistance

proteins MRP1, MRP2, MRP4, MRP5, and MRP7 have been found in CTCs. These can provide useful information for the elucidation of downstream pathways and their mechanisms of action. CTCs serve as viable tools for the isolation, detection, and prognosis of the disease.[9,10,11] For example, nuclear PD-L1 was believed to be a molecular diagnostic marker in patients with CRCs in stage IV, and prostate cancer stage VI while the survival was less in patients with expression of nPD-L1.[12]

1.3.1.2 Angiogenesis

Angiogenesis is a crucial process of forming new blood vessels from pre-existing ones which are essential for the primary growth of the tumor, invasion, and metastasis[13] and therefore it is a vital and appealing target for therapeutic intervention. Tumors with a size of 1-2 mm receive a supply of oxygen and nutrients by simple diffusion. For the further progression of the tumor, malignant cells secrete growth factors which are responsible for forming new blood capillaries by activating endothelial cells[14] and finally infiltrate the tumor mass.[15]

A rapidly expanding endothelial surface allows tumor cells to enter the circulation and metastasize whereas the release of anti-angiogenic factors explains the control exerted by primary tumors over metastasis. This indicates that a balance between pro-angiogenic and anti-angiogenic growth factors and cytokines markedly control angiogenesis.[15] Tumor angiogenesis results by increased secretion of angiogenic factors and/or down-regulation of angiogenesis inhibitors.[16] Several proangiogenic molecules such as the vascular endothelial cell growth factor (VEGF), which is highly specific for endothelial cells, the fibroblast growth factors (FGFs), the matrix metalloproteinases (MMPs), methionine aminopeptidase-2 (MetAP-2), tubulin, cyclooxygenase-2 (COX-2), angiopoietins and the angiogenesis inhibitors such as platelet factor-4, angiostatin, endostatin, and vasostatin are involved in the regulation and control of the angiogenic process.

Inhibition of angiogenesis can prevent diseases such as cancer, diabetic nephropathy, arthritis and psoriasis.[15,17] Approaches to novel anti-neoplastic therapy include targeting the growth signal transduction within cancer cells i.e., the mechanisms involved in cell invasion and metastatic spread, apoptosis and the cell cycle, and tumor-related angiogenesis. Molecularly targeted anticancer therapies like small-molecule tyrosine kinase inhibitors (TKIs) and monoclonal antibodies have been successfully introduced to treat patients with various cancers including breast cancer, colorectal cancer (CRC), chronic myeloid leukemia (CML), and gastrointestinal stromal

tumor (GIST)[13]. One of the most promising targeted therapies to treat cancer is the addition of antiangiogenic therapy to the therapeutic regimen. The real potential of antiangiogenic agents for cancer therapy resides in strategic combinations with treatment modalities such as chemotherapy, radiation, and tumor-targeting agents such as radioimmunotherapy.[18] Colon cancer requires angiogenesis for progression and metastasis and thus inhibition of angiogenesis can be a promising target for colon cancer therapy.[19]

1.3.2 Antibody based immunotherapy

The targeting of immune cells rather than cancer cells is one of the emerging strategies available along with conventional treatment. Antibodies are designed in such a way that they target the surface antigen expressed on the tumor cells and induce cell death through processes known as antibody-dependent cell-mediated cytotoxicity (ADCC). These immunomodulatory antibodies either activate immune-stimuli responses or antagonize immunosuppressive pathways.[20]

Many FDA approved immunomodulatory antibodies are available in the market which are used therapeutically to activate antineoplastic immune responses. The epithelial growth factor receptor (EGFR) is a tyrosine kinase receptor which is overexpressed in colon cancer. Cetuximab and panitumumab are specific EFGR antibodies used to treat metastatic colorectal cancer (mCRC)[20,21] in combination with 5-FU as an adjuvant chemotherapeutic agent. They inhibit EGFR signalling and thus prevent receptor dimerization resulting in the cell death in tumor cells. Human epidermal growth factor receptor 2 (HER-2) is overexpressed in breast cancer. Trastuzumab was the first anti-HER2 antibody, approved by FDA in 2006 for treatment of HER2+ breast cancer along with chemotherapy. Pertuzumab was recently approved in 2017 and used along with chemotherapy as adjuvant treatment. Even though they are clinically proven immunomodulators, their use in therapeutic regimen causes many toxic effects.

1.4 Current challenges in cancer chemotherapy

Cancer is one of the prime causes of premature death even though there are so many developments in drug discovery and numerous chemotherapeutic agents available in the market. One of the main reasons for this is that chemotherapeutic agents attack the rapidly growing cancerous cells as well as fast-growing healthy cells (bone marrow/blood cells, cells of the hair follicles, cells lining the digestive and reproductive tracts). Thus toxicity and severe side effects are involved with the use of chemotherapy drugs. The quest to minimize these side effects has always been of much interest to researchers.

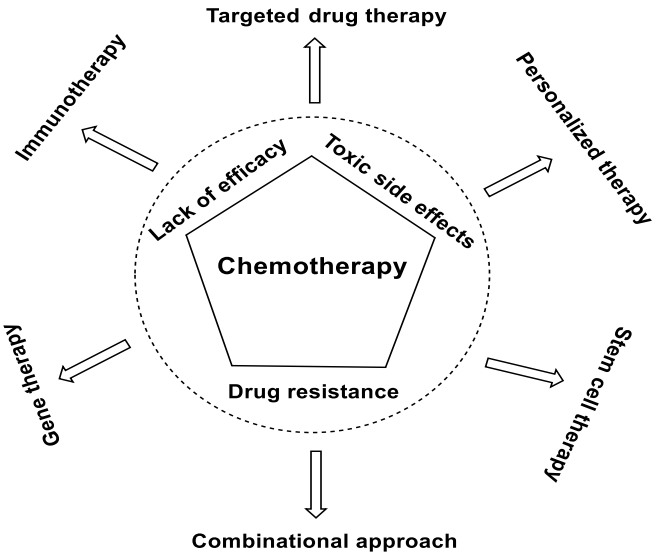

Figure 1.1 : Representation of factors responsible for chemotherapy failure and newer approaches to treat cancer.

Targeted and smart drug therapy to one or more specific sites of action seeks to treat cancer more efficiently because of the greater understanding of the molecular changes involved in cancer progression. These drugs target specific molecules involved in tumor growth and usually have less severe side effects than chemotherapy drugs and greater drug uptake as well as increased patient compliance.

Another hurdle with the use of chemotherapy is the problem of drug resistance. Resistance can be natural or acquired. Natural resistance is observed when a tumor is not responsive towards drug therapy probably because the malignant cells are in a plateau growth phase with less growth fraction and thus are insensitive towards drugs. Acquired resistance is seen when drugs are

effective to neoplasms but later fail to show responsiveness because of a number of mechanisms.[7] When tumors are treated with chemotherapeutics, malignant cells are killed and tumor size decreases. However, resistant clones develop on continuous exposure to chemotherapeutic drugs, and their division leads to the rebuilding of the tumor network by constant multiplication. Thus the chemotherapy is no longer as efficacious as it was previously. Resistance can be developed by a number of mechanisms such as intracellular inactivation or metabolic bypass of the drug before reaching the target, alteration of the target site to avoid binding and low cell permeability which impairs the influx/efflux of drug.[22]

Multidrug resistance (MDR) is problematic as resistance develops not only against a single agent but also against other drugs that fall into the same class. Mechanistic investigations show the role of membrane transporter proteins. P-glycoprotein (P-gp) is the efflux protein belonging to the ABC superfamily of transporters and is encoded by the MDR1 gene. Drugs are less effective as its intracellular concentration is significantly reduced because of increased activity of the energy-dependent efflux pump which is a result of overexpression of P-gp. Various drugs belonging to the class of calcium channel blockers, antiarrhythmics and cyclosporine A analogues modulate P-gp *in vitro* but limited efficacy is seen clinically.[7]

The p53 gene is the first tumor suppressor gene discovered by scientists and research reveals that the p53 pathway is significantly altered in cancer cells. In cancer cells under stress conditions and DNA impairment, p53 is activated and downregulated to induce cell cycle arrest, apoptosis, DNA repair and inhibition of angiogenesis. The mutation of p53 is unable to induce apoptosis in the cells and may finally lead to uncontrolled cell multiplication. Over 75% of its mutations are the result of a single amino substitution making it genetically unstable and thus favouring a tumor initiation environment. Overexpression of the MDM2 gene is responsible for p53 inactivation.[6]

Anticancer drugs have been developed with the aim to target enzymes or biological processes, such as tyrosine kinase inhibitors which use p53 as an anti-cancer agent, angiogenesis and metalloproteinase inhibitors, cyclooxygenase inhibitors, antisense oligonucleotides, reverse multidrug resistance drugs as well as gene therapy. There is a great need to understand the potential mechanisms of action of resistant proteins and an urgency to develop new novel chemotherapeutic agents which display selectivity towards cancer cells and are effective against MDR tumors.

1.5 Chemosensitivity of tumors to antineoplastic agents

As mentioned earlier, various mechanisms are responsible for the failure of chemotherapeutic agents. However the concept of chemosensitivity came to light as one of the efforts to overcome the problems of drug resistance and drug toxicity. The basic principle of chemosensitization is that tumors are sensitized to anticancer agents which potentiates the efficacy of the latter in cancer treatment. This process can also result in a dose reduction of the anticancer agent when tumors have already been treated by chemosensitizers. Chemosensitizers can either be drugs, synthetic organic compounds, natural products, modulators of thiol concentration or miscellaneous compounds. Figure 1.2 depicts an approach to chemosensitize a neoplasm prior to antineoplastic drug treatment.

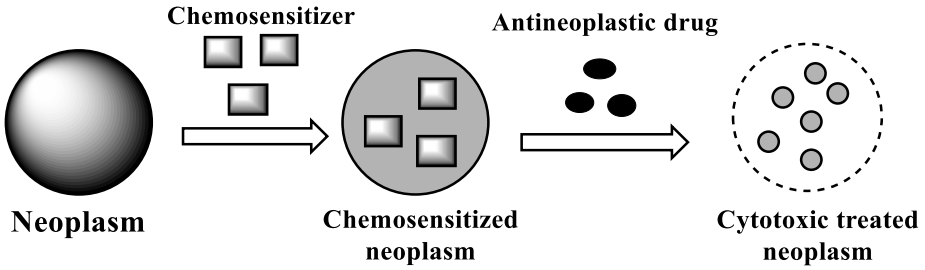

Figure 1.2 : Representation of the effect of a chemosensitizer to a tumor prior to antineoplastic drug treatment.

One of the main advantages in using an existing drug as a chemostimulant is the awareness of its pharmacokinetic profile and established pharmacodynamic effects. Synergistic effects can be seen when either the drugs having similar mechanisms of action or are acting on different targets. However, the latter is considered more fruitful particularly in the case of MDR.

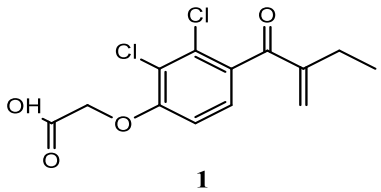

1

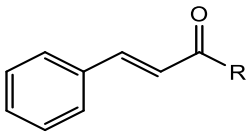

2

2a: R = H; **2b**: R = CH_3; **2c**: R = OCH_3; **2d**: R = OH

As an example, ethacrynic acid **1** having an α,β-unsaturated keto group interacts with the thiol groups in the renal tubules and sensitizes malignant cells to cytotoxins. Series **2** are derivatives of cinnamaldehyde and are highly reactive towards cellular nucleophiles as they act as Michael

acceptors. Compound **2a** is highly cytotoxic towards human SK-MEL19 and SK-MEL23 melanoma cells. Synergism is observed when compound **2** is administered in the presence of compound **1**. The high reactivity of cinnamaldehyde and its lipophilicity contributed towards its cytotoxicity.[23]

As discussed earlier, cellular membrane proteins like P-gp act as efflux pumps and thereby they decrease the intracellular drug concentration. Inhibition of P-gp as seen in Figure 1.3, by a chemosensitizer can be one of the ways to prevent MDR.

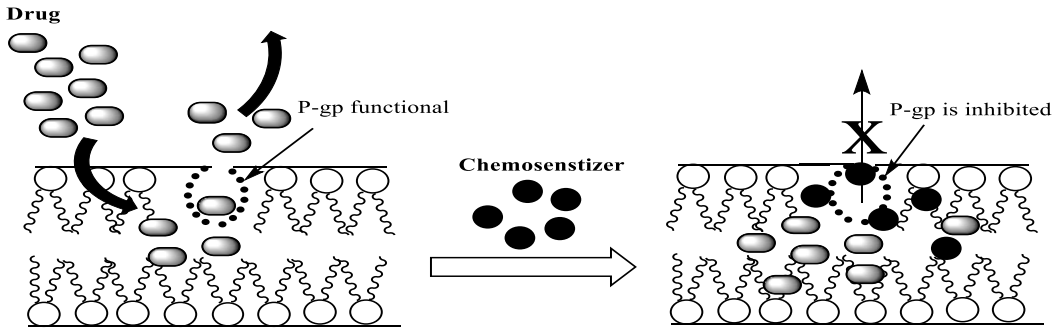

Figure 1.3 : Effect of P-gp expression in the presence of a chemosensitizer.

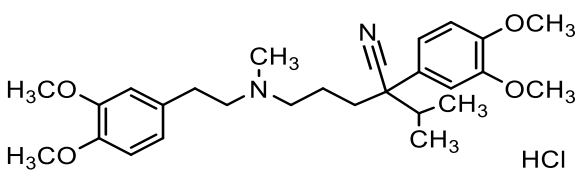

3

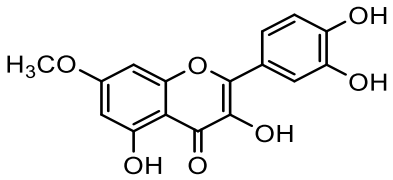

4

As an example, verapamil **3** is a calcium channel blocker, mainly used to treat hypertension and angina. It plays a crucial role in the inhibition of the activity of P-gp. Verapamil **3** increased cytotoxicity and induced apoptosis by sensitizing the proteasome inhibitors MG132, bortezomib and carfilzomib towards MDA-MB-231 TNBC. Increased cytotoxicity was observed when nicardipine, a P-gp inhibitor, was combined with bortezomib or carfilzomib.[24]

Rhamnetin **4** is a natural flavanol which can be isolated from clove. Recent studies showed that rhamnetin was a potential sensitizer of hepatocellular carcinoma (HCC) cells to paclitaxel, etoposide and sorafenib. The Notch-1 pathway upregulation in cancer cells is responsible for greater cell survival and thereby inhibits apoptosis. In the presence of rhamnetin, downregulation

of the Notch-1 pathway was seen thereby resulting in reducing MDR and there was a marked reduction in the expression of MDR-related proteins like P-gp and BCRP in HepG2/ADR cells.[25]

There are several mechanisms identified through which tumors are sensitized. Chemosensitization influences various cellular processes at the mitotic stage by inhibiting tubulin polymerization[26] as well as modulating genes involved in the cell-cycle. They potentiate the activity of protein kinase enzymes[27] and transcription factors, control ROS levels in tumor cells[28,29], causes apoptosis by PARP cleavage[26], change levels of cellular thiols or by inhibition of GSTs.[30] The use of chemosensitizers is an encouraging approach accounting for MDR reversal, toxicity reduction by decreased dose intake as well as selectivity towards cancer cells rather than normal cells.

1.6 Importance of conjugated α,β-unsaturated carbonyl compounds in chemotherapy

Compounds possessing an α,β-unsaturated carbonyl moiety are highly reactive as they are considered to be a Michael acceptor for cellular nucleophiles.[31] Many natural products such as chalcones, curcumin and coumarin contain an α,β-unsaturated carbonyl group and display a number of biological activities including anticancer, antioxidant, anti-inflammatory, antimicrobial, antiprotozoal, antiulcer, antihistaminic and multidrug resistance reversal properties.

Chalcones (1,3-diaryl-2-propen-1-ones) emerged as 'magic bullets' due to their selectivity towards cancer cells without affecting normal cells.[32] Clinical trials have shown that these compounds reached reasonable plasma concentrations and are well-tolerated.[33] Four groups of bioactive compounds which possess the α,β-unsaturated keto group are 1,3-diaryl-prop-2-en-1-ones (chalcones), 1,5-diaryl-3-oxo-1,4-pentadienes, 1,5-diaryl-pent-1en-3-ones and 1,7-diaryl-hept-3-en-5-ones (Figure 1.4).[34]

Over the years, our lab has focused on developing and synthesizing various α,β-unsaturated keto derivatives as cytotoxic alkylating agents based on the following important considerations. (1) These agents have a distinct affinity towards thiols rather than amino or hydroxyl groups. This specificity is useful to avoid toxic affects that arise from the interaction of anticancer drugs with genetic material.[35] (2) Elevated thiols levels are usually noted in malignant cells[36] as compared to normal cells. These compounds decrease thiol concentrations and may significantly impair various regulatory processes including MDR by sensitization of malignant cells to antineoplastic agents. (3) These agents can be cell cycle specific interfering with the mitotic phase of cell division during which thiol concentrations are higher. (4) These agents are promising when the cytotoxins have

MDR-revertant properties.

Thus new paradigms are emerging to synthesize novel α,β unsaturated ketones for selective toxicity to malignant cells and for treatment of MDR tumors.

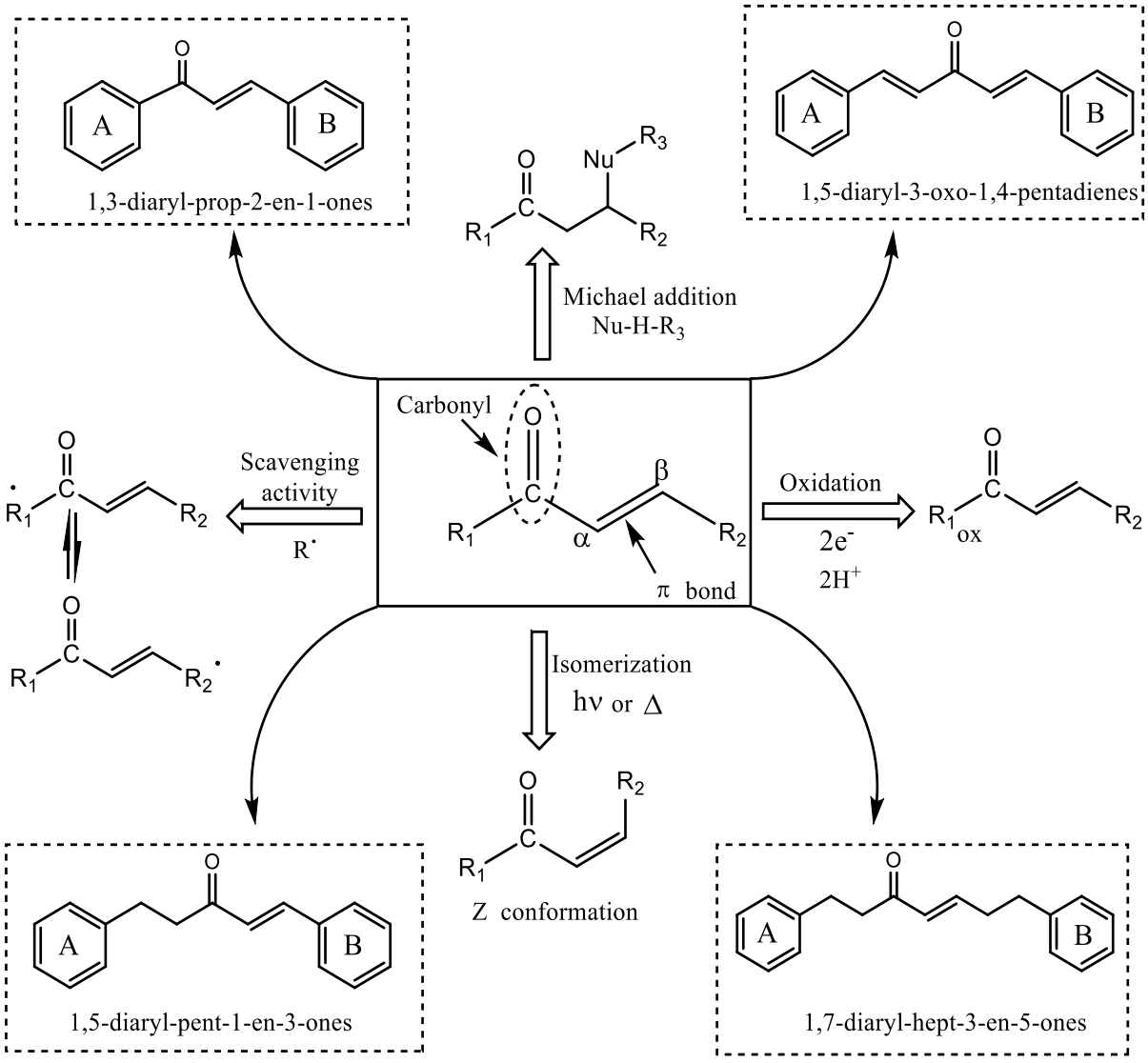

Figure 1.4 : Reactivities and important series of α,β-unsaturated carbonyl compounds.

1.7 Novel curcumin-based cytotoxic agents

Curcumin, a polyphenol, obtained from *Curcuma longa* L., has been traditionally used as a spice in cooking. It has been used conventionally as a carminative, laxative, for stomach pain and as a condiment in food.[37] However over the years this natural product has shown antioxidant,

antiinflammatory, antibacterial, antiviral, antifungal, antiparasitic and antispasmodic properties.[38,39] Another advantage of curcumin is that it is safe and effective and probably shows no or less toxicity than chemotherapeutic agents. The keto form of curcumin is symmetrical in structure with two aryl methoxy and two hydroxy groups linked by diendione moiety.

Curcumin [1,7 bis(4-hydroxy-3-methoxyphenyl)-1,6-heptadien-3,5-dione] has been extensively explored for its anticarcinogenic characteristics in the colon, gastric tract, ovary, prostate and lymph.[37] Recent studies involve the use of curcumin as a potential candidate to treat hyperlipidemia[40], obesity[40], multiple sclerosis[41] and systemic lupus erythematosus.[42] One of the studies highlights that curcumin can serve as a future target for Zika and Chikungunya viruses by inhibiting their replication processes.[43] However curcumin is considered a poor lead compound despite its clinical benefits, because of its poor pharmacokinetic and pharmacodynamic profiles. The phenolic -OH groups in curcumin undergo phase II transformation into glucuronides and sulfates by transferases *in vivo* resulting in a rapid elimination of water soluble metabolites[44,45,46] and shorter half-life of 6-7 h.[47] Low solubility and bioavailability, aqueous instability and extensive metabolism have restricted its therapeutic use.

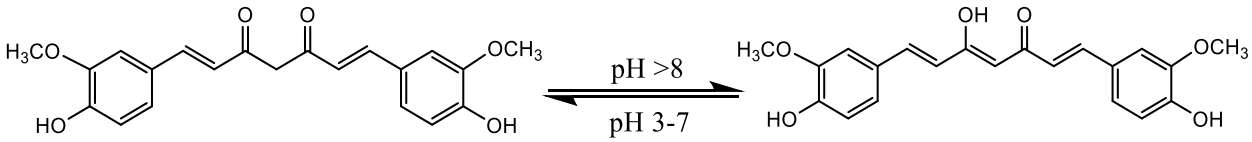

Bis-keto form **5a** enolate form **5b**

Curcumin **5**

Figure 1.5 : Tautomerism of curcumin.

NMR studies detected only the enolate form **5b** in solvents. The enol form **5b** is believed to be more stable because of intramolecular hydrogen bonding. Curcumin undergoes chemical degradation in alkaline pH, autooxidation and photodegradation to break into various moieties including vanillin, ferulic acid, bicyclopentadione and ferulic aldehyde.[48] To solve this problem, different formulation approaches have been employed such as nanoparticles, nanocrystals, emulsions and liposomes to make curcumin more stable *in vivo*.

In recent years, several strategies have been pursued by researchers to make structural modifications in curcumin by the addition of functional groups to increase the potency and efficacy at the therapeutic level. Figure 1.6 highlights a few of the approaches to overcome the pharmacokinetic disadvantages mentioned earlier.

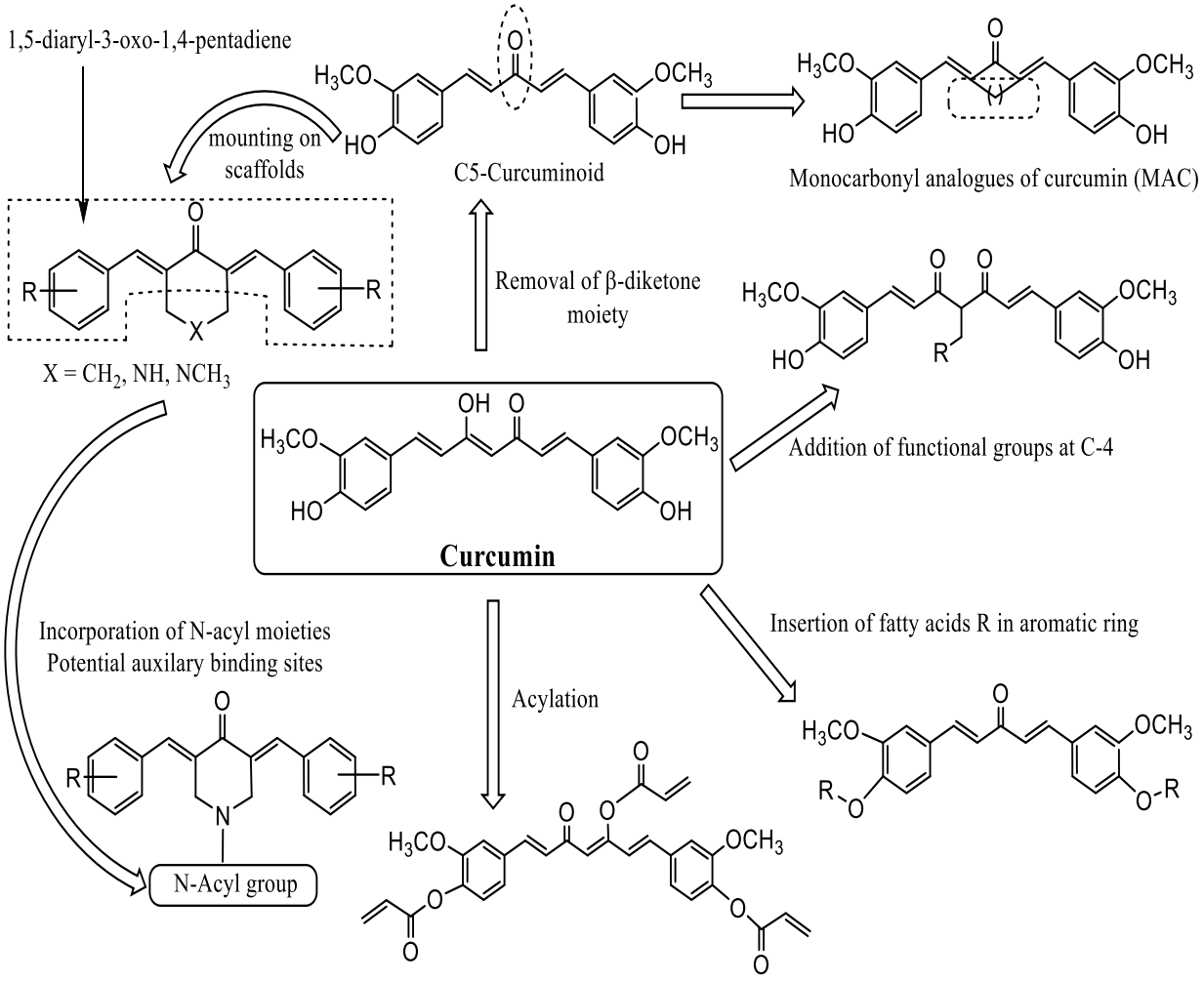

Figure 1.6 : Molecular modifications of curcumin.

Two different curcumin analogues were synthesized with the addition of an ester and acid groups at carbon atom 4 of curcumin to give rise to **6** and **7**. Addition of the alkyl chain at C-4 position in **6** and **7** increased the stability *in vitro* resulting in greater cytotoxicity than curcumin.

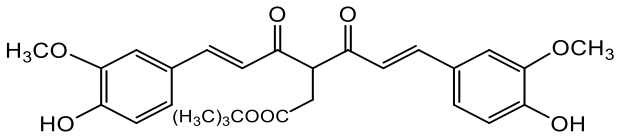

6

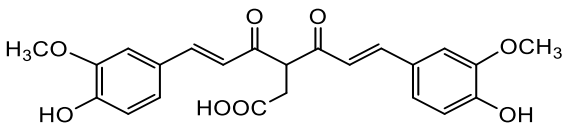

7

The presence of a Boc functional group in **6** kept the curcumin backbone intact with no degradation and was highly lipophilic as compared to **7** accounting for its faster cellular uptake and selectivity towards colon HCT 116 and LoVo cancer cells. The addition of an electron-withdrawing group

stabilizes keto-enol tautomerism. The presence of phenolic OH groups on the aromatic rings contributes to the antioxidant activity of compounds **6** and **7**.[37]

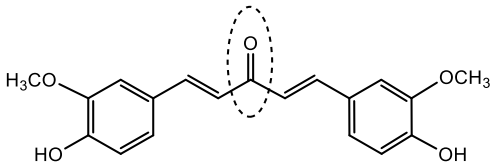

C5-Curcumin **8**

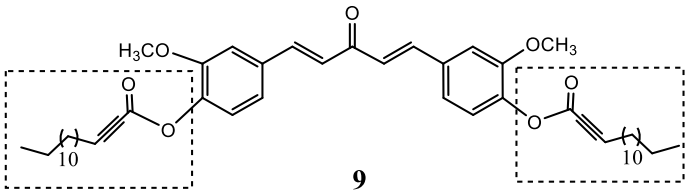

9

Another study outlined the conversion of 2-hexadecynoic acid to a C5-curcumin. C5-Curcumin **8** is formed by the removal of the β-diketone moiety. It was found to be active against various strains of bacteria such as *E. coli* and *S. aureus*. C5-curcumin-2-hexadecynoic acid **9** was synthesized and it was found to be active towards multidrug resistant bacterial strains like methicillin resistant *Staphylococcus aureus* (MRSA) with a minimum inhibitory concentration between 31.3-62.5 µg/ml. It was noted that the presence of a triple bond at the C-2 position in 2-hexadecynoic acid resulted in 4-8-fold higher anti-bacterial activity. Compound **9** was also found to restrict the supercoiling activity of DNA gyrase and inhibited DNA topoisomerase which alters various replication, recombination and transcription processes. A similar study was carried out previously by one of the research groups wherein palmitic acid was conjugated with curcumin. Addition of palmitic acid was advantageous as the ester bonds in Curcumin-PA conjugate were hydrolyzed by carboesterases resulting in a decreased rate of metabolism of curcumin.[49]

Quaternary piperazine curcuminoids were developed to improve the physicochemical properties of curcumin. These curcuminoids were synthesized by the Baylis-Hillman (BH) reaction wherein BH derived allyl bromides were first synthesized which are highly reactive electrophiles and may interact with molecules like DNA, GSH or cysteine. These quaternary ammonium curcumin derivatives are highly soluble in the range of >100 µg/ml.

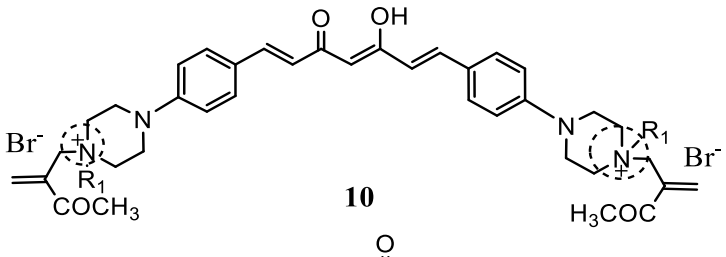

10

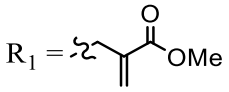

Compound **10** was cytotoxic against human triple negative breast cancer MDA-MB-231, metastatic murine breast cancer 4T1 and human pancreatic cancer MIAPaCa-2. *In vivo* toxicity studies of compound **10** suggested that it was well tolerated in mice with no significant changes in body weight or stress conditions. Furthermore compound **10** was used *in vivo* to treat pancreatic tumors by passaging MIAPaCa-2 cells in nude mice. Compound **10** inhibited tumor growth by 42% while gemcitabine inhibited the tumor growth by 47% .[50]

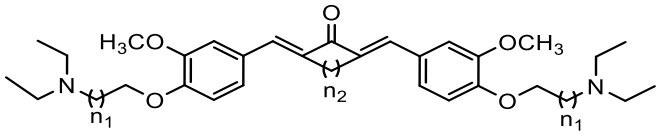

11

11a: $n_1 = 2$; $n_2 = 3$

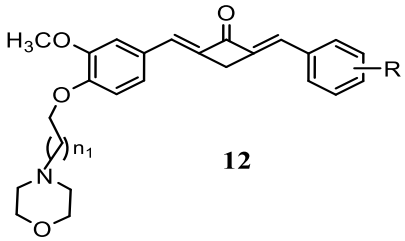

12

12a: R = 2-OCH_3 , $n_1 = 2$

12b: R = 2,3-$(OCH_3)_2$, $n_1 = 2$

To improve the pharmacokinetic stability of curcumin, the β-diketone moiety was replaced by a single carbonyl group. Such monocarbonyl curcumin analogues (MACs) having electron-withdrawing substituents are thought to display greater cytotoxicity than curcumin. Moreover, para substitution in these analogues serves as secondary binding sites of the target molecules. Compounds **11a**, **12a** and **12b** showed apoptosis in gastric cancer cells SGC-7901. All three compounds induced apoptosis by downregulating capase-3 and Bcl-2 expression and upregulating cleaved PARP expression. Compound **12a** displayed greater activity as compared to the others and showed 48% tumor efficacy *in vivo*.[51]

Novel bis(hydroxymethyl) alkanoate analogues of curcumin were designed as potential anti-cancer agents. Compound **13** was synthesized by esterification of both phenolic -OH groups and incorporation of bulky groups onto the aliphatic hydroxyl group. This strategy resulted in better solubility than curcumin. The logP value of compound **13** was found to be 1.73 as compared to 3.38 for curcumin. Compound **13** was 6.1 times more potent in MDA-MB-231 breast cancer cells than curcumin. If the methyl group was substituted by an ethyl group then a slight decrease in the cytotoxicity was found.

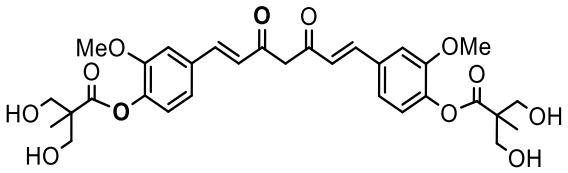

13

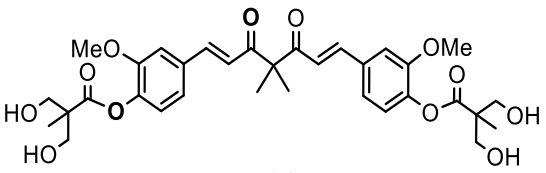

14

The important difference between compound **13** and **14** was tautomerism. Compound **13** existed in convertible enol and keto forms with the enol form considered to be the most stable whereas compound **14** is in the keto form and is not able to tautomerize because of the additional methyl groups restricting its conformation. The IC_{50} values of compounds **13**, **14** and curcumin towards MDA-MB-231 cells was found to be 1.98 µM, 2.67 µM and 16.23 µM, respectively. When doxorubicin was used in combination with compound **13**, synergism was observed *in vitro* as well as *in vivo*. Compound **13** resulted in apoptosis by cell cycle arrest in the G_2/M phase. It is a potential antioxidant as it leads to the expression of the heme oxygenase 1 enzyme in MDA-MB-231 cells. Because of lower toxicity *in vivo*, it could be a potential drug for treating triple negative breast cancer.[52]

Another study found that a C5-curcumin conjugated with fatty acids to form C5-curcumin-fatty acid (C5-Curc-FA). Conjugates possessing decanoic acid or palmitic acid were found to be more cytotoxic against colorectal adenocarcinoma CCL-229 cells than curcumin. Moreover structure-activity relationships revealed that decanoic acid in the *meta* position is essential for antineoplastic activity.

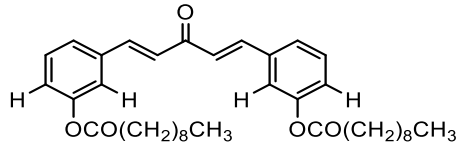

15

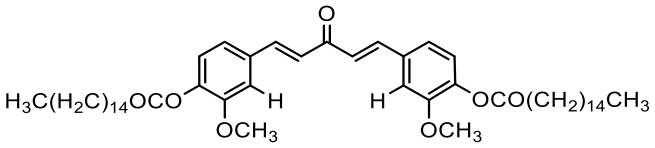

16

It was also noted that anticancer potencies were greatly influenced by the number of carbon atoms in the fatty acid chain. Cytotoxicity was increased with a decrease in the number of carbon atoms in the fatty acids. Nuclear factor kappa B (NF-κB) plays a crucial role in inflammation signalling as well as apoptosis. Compound **15** inhibits the activity of NF-κB probably because of its favourable lipophilicity. Furthermore various bioassays revealed some of the possible mechanisms of cell death of these conjugates. Compound **15** induces apoptosis, decreased MMP (caused 68 % depolarization), activated caspases-3 and caspases-7 which in turn stimulate nucleases to alter

nuclear expression. Compound **15** is 5-10-fold more effective for inhibiting DNA topoisomerase I as compared to compound **16** due to the presence of the fatty acid group at the *meta* position.[53]

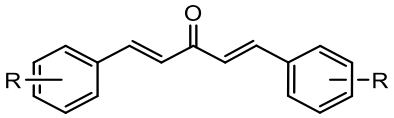

17

17a: R = 2F; **17b**: R = 3F; **17c**: R = 4F

Substitution in the aromatic ring of a curcuminoid with a fluoro group was undertaken to evaluate their efficacy towards lung cancer. Analogues designed with fluoro substituents have contributed towards greater binding capacities and pharmacokinetic stability. Compound **17a** was found to be 4 times more cytotoxic than curcumin towards lung NCI-H460 cancer cells. The relative cytotoxicity can be represented as **17a** > **17b** > **17c**. The analogue with an *ortho* substituent was highly toxic to NCI H460 cells as compared to compounds possessing *meta* and *para* substituents. Fluoro substitution may have stabilized the molecule and as a result more cellular uptake was observed in NCI-H460 cells as compared to curcumin. Dose-dependent apoptosis was induced by **17a** which in turn was corelated with an increase in the generation of reactive oxygen species (ROS). This possible mechanism of cell death was confirmed by a decrease in the mitochondrial membrane potential, induction of lipid peroxidation and a decrease in GSH/GSSG levels.[38]

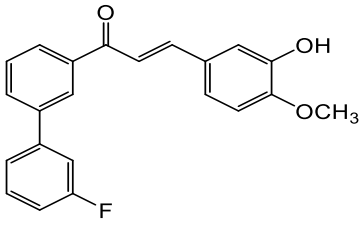

18 MC37

MC37 is a novel analogue of curcumin with fluorine as a key substituent. Compound **18** was cytotoxic towards colon cancer cells and impeded the cell-cycle at the G_2/M phase. The average IC_{50} values of **18** and curcumin towards colon carcinoma cells (HCT-8 and SW480) were 0.34 µM and 12.36 µM, respectively. Further possible mechanisms of cytotoxicity were investigated and the findings revealed that collapsed mitochondrial membrane potential, activation of capases-3 and caspases-9, upregulated Bax/Bcl-2 ratio and downregulated cyclin dependent kinase 1 (CDK1) which is a protein essential for regulation of the cell cycle, contributed to cytotoxicity.[39]

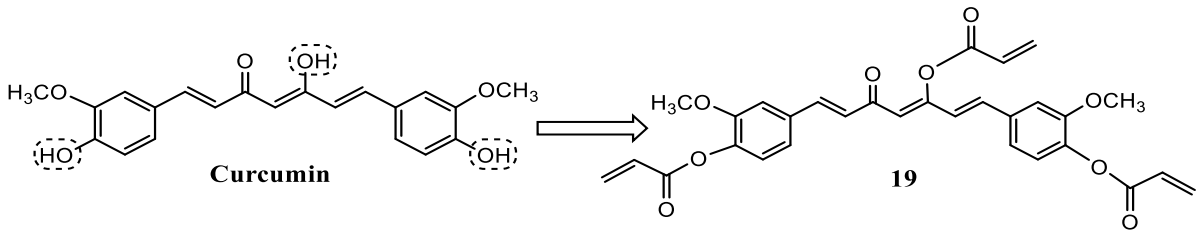

In a recent reference, curcumin analogues were synthesized with the incorporation of acrylate functional group in curcumin. Curcumin multiacrylate species were developed by alkylating the three hydroxy groups in curcumin with acryloyl chloride to obtain mono-, di- or triacrylate derivatives. The ratio of curcumin : acryloyl chloride plays an important role to form the corresponding derivatives. Various techniques such as HPLC, LCMS and NMR were used to characterize different curcumin based multiacrylate moieties.[54] Previous studies highlighted the use of curcumin acrylation to improve the stability as well as solubility by formulating hydrogels[55] and microspheres.[56]

1.8 Development of 1,5-diaryl-3-oxo-1,4-pentadienes as potential cytotoxic agents

Over the past few years, various approaches have been made to incorporate additional functional groups to compounds possessing the 1,5-diaryl-3-oxo-1,4-pentadienyl group with the following objectives. (1) It is well known that the possibility of drug resistance increases if the drug continuously binds to only one active site. This problem can be overcome if the drug candidate has more than one potential active binding sites which interacts with cellular moieties. Thus the efficacy of a drug can be increased. (2) A drug candidate with different potential interactive sites may undergo extensive metabolism in such a way that it is removed from the body resulting in low or no chances of toxicity. (3) It is more fruitful to use a single drug acting on many targets rather than using several drugs for various targets. Multitargeted drugs may work through different biochemical pathways and may also have pharmacological effects to treat comorbid conditions. This approach may reduce the side effects associated with using several drugs at the same time. To design novel cytotoxic agents, researchers mounted the 1,5-diaryl-3-oxo-1,4-pentadienyl group onto several scaffolds such as piperidones, cycloalkanones and 2-tetralones and significant potency against neoplastic cells was observed.

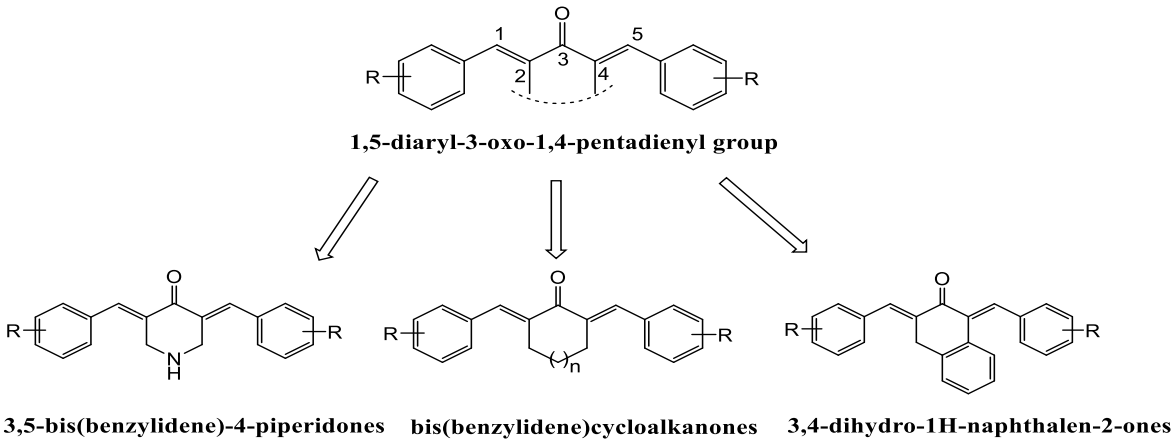

Figure 1.7 : The incorporation of the 1,5-diaryl-3-oxo-1,4-pentadienyl pharmacophore to form potential cytotoxic agents.

As mentioned earlier, various chemotherapeutic agents used in cancer treatment exhibited effects on both neoplasms as well as normal cells. This results in various side effects associated with these agents. Thus there was a need to develop antineoplastic agents which are selectively toxic towards malignant cells and not non-malignant cells. Hence the theory of sequential toxicity came into the picture. It was proposed that successive chemical attacks could damage cancer cells to a greater extent as compared to normal cells. For example, as indicated in Figure 1.8, intracellular thiols can interact at position 1 of the 1,5-diaryl-3-oxo-1,4-pentadienyl pharmacophore. Subsequently thiols can bind at position 5. If the neoplasms are damaged more than the normal cells with the initial chemical insult, then chemosensitization of the tumors will have occurred. A second interaction with a cytotoxin may lead to tumor-selective cytotoxicity.[57]

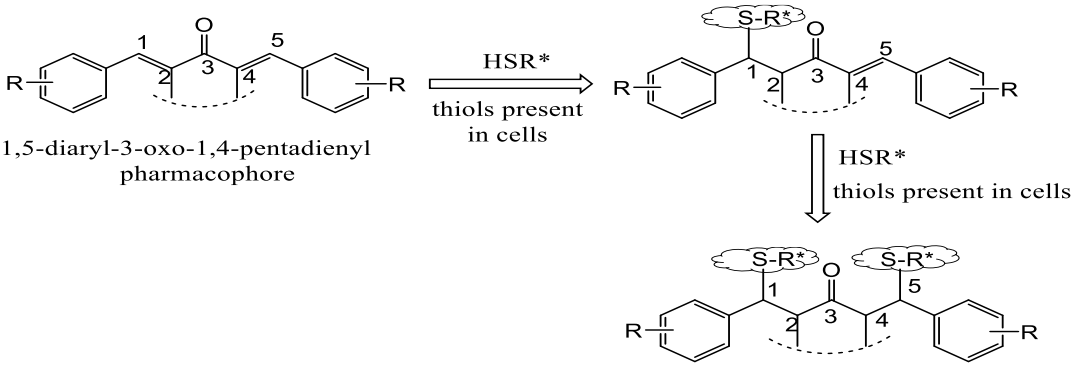

Figure 1.8 : Sequential interaction of cellular thiols with compounds possessing the 1,5-diaryl-3-oxo-1,4-pentadienyl moiety.

1.8.1 Mannich bases

Over the years, our lab's research work has focused on Mannich bases. Dr. Dimmock and his team have contributed significantly towards the design and synthesis of Mannich bases and their role in cancer treatment. A Mannich reaction is the condensation between a compound having a labile hydrogen atom next to a carbonyl function, an aldehyde (generally formaldehyde) and a primary or secondary amine or ammonia.

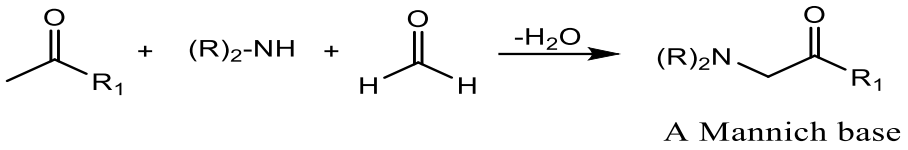

Scheme 1.1 : A Mannich reaction between a substrate, formaldehyde and secondary amine.

Mannich bases have various pharmacological activities including antiinflammatory, antibacterial, antifungal, anticonvulsant, antitubercular, analgesic, anti-HIV, antimalarial, antiviral and anticancer properties. Mannich bases inhibit various endogenous enzymes such as cholinesterase, α-glucosidase and purine nucleoside phosphorylase that play key roles in the regulation of molecular processes. Previous research work from our lab have revealed that Mannich bases as well as the α,β-unsaturated keto moiety contribute towards the cytotoxicity of neoplasms as hypothesized by the sequential cytotoxicity theory.[35]

1.8.2 Acyclic Mannich bases

Dimmock *et al* synthesized a series of acyclic Mannich bases or β-aminoketones which had either one or two centres for nucleophilic attack by cellular constituents. Compounds **20** and **21** were evaluated against the WiDr colon cancer and their IC_{50} values were found to be 0.8 μM[58] and 0.45 μM, respectively, as compared to 5-FU with an IC_{50} value of 1.61 μM.[59]

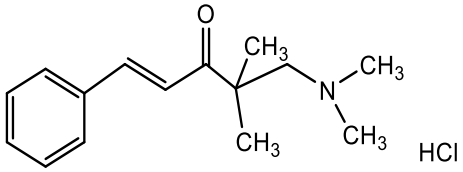

20

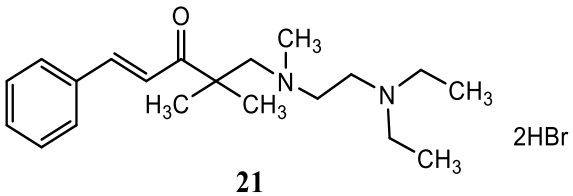

21

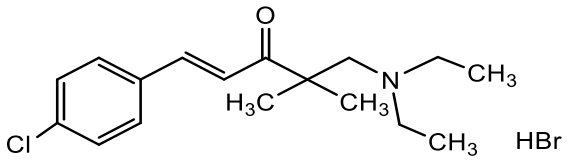

22

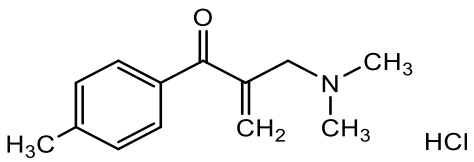

23

CDDP **22** is an acyclic Mannich base which inhibited various isoenzymes of GST. This compound was synthesized with the hypothesis that if a tumor having a lower level of α-GST isoenzyme than normal cells and the alkylating agent has a selectivity towards this isoenzyme, then a second chemical insult may be more damaging to tumors as compared to normal cells having higher concentrations of α-GST.[60] Compound **23** inhibits the growth of WiDr colon cancer with an IC_{50} value of 2 μM and was found to be less toxic towards human CRL-2522 fibroblasts. Compound **23** is a lead compound with greater potency than cisplatin.[61] Some of the Mannich bases obtained from 1-aryl-4-methyl-1-penten-3-ones showed greater cytotoxic potency than the precursor ketones towards murine P388 and L1210 leukemic cells and human tumor cell lines. Some Mannich bases are effective in treating drug resistant tumors.[62]

1.8.3 Cyclic Mannich bases

1.8.3.1 3,5-bis(Benzylidene)-4-piperidones

Although the Mannich bases **24** are highly cytotoxic, they caused respiratory depression in mice. Hence, structural modifications were made by adding a second benzylidene group as a potential alkylating site while retaining the arylidene keto and carbonyl functionality. This approach reduced the flexibility and restricted the conformation of the molecules as compared to **24**. Compound **25a** is a lead compound developed by Dimmock and coworkers and has 5800 times greater cytotoxic potency than the anticancer drug BCNU towards P388D1 leukemic cells.[63]

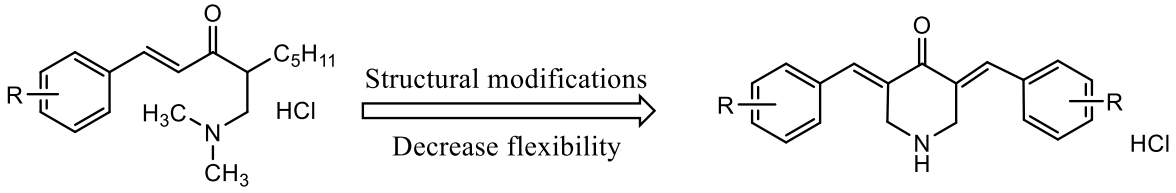

24 **25**

Figure 1.9 : The design of 3,5-bis(benzylidene)-4-piperidones as potential antineoplastic agents.

3,5-bis(Benzylidene)-4-piperidone **25a** is a thiol alkylating agent as it interacts with cellular thiols by lowering the hepatic glutathione levels in mice and is well tolerated in mice (with a daily dose of 240 mg/day for 5 consecutive days). It is highly cytotoxic against murine P388D1 leukemic cells *in vitro* with an IC_{50} value of 16 pM but was inactive *in vivo*. It is believed that due to poor pharmacokinetic parameters, its penetration and transport across membranes was difficult.[63] Hence to overcome this problem, many analogues of 3,5-bis(benzylidene)-4-piperidone were synthesized and evaluated with the aims to improve permeability, higher selectivity towards neoplasms and effectiveness against MDR tumors. Molecular descriptors like Hammett σ (electronic parameter), Hansch π (solubility parameter), molecular refractivity (steric parameter) of substituents, partition coefficients (solubility parameter), dipole moment, molecular geometry were taken into consideration in the design and development of 3,5-bis(benzylidene)-4-piperidone analogues.

Compounds **25a-d** displayed cytotoxic potency towards human Molt4/C8 and CEM T-lymphocytes, murine P388 leukemic cells as well as murine L1210 neoplasms.[64] In addition, these compounds showed greater toxicity to malignant cells (human HSC-2 and HSC-4 squamous cell carcinomas and human HL-60 promyelocytic leukemic cells) than non-malignant cells (human HGF gingival fibroblasts, HPC pulp cells and HPLF periodontal ligament fibroblasts). The selective index values of **25a-d** are 10, 4.3, 13 and 29, respectively, suggesting that they are highly tumor-selective cytotoxins.[65] Incorporation of the electron-donating dimethylamino group in **25h** (IC_{50} = 36.4 μM) displayed 15-fold less potency than the unsubstituted **25a (**2.5 μM), which is the parent compound, in L1210 cells. This effect may be due to a reduction in the positive charge on olefinic carbon atoms.[66]

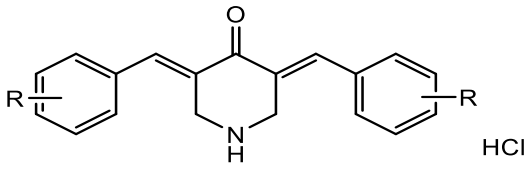

25

25a: R = H; **25b**: R = 4-Cl; **25c**: R = 4-NO_2; **25d**: R = 4-CH_3; **25e**: R = 4-OCH_3

25f: R = 4-F; **25g**: R = 2-F; **25h**: R = 4-$N(CH_3)_2$

Apart from being cytotoxic agents, compound **25a-c** display antimycobacterial activity with minimum inhibitory concentrations of 3.13 μM, 6.25 μM and 0.2 μM respectively. These compounds stimulate respiration in mitochondria isolated from rat livers. The compounds are well

tolerated in a short term toxicity evaluation in mice which means these analogues may be promising agents for the treatment of tuberculosis.[67] Moreover, **25a-d** show potent antimalarial activity against drug sensitive D6 as well as drug resistant C235 strains of *Plasmodium falciparum*.[68]

Compound **25g**, **EF 24** is a novel curcumin analogue possessing a fluoro group at the ortho position of the aryl rings and exhibited remarkable potency as compared to cisplatin. It was 23.3 and 9.8-fold more efficacious than cisplatin and curcumin, respectively, against a panel of tumor cell lines screened by the NCI *in vitro*. **EF 24** was highly cytotoxic as compared to the antiangiogenic drug TNP-470. Further *in vivo* investigation revealed that it greatly reduced the size of a breast tumor in female nude mice.[69] The possible mechanism of cell death includes redox-dependent apoptosis and cell-cycle arrest in MDA-MB-231 human breast cancer cells and DU-145 human prostate cancer cells.[70] Further investigations revealed that it can also disrupt the microtubule cytoskeleton[71] and suppress NF-κB pathways in cholangiocarcinoma (CCA) cells.[72] **EF 24** also acts as antibacterial agent against *E.coli* and *S. aureus*.[73]

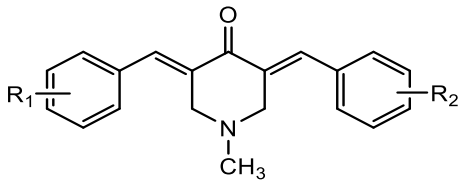

26

26a: $R_1 = R_2 = H$; **26b**: $R_1 = R_2 = 4\text{-}B(OH)_2$; **26c**: $R_1 = R_2 = 4\text{-}CF_3$; **26d**: $R_1 = R_2 = 3\text{-}Br$;

26e: $R_1 = 2\text{-}F$, $R_2 = 3,4,5\ (OCH_3)_3$; **26f**: $R_1 = 3,4\ (OCH_3)_2$, $R_2 = 3,4,5\ (OCH_3)_3$;

26c: $R_1 = 3,4,5\ (OCH_3)_3$, $R_2 = 4\text{-}CN$; **26h**: $R_1 = 3\text{-}NO_2$, $R_2 = 4\text{-}CF_3$

Compound **26a** shows potency against number of cancer cell lines with average IC_{50} of 4.69 μM.[57] Compound **25a** exhibits 57-fold higher potency than the N-methyl adduct **26a**. 3,5-bis(dihydroxyborinyl-benzylidene)-1-methyl-4-piperidone **26b** showed high cytotoxicity against colon HCT 116 cancer cells which were p53 sensitive (HCT 116 p53 +/+) as compared to the ones which lacked p53 (HCT 116 p53 -/-). This compound was also cytotoxic against breast cancer cells with an IC_{50} value of 3.5 μM towards MCF-7 and MDA-MB-231 cells[74]. A recent study shows that compounds **26c** and **26d** are not only potent cytotoxic agents but also have multidrug resistant reverting properties. These trifluoromethyl and bromo analogues showed marked selectivity

against a panel of cancer cells as compared to normal human umbilical vein endothelial cells (HUVEC). Such compounds displaying dual effects are promising lead molecules.[34]

Novel dissymmetrical compounds **26e-h** having aryl 3,4-dimethoxy and 3,4,5-trimethoxy groups or electron withdrawing groups 2-F, 4-CN, 3-NO_2 and 4-CF_3 inhibit the growth of HepG-2 and THP-1 cells *in-vitro* and exhibited low cytotoxicity towards normal LO2 cells. The fluoro substituted compound **26e** is the most potent compound towards HepG-2 cells and exhibits dose-dependent apoptosis by up-regulating BAX expression and down-regulating Bcl-2 expression. A further *in vivo* investigation showed that compound **26e** is well tolerated and supresses the growth of the HepG2 tumor in mice.[75]

Another study was undertaken with compounds **27a-c** which possess the dual properties of cytotoxicity as well as MDR reverting properties. They have anti-proliferative activity against a panel of cancer cell lines among which Hela, K562 and U87 cancer cells are the most sensitive. The compounds possessing a trifluoromethyl group in the aryl ring were the most cytotoxic probably because the nucleophilic attack by cellular thiols is easier as electron-withdrawing groups reduce the electron density on the olefinic carbon atoms.

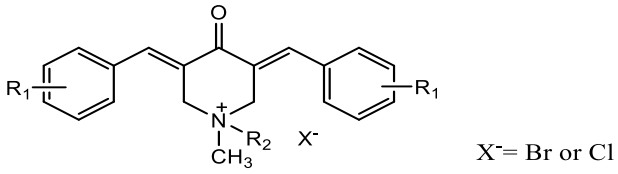

X^-= Br or Cl

27

27a-c: R_1 = 4-CF_3 **27d-f**: R_1 = 3-Br

27a, **27d**: R_2 = 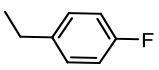 **27b**, **27e**: R_2 = 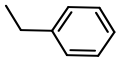 **27c**, **27f**: R_2 = 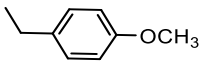

All compounds were selective towards cancer cells as compared to HUVEC normal cells. The selectivity of compound **27b** is 39 which is noteworthy and merits further considerations. Compounds **26c** and **27a-c** with a trifluoromethyl group and compounds with a 3-bromo substitution (**26d**, **27d-f**) decrease the expression level of the resistant gene MDR1 by 11-38% and 31-46% respectively. Thus compounds **26c** and **26d** displayed strong potency and more MDR reverting properties than their corresponding N-substituted groups.[34]

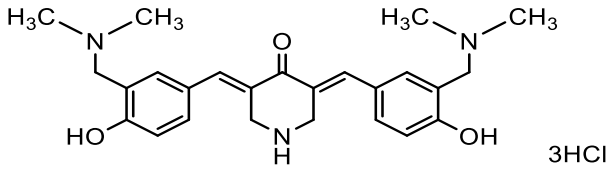

28

A recent study revealed that the incorporation of hydroxyl groups and substitution by alkylaminoalkyl groups in the aryl rings may reduce the lipophilicity of compound **25a**. Physicochemical parameters such as torsion angles between the aryl rings and adjacent olefinic groups and logP values had a significant impact on cytotoxicity. When another dimethylaminomethyl group was introduced into compound **28** it displays remarkably decreased cytotoxicity (IC_{50} > 500 µM) towards Molt 4/C8, CEM and L1210 leukemic cells. Compound **28** was highly cytotoxic against a subpanel of human colon cells (COLO205, HCC-2998, HCT 116, HCT 15, HT29, KM12, SW-620) with average IC_{50}, TGI and CC_{50} value of 1.26 µM, 3.09 µM, 7.25 µM respectively; while for 5-FU the average IC_{50}, TGI and CC_{50} values are 14.8 µM, >1862 µM, >2512 µM, respectively. 3,5-bis(3-Dimethylaminomethyl-4-hydroxybenzylidene)-4-piperidone trihydrochloride **28** is a promising lead antineoplastic agent and its mode of action was investigated and shown to cause apoptosis, DNA fragmentation and cleavage of PARP1 in HSC-2 and HL-60 cells.[76]

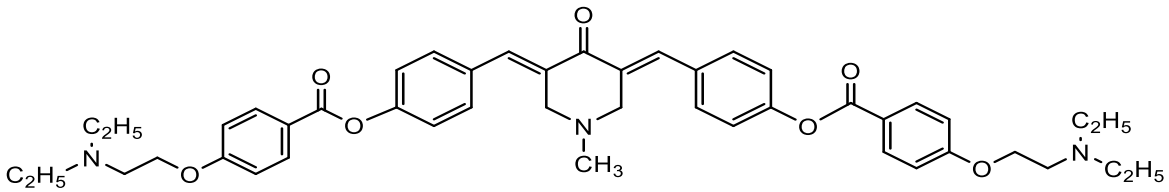

29

Compound **29** was synthesized in our lab based on the hypothesis that auxiliary binders on the arylidene benzene ring will be more potent than the corresponding N-methyl substituted 4-piperidones. Compound **29** emerged as a lead compound with high potency towards a panel of cancer cell lines such as leukemia, lymphoma, prostate, colon, and breast cancers. It was more potent than curcumin and **EF 24** which is a curcumin analogue. It remarkably inhibited the growth in Ramos, RAJI and EL4 cells by 90%, 70% and 60%, respectively, at 1 µM concentration. The selectivity index was greater than 1 which means that its toxicity is more towards malignant cells than normal cells. It has high selectivity (11.1) against T-leukemic cells as well as cytotoxicity

with a CC_{50} value of approximately 0.45 μM. It also exhibited MDR reverting properties. A mechanistic investigation revealed that cell death was caused by apoptosis by activation of caspase-3 and caspase-7 and mitochondrial depolarization in Jurkat cells.[77,78]

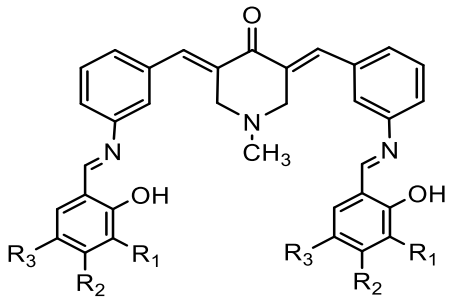

30

30a: $R_1 = R_2 = R_3 = H$; **30b**: $R_1 = R_2 = H$, $R_3 = OH$; **30c**: $R_1 = R_2 = OH$, $R_3 = H$

In another series of novel curcumin analogues, the N-methyl-4-piperidone moiety and incorporation of the hydroxyl groups favoured anticancer activity. Compounds **30a** and **30b** displayed high potency against THP-1 leukemic cells *in vitro* with IC_{50} values in the range of 0.69-0.96 μM. They were also cytotoxic against a number of cell lines namely HepG2, Hela and K562 cells. Moreover, the phenolic -OH groups contributed to the higher solubility in 20 mM PBS as compared to **30a**.[79]

1.8.3.2 N-Acyl-3,5-bis(benzylidene)-4-piperidones

These analogs were developed based on the following considerations: (1) An acyl group that serves as an auxiliary binding site was introduced onto the piperidyl nitrogen atom of the 1,5-diaryl-3-oxo-1,4-pentadienyl pharmacophore to investigate whether it increases or retains cytotoxicity. (2) It is challenging for 3,5-bis(benzylidene)-piperidones to pass through the cell membrane as they tend to ionize in the body under various physiological conditions. Addition of a N-acyl group onto the piperidyl nitrogen atom will prevent possible ionization of the piperidyl nitrogen and hence the permeability in neoplasms may increase.

Two important characteristics of these compounds are that these groups can form van der Waals, hydrogen and ionic bonds with cellular moieties. These analogs can also act as prodrugs undergoing amidic hydrolysis and releasing 4-piperidones into cells.[57]

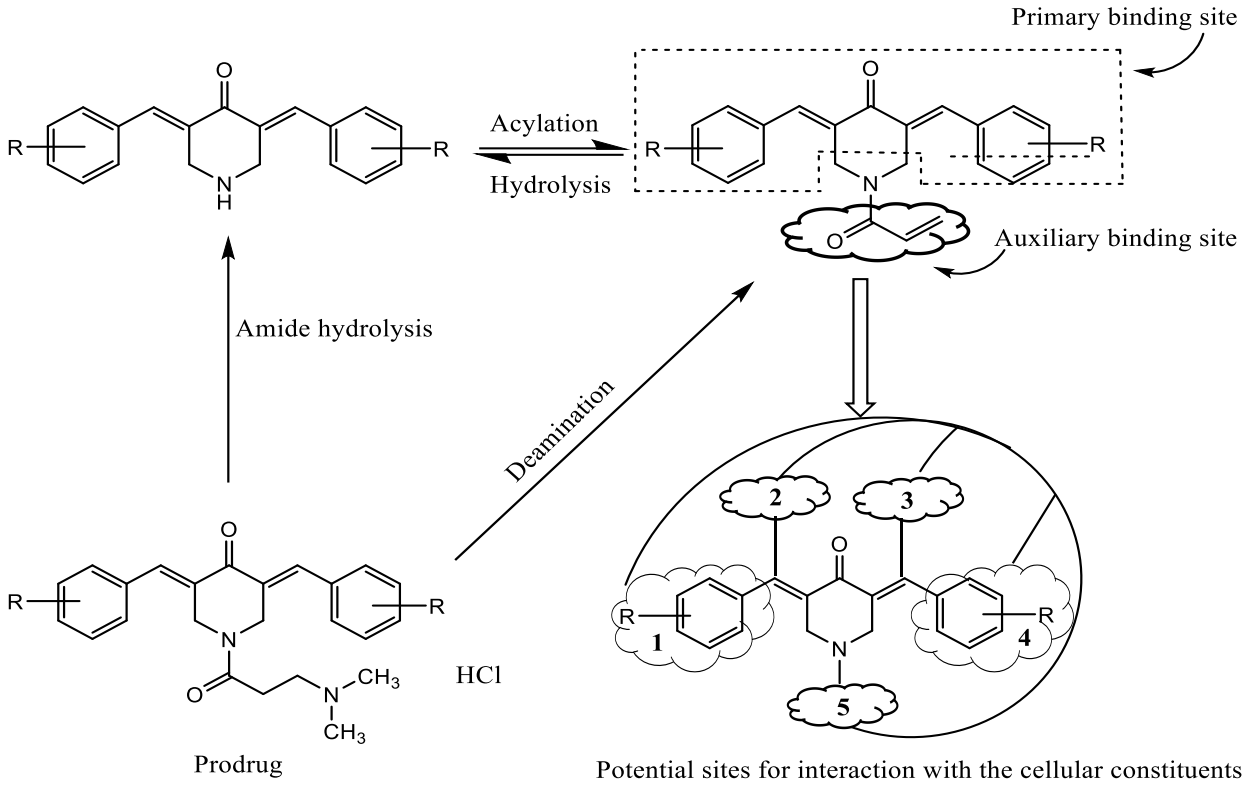

Figure 1.10 : N-Acylation of 3,5-bis(benzylidene)-4-piperidones.

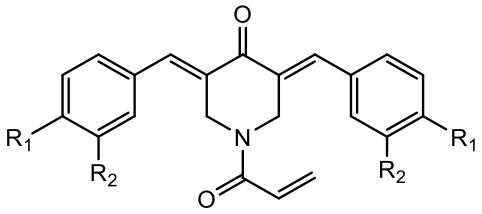

31

31a: $R_1 = R_2 = H$; **31b**: $R_1 = Cl$, $R_2 = H$; **31c**: $R_1 = R_2 = Cl$; **31d**: $R_1 = F$, $R_2 = H$; **31e**: $R_1 = NO_2$, $R_2 = H$

These compounds were prepared with the aim to increase cytotoxic potencies and display selectivity towards malignant cells and interact at a N-acyl binding site. The N-acryloyl derivatives displayed greater antineoplastic activity against four different cell lines namely murine P338, L1210 leukemic cells, human Molt 4/C8 and CEM neoplasms than the analogues in which a hydrogen atom was present on the piperidyl nitrogen atom. The average IC_{50} values of **31a-e** were 0.28 μM (P388), 4.71 μM (L1210), 0.96 μM (Molt 4/C8) and 1.13 μM (CEM), respectively. Overall, there was 25-fold increase in cytotoxicity for N-acryloyl analogues when their average IC_{50} values were compared with the corresponding parent compounds in these four cell lines. The results also show that the addition of the N-acryloyl group **31a** (IC_{50} = 0.8 μM) increases potency

3-fold as compared to the corresponding 3,5-bis(benzylidene)-4-piperidone **25a** (IC_{50} = 2.5 μM) against the L1210 leukemic cells *in vitro*. Thus the addition of third alkylating site led to an increase in potency of the cytotoxins.[80]

Moreover, NCI screening of **31a** against a series of 56 different cancer cell lines revealed it had an average IC_{50} value of 1.45 μM. This means that **31a** is approximately 18-fold more potent than a reference alkylating cytotoxic drug melphalan (IC_{50} = 26.30 μM).[80] Although substitution of the carboxyl moeity (R=COCH=CHCOOH) increased potency 700 times compared to BCNU (IC_{50} = 134 pM) in P338 cells, it was less active than **25a** and it is believed that the polar carboxyl group may have hindered its permeation into the cells. However, hepatic glutathione levels were reduced by 29% when a dose of 0.87 mmol/kg was administered in mice.[63] Further, **31e** inhibits DNA, RNA, and protein synthesis in murine L1210 cells whereas **31c** induces apoptosis in human Jurkat leukemic cells. Structure-activity relationships shows that electronic parameters influence cytotoxicity. The contributing features towards enhancement of potency can be the incorporation of strong electron-withdrawing groups in the arylidene benzene ring, addition of substituents of varying sizes in the ortho position of the aryl rings to increase the torsion θ values and insertion of groups having lower redox potentials.[64] Another important characteristic of **31a-e** is that they show higher selectivity towards neoplasms than normal cells. N-Acryloyl-3,5-bis(benzylidene)-4-piperidone **31a** is considered a lead compound.

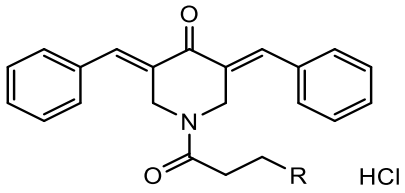

32

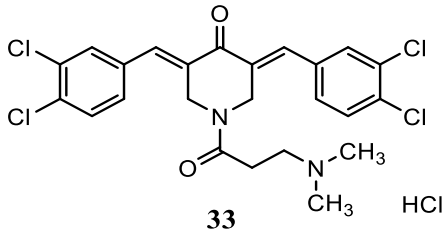

33

32a: R= $N(CH_3)_2$; **32b**: R= $N(C_2H_5)_2$

32c: R=  ; **32d**: R=  ; **32e**: 

All the compounds in series **32** were potent inhibitors of L1210 leukemic cells. Compound **32b** displayed 1.6-fold greater potency than **31** while the dimethylamino and pyrrolidino analogues showed similar potency as **31**. Substitution of electron-withdrawing groups to the arylidene aryl ring **33** further increased their cytotoxicity 4-fold and 13-fold compared to the corresponding unsubstituted compound **32a** and precursor compound **25a**. As β-aminoketones tend to deaminate,

compounds **32** were designed as prodrugs which are believed to liberate **31**. Solubility studies showed that all the compounds were poorly soluble in PBS except **32a** and **32b** which were dissolved in a mixture of PBS-d: DMSO-d_6. ^{1}H NMR studies after incubation at 37°C for 48 h revealed that compound **32** liberates **31** which was unstable in the solvents used in the experiments. It was also noted that the potency of compound **32** was greater before its decomposition. Thus decomposition of N-acyl group can be avoided if methyl groups can be introduced adjacent to the N-acyl group.[80]

Another novel series of N-acyl analogues of 3,5-bis(arylidene)-4-piperidone **34** and **35** were developed as potential cytotoxins which supports the hypothesis that the N-acyl moiety will act as a third alkylating site capable of forming van der Waals, hydrogen and ionic bonds with the receptor. The 1-[4-(2-alkylaminoethoxy)phenylcarbonyl]-3,5-bis(arylidene)-4-piperidone hydrochlorides **34** are cytotoxic against a panel of human colon cancer cells displaying IC_{50} values in the submicromolar to nanomolar range and the average IC_{50} values are lower than a reference drug 5-FU.

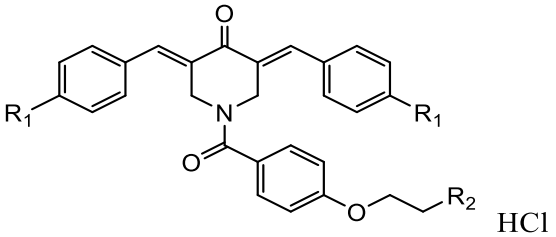

34

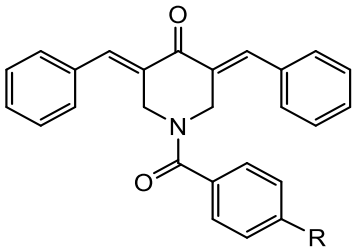

35

R_1: same as series **25a-e**

R_2=$N(CH_3)_2$, $N(C_2H_5)_2$, 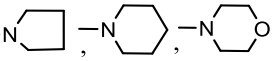

34a : R_1 = H, R_2 =  ; **34b** : R_1= Cl, R_2 = 

34a : R_1= CH_3, R_2= 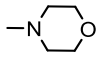

35a: R = H; **35b**: R = OCH_3

35c : 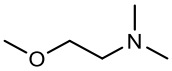

The structure-activity relationships were developed by incorporating different substituents with varying Hammett σ and Hansch π values in the arylidene aryl rings and incorporating a number of various amines with different sizes and basicity in the N-acyl side chain. The potencies of the compounds in series **34** are either increased, equipotent or decreased in 48%, 35% and 17%, respectively, to the corresponding analogues of the parent compound **25**. Overall, higher cytotoxic properties are observed where R_1 is a nitro group. Compounds **34b** and **34c** showed 48 times and

38 times higher potencies than the reference drug melphalan. Compound **34b** was a lead compound with IC_{50} = <5 nM against colon cancer HCC-2998 cells.[81] The compounds in series **34** demonstrated greater toxicity to the neoplastic HL-60, HSC-2 and HSC-4 tumor cells than non-malignant HGF, HPC and HPLF normal cells. Compound **34b** possessing morpholine as the terminal base displayed higher selectivity towards neoplasms with a SI value of 69 which is noteworthy. This observation suggests that the N-acyl group contributes to the preferential cytotoxicity to the malignant cells compared to the normal cells. This compound induces apoptosis by activation of caspase-3 and internucleosomal DNA fragmentation in HL-60 cells. Additionally, it caused autophagy in HSC-2 cells.[82] Moreover, these compounds are well-tolerated in mice up to a 300 mg/kg dose without noteable toxicities.[67] Compounds **35a** and **35b** showed similar potencies as the parent compound **25a** whereas the presence of a dimethylaminoethoxy group in **35c** displayed greater potency (IC_{50} = 0.58 μM) than **25a** (IC_{50} = 1.67 μM) in Molt 4/C8 cells supporting the hypothesis that the 4-(2-aminoethoxy) fragment serves as auxiliary binders interacting with the cellular constituents. Thus, the N-[4-(2-aminoethoxy)phenylcarbonyl] side chain is believed to interact at auxiliary binding sites and contributes to the increased potencies.

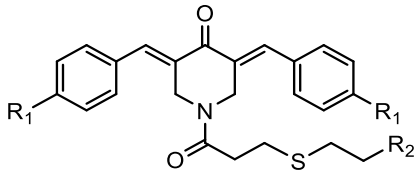

36

36a: R_1 same as series **25a-e**, $R_2 = SO_3H$

36b: $R_1 = OCH_3$, $R_2 = SH$

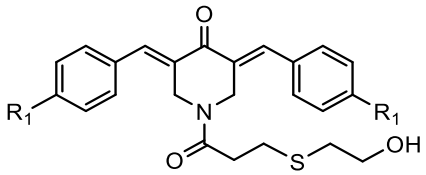

37

37: R_1 same as series **25a-e**

A series of novel compounds **36** were prepared from our lab with mercaptosulfonic acid which are potential cytotoxins based on the hypothesis that mercaptosulfonic acid will be released *in vivo* by undergoing dethiolation under suitable physiological conditions. The sodium salt of mercaptosulphonic acid (mesna) acts as a chemoprotectant when co-administered with antineoplastic agents and thus it was hypothesized that incorporation of this group will demonstrate selective toxicity towards neoplasms. However, compound **36a** showed poor potency towards HSC-2 and HSC-4 squamous carcinoma cells, murine L1210, HL-60 and Molt/C8 and CEM T-lymphocytes as well as no selectivity towards cancer cells and it is believed that the incorporation of the hydrophilic sulfonic acid group might have restricted its transport across cell membranes.

Stability studies shows that derivatives of **36a** at 37°C for 24 h do not release 1-acryloyl-3,5-bis(benzylidene)-4-piperidones and mesna. To overcome this problem, the sulfonic acid group was replaced by a mercapto group **36b** which increased the logP value to 3.23. In general, an analogue **36b** possessing a nitro group in the benzylidene ring displayed more potency than other substituents and greater potency than **36a**.[65] This thiol **36b** is equipotent to melphalan against Molt 4/C8 and CEM cell lines.[83]

A related series of dienones such as 3,5-bis(benzylidene)-1-[3-(2-hydroxyethylthio)-propanoyl]-piperidin-4-ones **37**, displayed high potencies against a wide range of cancer cell lines especially colon cancers and leukemias with IC_{50} values in the submicromolar range and are significantly more potent than the reference drug melphalan. The compound possessing nitro substituents in series **37** was found to be the most potent with IC_{50} values in range of 0.02-0.28 μM against a panel of cancer cells. It displayed 96 times greater potency than melphalan. Statistical analysis showed a negative correlation between the σ values of the aryl substituents and CC_{50} values in HL-60, HSC-3 and HSC-4 bioassays suggesting that by increasing the electron-withdrawing properties of the aryl substituents will result in a higher positive charge on the olefinic carbon atoms and thereby increase potency. Moreover a positive correlation was observed between the σ values of aryl substituents and SI values of compounds in series **37** in the HL-60, HSC-3 and HSC-4 bioassays suggesting that with increases in the electron-withdrawing properties of the aryl substituents, greater toxicity is observed towards cancer cells than the normal cells. The compounds in series **37** with nitro and chloro substituents at the para position emerged as potential cytotoxins against malignant cells compared to normal cells.[83]

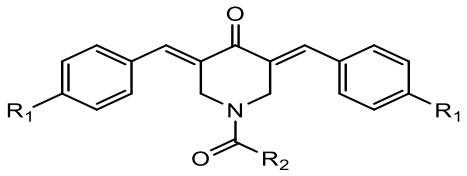

38

38 : R_1 same as series **25a-f**

38a : R_2 = 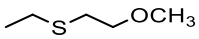

38b : R_2 = 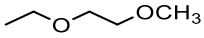

38c : R_2 = 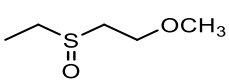

38d : R_2 = 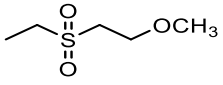

Another series of dienone derivatives **38** were prepared by replacing the polar hydroxyl group in the terminal N-acyl chain of **37** to a methyl ester and by replacing the sulphur atom to an isosteric oxygen atom and by incorporating groups having different sizes, electronic parameters and hydrogen bond forming capacities. These novel dienones are potent cytotoxins against Molt4/C8 and L1210 leukemic cells and displayed higher toxicity than melphalan. The results in this study supports the hypothesis that addition of the 3-(2-methoxyethylthio)-propionyl group in **38a**, shows higher potency or are equipotent than their corresponding parent analogues **25** and **37** when comparisons were made. This suggests that these compounds undergo interactions at secondary binding sites. Compound **38a** having a 4-nitro substituent (CC_{50} = 0.36 μM in HSC cell lines) was 35 times more potent than the reference drug melphalan. Furthermore addition of an isosteric oxygen atom in **38b** remarkably lowered the potency. Compounds in series **38c-d** with a 4-fluoro substituent at the R_1 position were found to be more cytotoxic than the corresponding parent compound **25** and twice as potent as the 4-fluoro analogues in **38a**. Overall, replacing sulphur atoms with large sized atoms results in higher electron-attracting properties thereby increasing or retaining potency. Compounds with terminal polar -OH groups resulted in lower IC_{50} values than **38a** possessing a methoxy group. The 3,4-dimethoxy analogues in **38a** were potent with an average CC_{50} figure of 0.83 μM and selectivity index of 13. Compounds in **38a** with R_1 having nitro and 3,4-dimethoxy groups showed apoptotic death by cleavage of PARP1 in HSC-2 cells. [84]

In general, it can be concluded from the literature studies that N-acyl derivatives of 3,5-bis(benzylidene)-4-piperidones are a novel class of antineoplastic agents that may possess tumor-selective properties. Hence, incorporation of a novel N-acyl group into the 3,5-bis(benzylidene)-4-piperidone moiety may increase or retain cytotoxic potencies.

1.8.3.3 Other 3,5-bis(benzylidene)-piperidone derivatives

Various groups have been placed on the piperidyl nitrogen atom to observe the potential interaction of auxiliary binders with the cellular constituents.

Another series of dienone derivatives, the N-diethylphosphono-4-piperidones **39** and 3,5-bis(benzylidene)-4-oxo-1-phosphonopiperidines **40** have been developed which inhibits the growth of human Molt4/C8 and CEM T-lymphocytes and murine L1210 leukemic cells. Overall, compounds **39a-c** and **40c** displayed 58-, 35- 93- and 15-fold greater potency than melphalan towards 60 human tumor cell lines.[85] Compounds **39b** and **40b** were potent tumor-specific

cytotoxins meeting the criteria of PL10 status (that is compounds are identified as promising lead molecules if they have CC_{50} values of 10 μM or less and SI of 10 or more).

The average CC_{50} figures (SI values in parentheses) of **39b** and **40b** were 1.20 μM (46) and 3.35 μM (25) respectively. Moreover, all the compounds showed selectivity towards neoplastic cell lines (HL-60, HSC-2, HSC-3 and HSC-4) compared to human normal cells (HGF gingival fibroblasts, HPC pulp cells and HPLF periodontal ligament fibroblasts).[86]

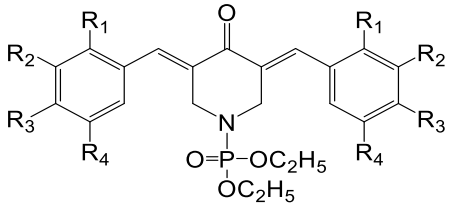

39

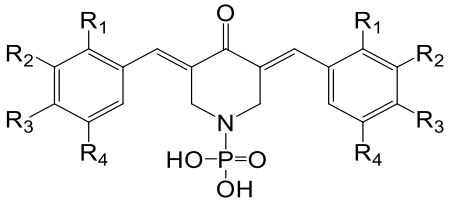

40

39a : $R_1 = R_2 = R_3 = R_4 = H$;

39b : $R_1 = R_2 = R_4 = H$, $R_3 = OCH_3$;

39c : $R_1 = R_2 = H$, $R_3 = R_4 = OCH_3$;

39d : $R_1 = NO_2$, $R_2 = R_3 = R_4 = H$

40a : $R_1 = R_2 = R_3 = R_4 = H$;

40b : $R_1 = R_2 = R_4 = H$, $R_3 = OCH_3$;

40c : $R_1 = R_2 = H$, $R_3 = R_4 = OCH_3$;

40d : $R_1 = NO_2$, $R_2 = R_3 = R_4 = H$

Compound **40d** was identified as lead molecule with IC_{50} value of 34 nM against both Molt 4/C8 and CEM T-lymphocytes. It displayed 90-fold and 76-fold more potency than melphalan in the Molt4/C8 and CEM tests respectively. It was concluded from QSAR studies that substitution of large electron-withdrawing groups with low hydrophobicity in the benzylidene ring could be fruitful in the development of potent cytotoxins. The positive correlation between IC_{50} values and ClogP suggests that hydrophilic groups like the phosphonic acids **40** have lower potency than the ester moiety **39** in L1210 cells and therefore increasing Hansch π values in the aryl substituents may be fruitful. In general, series **40** has greater growth-inhibiting properties than series **39**. Compounds **39a** and **39b** were potent towards RPMI leukemic cells with IC_{50} values of <10 nM and 32 nM, respectively, which is noteworthy. A further investigation revealed that **40d** induced apoptosis in HT-29 colon cancer cells at a concentration of 5 μM with a 29-fold increase in the sub-G_1 phase and inhibited cellular respiration. Moreover compounds **39** and **40** possess MDR reverting properties which is discussed later in the mechanism of actions section.[85]

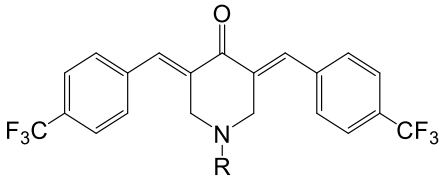

41

41a: H ; **41b**: 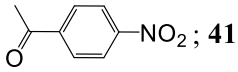 ; **41c**: 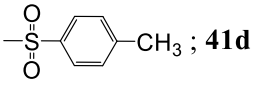 ; **41d**: 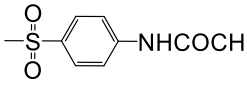 ; **41e**: 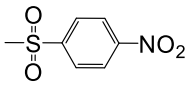

A series of novel fluorescent antitumor agents were synthesized with the aim that these agents will not only be cytotoxins but will also possess fluorescent properties which can be useful to trace targets in the cell. These compounds were potent inhibitors of the growth of five malignant cell lines namely, SW1990 and MIA PaCa-2 (human pancreatic carcinoma), PG-BE1 and NCI-H460 (human lung carcinoma) and SK-BR-3 (human breast cancer). Compounds **41a**, **41d** and **41e** were the most potent with average IC_{50} values of 0.98 μM, 0.67 μM and 0.36 μM, respectively, in these cell lines. It is possible that the electron-withdrawing trifluoromethyl group and the interaction of the N-substituent with cellular constituents contributed to the higher potencies than the parent compounds. Moreover, X-ray crystallography suggests that the short distances between the N-substituent (4-nitrophenylsulfonyl groups) and 3,5-bis(benzylidene)-4-piperidones results in an interconjugated system and thereby contributes towards the fluorescent properties. The fluorescent intensities of **41a-e** with trifluoromethyl substituents were not as strong as compared to compounds possessing electron-donating groups like dimethylamino. In addition, there exists an inverse relationship between cytotoxicity and fluorescent properties. The N-aroyl derivatives **41a-e** are potent cytotoxins but exhibit weak fluorescence.[87]

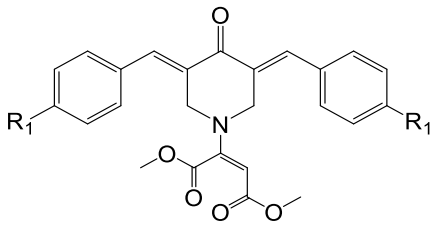

42

42a: R_1 = H ; **42b**: R_1 = Cl

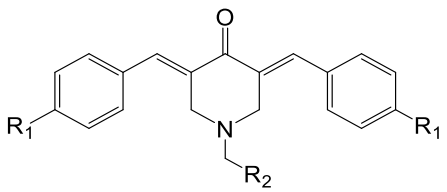

43

R_1 = H ; Cl

43a: $R_2 = CH_2COOCH_3$; **43b**: $R_2 = CH_2COOCH_3$

43c: $R_2 = COOCH_2CH_3$

The following study highlighted the incorporation of small N-substituents in 3,5-bis(benzylidene)-4-piperidones. The diesters **42a-b** had shown poor cytotoxicity against four human adherent carcinoma cell lines Hela, A2780, MCF7 and A431 compared to the parent analogues **25**. On the other hand, the dienones **43** were potent cytotoxins against these four malignant cell lines. It can be noted that compounds **43** are potent antineoplastic agents as they possess oxygen atoms which can interact with the auxiliary binding sites by forming hydrogen bonds. Compound **43a** with R_1 having a chloro substituent (average IC_{50} = 0.84 μM) was more potent than unsubstituted analogue (R_1= H, average IC_{50} = 2.61 μM) and displayed 28 times greater potency than cisplatin which is a drug used in chemotherapy. Moreover, the long chain monoesters **43b** had a 2.4-fold increased cytotoxicity than **43c**. The positive correlation of the atomic charges of the olefinic carbon atoms in the aryl ring and cytotoxicity suggests that chlorobenzylidene derivatives are more potent than corresponding benzylidene ones.[88]

1.9 Importance of N^1-acylhydrazide derivatives

Hydrazide and hydrazone functional groups which are present in many biomolecules contributing towards various pharmacological activities such as anti-inflammatory, antiviral, antibacterial, antitubercular, antifungal, antiprotozoal and anticancer activities. The azomethine group in hydrazones (NH-N-CH=) bridged with the carbonyl group mainly contributes towards its biological activity as well as the synthesis of various heterocyclic scaffolds like 1,3,4-oxadiazolines, azetidin-2-ones, coumarins, 1,3-benzothiazin-4-ones and 1,3-thiazolidin-4-ones.[89,90] Isoniazid (isonicotinylhydrazide) is a well known first line drug used to treat tuberculosis.

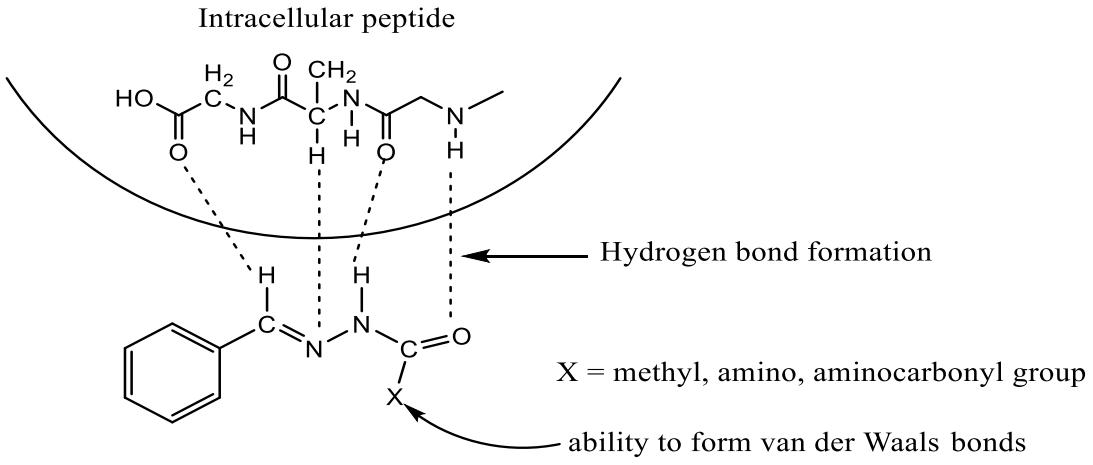

44 aryl semicarbazones

Dimmock *et al* synthesized various acetylhydrazone and semicarbazone derivatives **44** which showed promising anticonvulsant activity. These compounds were believed to interact with cellular peptides by forming hydrogen bonds as shown in the figure, as well as with an aryl binding site. If the terminal group is methyl then it facilitates van der Waals formation and with amino and aminocarbonyl groups, there is formation of hydrogen bonding with the binding site.[91]

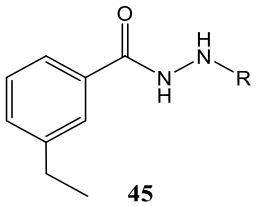

45

45a: R = 2-cyanoethyl

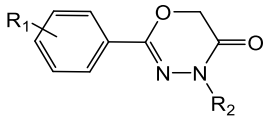

46

46a: R_1 = 3,4,5 $(OCH_3)_3$, R_2 = nonan-5-yl

A series of nitrogen containing heterocyclic 4H-1,3,4-oxadiazin-5(6H)-ones derivatives were synthesized by cyclization reaction of N-aroylhydrazines with chloroacetyl chloride. Compound **46a** having a trimethoxy moiety was the most potent growth inhibitor of human lung A549 cancer cells and human prostate PC-3 cell lines with IC_{50} values of 9.91 µM and 14.42 µM, respectively. In another assay, compound **45a** displayed monoamine oxidase (MAO) inhibitory activity with an IC_{50} value of 0.24 mmol/L.[92]

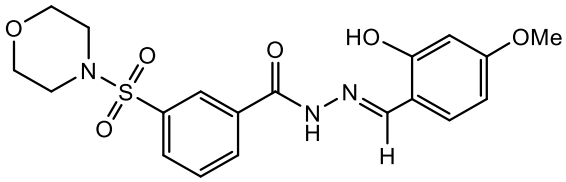

47

In a recent study, the hydrazone derivative **47** emerged as a lead cytotoxin towards esophageal cancer cells EC9706 and EC109 with IC_{50} values of 1.09 µM and 2.79 µM, respectively. This compound was synthesized by the conjugation of a hydrazone and sulfonamide moiety in an approach to study potential synergistic effects of these scaffolds. Structure-activity relationship revealed that the substitution on the phenyl ring has significant effects on cytotoxicity. The hydroxyl group at the ortho position of the phenyl ring improved the cytotoxic potency. The replacement of the phenyl ring with furan or thiophene groups led to compounds with IC_{50} values in excess of 100 µM; however in the case of the pyridine moiety, the cytotoxicity was increased to some extent. A mechanistic investigation shows that compound **47** induces cell-cycle arrest in

the G_0/G_1 phase, collapses the mitochondrial membrane potential, increases ROS levels, upregulates the pro-apoptopic protein Bax and p53 as well as downregulates anti-apoptopic Bcl-2 by activating caspase-9 in EC9706 and EC109 cells. Furthermore it was well tolerated in mice with a dose of 2 g/kg for 2 weeks and no signs of toxicities were noted.[93]

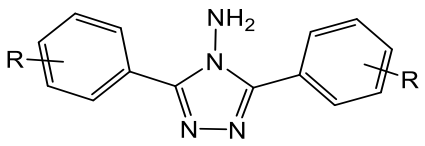

48

R = 3-NO_2 , 4-Cl, 3-NH_2

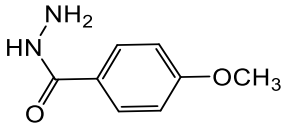

49

The triazole derivatives **48** and the acyl hydrazide **49** inhibit two main targets namely cathepsin B and cathepsin H in cancer which belong to the cysteine protease family. These cysteine proteases play important roles in the regulation of cellular proteins and increased enzyme levels are associated with tumor progression. Compounds having amino, nitro and chloro groups at the 3 and 5 positions of the 1,2,4 triazole ring and 4-methoxy benzohydrazide **49** inhibited the proteolytic activities in liver homogenate. The acyl hydrazide **49** inhibited cathepsin B competitively and cathepsin H non-competitively whereas the triazoles **48** inhibited cathepsin H in a non-competitive fashion.[94]

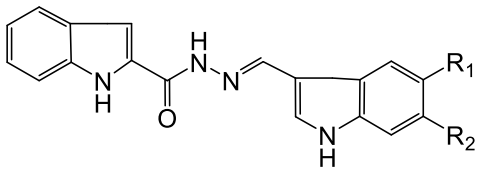

50

50a: R_1 = OCH_3, R_2 = H; **50b**: R_1 = H, R_2 = OCH_3

Novel bis(indolyl)-hydrazide **50** derivatives were synthesized wherein an indole ring is linked to an acyl hydrazone (-CO-NH-N=CH-) pharmacophore. These compounds are potent cytotoxic agents and display higher selectivity against human lung A549 cancer cells (**50a**: IC_{50} = 2 µM, **50b**: IC_{50} = 6 µM,) than normal human lung W138 fibroblasts (**50a**: IC_{50} = 48.5 µM) and peripheral blood mononuclear PBMC cells (**50a**: IC_{50} = 62 µM). SAR studies revealed that compound **50a** is the most potent cytotoxin. The mode of action studies involved cell-cycle arrest at the G_2/M phase, mitochondrial membrane depolarization and apoptosis by inhibiting microtubules (62%) with an IC_{50} value of ~7.5 µM. Moreover, high levels of expression of p53, Bax, caspase 3 and caspase 9

were noticed with a decrease in the level of Bcl-2 expression in A549 cells. Additionally, compound **50a** exhibited remarkable fluorescent properties on binding with tubulin.[95]

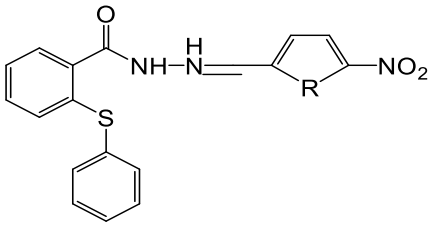

51

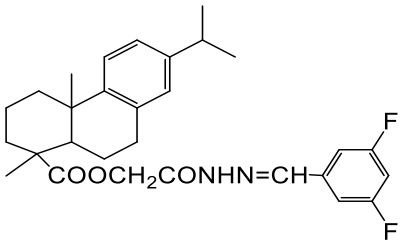

52

51a: R = O, **51b**: R = S

Compounds **51a** (furan substituent) and **51b** (thiophene substituent) were cytotoxic towards MCF-7 adenocarcinoma cells with IC_{50} values of 0.7 µM and 0.18 µM, respectively, as compared to doxorubicin as a reference drug with an IC_{50} value of 2.1 µM. Compound **51b** exhibited a 4-fold greater cytotoxic potency than **51a**. Moreover, it showed less toxicity towards normal human fibroblasts cells. Compound **51b** induced apoptosis by up-regulating Bax levels, downregulating Bcl-2 levels and activating caspase 3. It also inhibited the growth of a mammary tumor at doses of 10 mg/kg/day in mice.[96]

Another dehydroabietic acid-based acylhydrazone derivative **52** was synthesized by a condensation reaction. N′-(3,5-difluorobenzylidene)-2-(dehydroabietyloxy)acetohydrazide **52** is a potent cytotoxin against cervical HeLa cancer cells with an IC_{50} value of 2.21 µM which is a similar potency as cisplatin (IC_{50} = 1.94 µM). Moreover, it displayed cytotoxicity towards liver BEL-7402 cancer cells with an IC_{50} value of 14.46 µM which is the same potency as cisplatin (IC_{50} = 12.68 µM). SAR studies revealed that a methyl group at the para position, bromo at ortho position and bifluoro groups at the ortho, para and meta positions in the aryl ring of the acylhydrazone moiety increases cytotoxicity towards HeLa cells.[97]

Tolmetin, 2-[1-methyl-5-(4-methylbenzoyl)-1H-pyrrol-2-yl]-acetic acid belongs to the non-steroidal anti-inflammatory drug (NSAIDs) class known to inhibit prostaglandin synthesis but it also prevents cell proliferation in colon neoplasms. Tolmetin based hydrazide derivative **53** displayed antineoplastic activity against colon cancer HT-29 cells with an IC_{50} value of 76 µM. The mode of action studies revealed that Tolmetin and compound **53** significantly increases caspase-3, -8 and -9 concentrations as well as annexin V levels with a dose of 75-100 µM in colon HT-29 cancer cells.

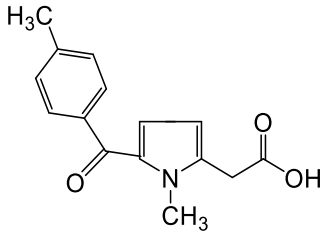

Tolmetin

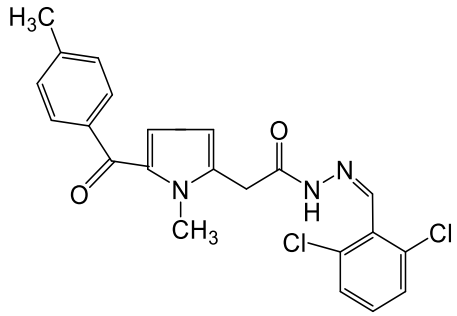

53

In addition, it also decreased the mitochondrial membrane potential in HT-29 cells at a concentration of 75-150 µM. Moreover, it is believed that cyclooxygenase-2 (COX-2) has elevated levels in colon adenomas. Computational studies predicted that both tolmetin and compound **53** bind selectively to the COX-1 active site rather than COX-2 enzyme. Moreover, compound **53** has higher binding affinity than tolmetin for COX-1. Thus compound **53** was considered to be a novel hydrazide derivative with antineoplastic activity.[98]

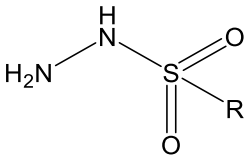

54

54a: R = CH_3; **54b**: R = CH_2CH_3; **54c**: R = $CH_2CH_2CH_3$; **54d**: R = $CH_2CH_2CH_2CH_3$

The homologous series of methane (**561a**), ethane (**54b**), propane (**54c**) and butane (**54d**) sulfonic hydrazide derivatives were synthesized by a nucleophilic substitution reaction of alkyl sulfonyl chloride with hydrazine hydrate. An *in vitro* cytotoxicity study showed that the compound with the lowest IC_{50} (15.41 µM) is **54d** as compared to docetaxel (IC_{50} = 7.24 µM) towards MCF-7 breast adenocarcinoma cells revealing that there is enhancement in cytotoxicity with an increase in the number of methylene groups. Furthermore the butane sulfonic acid hydrazide **54d** has shown remarkable antibacterial activity against Gram positive and negative bacterial strains as well as it inhibits carbonic anhydrase II isoenzyme.[99]

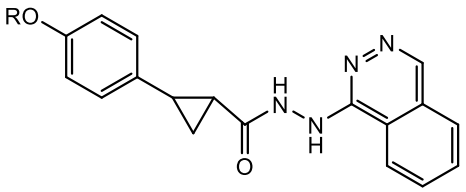

55

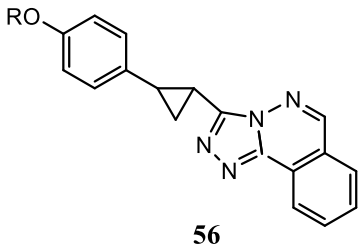

56

55: R = $(CH_3)_2C{=}CHCH_2CH_2C(CH_3){=}CHCH_2$ —

56: R = $(CH_3)_2C{=}CHCH_2$ –

In another study a 2-(4-alkoxyphenyl)-N'-(phthalazine-1-yl)cyclopropanecarbohydrazide **55** and a 3-(2-(4-alkoxyphenyl) cyclopropyl)-[1,2,4]triazolo[3,4-α]phthalazine **56** exerted anticancer activity via cytostatic effects rather than a cytocidal effect. SAR studies revealed that 1-phthalazines may be responsible for the inhibition of DNA synthesis in cancer cells by acting as DNA-intercalators. Moreover, it is believed that the phenyl cyclopropyl fragment contributes to potent cytotoxicity. Compounds **55** with geranyl and **56** with isopentyl side chains attached to 4-hydroxylphenyl frame were active against U373 glioblastoma (GBM, IC_{50} values 9 µM and 4 µM, respectively) and OE21 esophageal cancer cells (IC_{50} values 9 µM and 8 µM, respectively). These compounds impeded U373 tumor growth by decreasing cell proliferation rather than killing U373 tumor cells. Compound **55** showed mitosis dependent cytotoxic effects by prolonging the mitosis duration thereby reducing mitosis numbers in U373 GEM cells at 10 µM whereas compound **56** exerted independent cytotoxic effects by decreasing mitosis duration but there were no changes in mitosis numbers *in vitro*. [100]

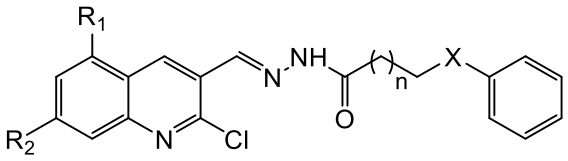

57

57a: X = S, n = 1, R_1 = H, R_2 = OMe; **57b**: X = O, n = 1, R_1 = H, R_2 = OMe;

57c: X = S, n = 1, R_1 = OMe, R_2 = OMe; **57d**: X = S, n = 4, R_1 = H, R_2 = OMe;

57e: X = O, n = 4, R_1 = H, R_2 = OMe

Novel quinoline based hydrazide-hydrazones analogues were synthesized based on the fact that conjugation of the quinoline moiety onto the hydrazide-hydrazones [(-C=O)NHN=CH] fragment would confer antineoplastic properties as well as affecting the expression levels of $p27^{kip1}$ which

plays a crucial role in the regulation of G_0 to S phase transition in cell-cycle via regulating cyclin-dependent kinases. All the compounds in series **57** inhibit the growth of SH-SY5Y and Kelly neuroblastoma as well as MDA-MB-231 and MCF-7 breast adenocarcinoma cells. However it was observed that these acyl hydrazone compounds display greater cytotoxicity and selectivity towards neuroblastoma cells rather than breast cancer cells. It was noted that **57c** possessing two methoxy groups was the most active against SH-SY5Y (IC_{50} = 2.9 µM), Kelly (IC_{50} = 1.3 µM), MCF-7 (IC_{50} = 14.1 µM), and MDA-MB-231 (IC_{50} = 18.8 µM), malignant cells respectively.

Moreover, compound **57b** having an ether linkage exhibited higher cytotoxic potency than compound **57a** possessing a sulfane linkage. Further SAR revealed that the hydrazides having short chains such as in compound **57a** (n = 1, X = S) reduced the cell viability up to 37% more than compound **57d** (n=1, X = S) in Kelly cells. Additionally, **57b** (n = 1, X = O) decreased cell viability up to 53% more than the compound bearing a long chain **57e** (n = 4, X = O) in SH-SY5Y cells. It was also found that the size of the heterocyclic moiety plays an important role in cytotoxicity. For example, replacement of the quinoline moiety with indole and phenyl derivatives lowered cytotoxicity whereas the naphthalene group showed similar cytotoxicity across cell lines as **57**. Mode of action studies revealed that **57c** increased proportions of the G_0/G1 phase as well as decreased the number of cells in the S and G_2/M phases at 10 µM concentration and induces cell cycle arrest by upregulating $p27^{kip1}$ in SH-SY5Y neuroblastoma cells. Thus, these hydrazide compounds are potential anticancer agents against neuroblastoma with less toxicity towards normal lung fibroblasts cells.[101]

1.10 Mitochondria: an important target for cell death

Mitochondria, the power house of the cell, is an important target for anticancer agents as it plays a vital role in the regulation of cellular processes such as ATP production, biosynthesis, metabolism and apoptosis. The disruption of mitochondria either by causing a loss of ATP production, the collapse of mitochondrial membrane potential or decreased oxygen consumption leads to cell death. These dysfunctions may be due to enzymatic, transport, structural or regulatory failure of mitochondria.[102]

Many significant differences have been noted between mitochondria present in cancer and non-cancerous cells. Under hypoxic conditions, cancer cells inhibit oxidative phosphorylation and induce glycolysis by overexpression of hexokinase II associated with the outer mitochondrial

membrane and also increases VEGF levels which allows the growth of tumors by angiogenesis. The overexpression of antioxidant enzymes such as GST in malignant cells helps to scavenge the high ROS levels. Inhibition of these enzymes in cancer cells could considerably increase ROS levels.[103] Moreover cancer cells have a more hyperpolarized mitochondrial membrane potential ($\Delta\psi_m$ ~ -220 mV) than the healthy cells ($\Delta\psi_m$ ~ -140 mV).

Mitochondrial membrane potential results from the transfer of protons across the inner mitochondrial membrane by the respiratory pumps during aerobic respiration. This build-up of proton force generates an electrochemical gradient across the hyperpolarized membrane to produce energy in the form of ATP. CCCP and 2,4-dinitrophenol are lipophilic uncouplers which can cross the membrane and accumulate inside the polarized mitochondrial matrix. These uncouplers, when targeted to cancer cells, depolarize the potential by opening the permeability transition pore and release pro-apoptotic agents such as cytochrome c into the cytoplasm and consequently induces apoptosis at higher doses.[104] The regulation of MMP in healthy cells is vital because high $\Delta\psi_m$ during the electron transport process results in an increase in ROS levels. On the contrary, if $\Delta\psi_m$ drops then there is less energy production and low ROS levels may dissipate cell homeostasis.[105] Therefore, the dysregulation of $\Delta\psi_m$ results in a loss of cell viability.

Reactive oxygen species generated in the electron transport chain across the membrane results in the oxidation of endogenous molecules initiating a caspase activation pathway.[106] Apoptosis, which may be defined as programmed cell death, depends on the activation of caspases wherein oxidative stress, Ca^{+2} overload, DNA damage, high ROS levels can directly lead to the initiation of apoptosis. Thus targeting mitochondria in cancer cells can be one of the key strategies for apoptosis which can achieved with different pathways such as damaging mitochondrial DNA, targeting metabolic pathways as well as effects on the mitochondrial membrane. Results from our lab have shown the effect of unsaturated carbonyl compounds on mitochondria.[107,108] Hence, mitochondrial membrane potential and evaluation of ROS levels have been undertaken to investigate the effect of developed cytotoxic agents on mitochondria.

1.11 Conclusion

Chemotherapy is a well-known treatment option for treating cancer however its debilitating effects such as nausea, vomiting, hair loss, susceptibility to infections and other health problems needs to be overcomed. Thus advances are being made by researchers to design and develop antineoplastic agents which can kill the tumors without having detrimental effects on normal healthy cells. Moreover tumors develop intrinsic or extrinsic resistance mechanisms to overcome the effects of the chemotherapeutic agent. Curcumin isolated from turmeric has shown proven efficacy treating cancer with a limited therapeutic profile. Hence, the need to develop synthetic analogs of curcumin with better therapeutic outcomes is a promising option.

CHAPTER 2 : HYPOTHESES AND OBJECTIVES

2.1 Hypotheses

1. The attachment of a suitable group on the nitrogen atom of antineoplastic 3,5-bis(benzylidene)-4-piperidones **63** will lead to analogs with increased cytotoxic potencies.[57, 64]

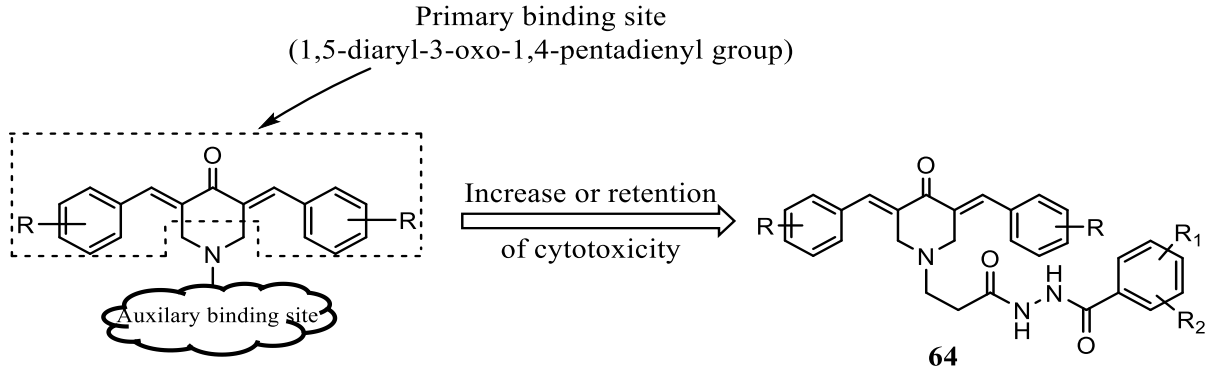

64

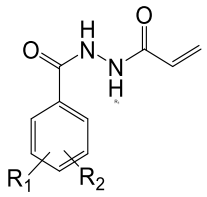

N^1-aroyl-N^2-acryloylhydrazines **60**

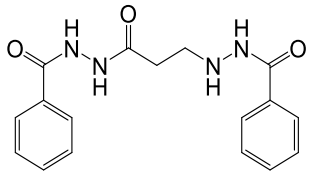

N^1-aroyl-N^2-3-arylcarboxamido-aminopropionylhydrazine **61**

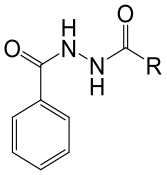

N^1-aroyl-N^2-acylhydrazines **62**

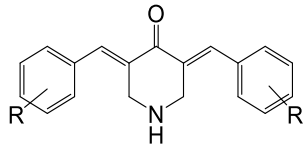

3,5-bis(benzylidene)-4-piperidones **63**

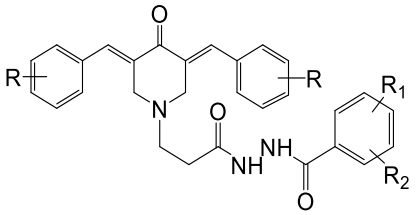

3,5-bis(benzylidene)-1-[3-(arylcarbonylaminoamino)-3-oxo-1-propyl]-4-piperidones **64**

2. Representative N^1-aroyl-N^2-acryloylhydrazines **60** will sensitize human HCT 116 colon cancer cells to 3,5-bis(benzylidene)-4-piperidones **63**.
3. N^1-aroyl-N^2-acylhydrazines in series **62** will be less cytotoxic than N^1-aroyl-N^2-acryloylhydrazines in series **60** towards human HCT 116 colon cancer cells.

4. An adduct **64** between a representative compound in series **60** and a 3,5-bis(benzylidene)-4-piperidone in series **63** will have greater potency than the corresponding compounds in series **60** and **63**.

2.2 Objectives

1. To synthesize a series of cytotoxic N^1-aroyl-N^2-acryloylhydrazines **60**, N^1-aroyl-N^2-3-arylcarboxamidoaminopropionylhydrazines **61**, N^1-aroyl-N^2-acylhydrazines **62** and 3,5-bis(benzylidene)-1-[3-(arylcarboxamidoamino)-3-oxo-1-propyl]-4-piperidone **64**.
2. To establish the activity of these agents against HCT 116, MCF-7 and MDA-MB-231 cancer cell lines. Selected compounds will be evaluated against non-malignant human CRL1790 colon cells.
3. To evaluate whether one or more representative compounds in series **60** sensitize HCT 116 cells to 3,5-bis(benzylidene)-4-piperidones **63**.
4. To investigate some of the mechanisms of action of representative compounds such as their effects on mitochondrial membrane potential, generation of reactive oxygen species (ROS) levels and antioxidant properties.

CHAPTER 3 : SYNTHESIS

3.1 Materials and Methods

All the chemicals and solvents used are of analytical grade and are used without further purification. Melting points (m.p.) were measured on a Gallenkamp instrument (MF370) and are uncorrected. Thin layer chromatography (TLC) was used to monitor the chemical reactions for which silica gel 60, F_{254} precoated plates were used and visualized under UV light or an iodine chamber. ^{1}H and ^{13}C Nuclear Magnetic Resonance (NMR) were recorded at 500 MHz and 125 MHz, respectively, using a Brüker Avance spectrometer equipped with a 5mm BBO probe. NMR spectra were obtained by dissolving the samples either in deuterodimethyl sulphoxide (DMSO-d_6) or deuterochloroform ($CDCl_3$) relative to tetramethylsilane (TMS) or solvent. The NMR spectra were determined in terms of the chemical shifts which are expressed in parts per million (ppm). Different designations were used to indicate the multiplicity namely, s (singlet), d (doublet), dd (doublet of doublet), t (triplet), q (quartet), m (multiplet) and br (broad). Mass spectra were obtained using QSTAR XL LC/MS/MS quadrupole / time of flight mass spectrometer with an ESI source.

3.2 General scheme for the synthesis of N^1-aroyl-N^2-acryloylhydrazine derivatives 60a-m

The general methodology for the synthesis of **60a-m** is presented in scheme 3-1.

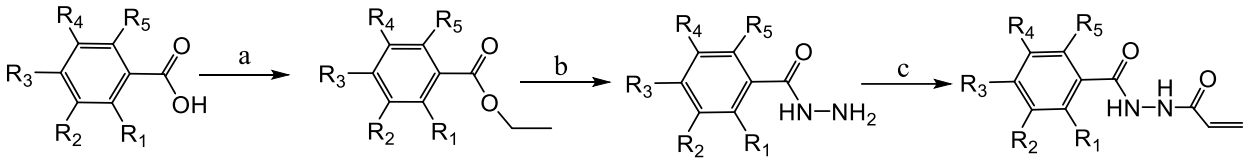

Scheme 3.1 : General scheme for the synthesis of N^1-aroyl-N^2-acryloylhydrazines **60a-m**.
The reaction conditions are as follows: a: ethanol/H_2SO_4, reflux temperature, 6-8 h; b: hydrazine hydrate/ethanol, reflux temperature, 8-12 h; c: acryloyl chloride/$CHCl_3$, $NaHCO_3$ /water, 0°C, 1 h. **a**: $R_1 = R_2 = R_3 = R_4 = R_5 = H$; **b**: $R_1 = R_2 = R_4 = R_5 = H$, $R_3 = F$; **c**: $R_1 = R_2 = R_4 = R_5 = H$, $R_3 = Br$; **d**: $R_1 = R_2 = R_4 = R_5 = H$, $R_3 = Cl$; **e**: $R_1 = Cl$, $R_2 = R_3 = R_4 = R_5 = H$; **f**: $R_1 = R_3 = R_4 = R_5 = H$, $R_2 = Cl$; **g**: $R_1 = R_4 = R_5 = H$, $R_2 = R_3 = Cl$; **h**: $R_1 = R_4 = Cl$, $R_2 = R_3 = R_5 = H$; **i**: $R_1 = R_3 = R_4 = R_5 = H$, $R_2 = CH_3$; **j**: $R_1 = CH_3$, $R_2 = R_3 = R_4 = R_5 = H$; **k**: $R_1 = R_2 = R_4 = R_5 = H$, $R_3 = CH_3$; **l**: $R_1 = R_2 = R_4 = R_5 = H$, $R_3 = OCH_3$; **m**: $R_1 = R_4 = R_5 = H$, $R_2 = R_3 = OCH_3$.

3.2.1 Synthesis of the esters 58a-m

Substituted or unsubstituted benzoic acids (0.0082 moles, 1 g), ethanol (0.085 moles, 5 ml) and sulphuric acid (0.0094 moles, 0.5 ml) were heated under reflux for 6-8 h.[109] Ethyl acetate and hexane (1:1) were used as the TLC solvent to monitor the reaction. In the case of **58g** and **58m**, a precipitate was formed from the solution at room temperature. In the case of the other compounds, the solvent was removed and the residues were collected. For purification, these residues were added to ethyl acetate (20 ml) and washed twice with saturated sodium bicarbonate solution (20 ml). The aqueous solution was discarded and the ethyl acetate solution containing the esters was rinsed with brine solution (20 ml), dried over sodium sulphate and further solvent evaporation *in vacuo* yielded the esters. All the esters prepared are liquid in nature except **58g** and **58m** which are solids. For all the esters synthesized, 1H NMR spectra obtained are consistent with their structure. Data for three representative compounds **58a**, **58g** and **58m** are as follows:

Ethyl benzoate (58a): Colorless liquid; Yield = 83%; ^{1}H NMR ($CDCl_3$): δ 8.08 (dd, J = 8.32 Hz, 1.31 Hz, 2H, Ar-H), 7.54 (m, 1H, Ar-H), 7.45 (m, 2H, Ar-H), 4.40 (q, J = 14.25 Hz, 7.12 Hz, 2H, CH_2), 1.39 (t, J = 7.12 Hz, J = 14.23 Hz, 3H, CH_3).

Ethyl 3,4-dichlorobenzoate (58g): Colorless crystals; Yield = 76%; m.p. 37°C (lit. m.p. 35-37 °C);[110] ^{1} NMR ($CDCl_3$): δ 8.12 (d, J = 1.92 Hz, 1H, Ar-H), 7.87 (dd, J = 8.36 Hz, 1.95 Hz, 1H, Ar-H), 7.52 (d, J = 8.38 Hz, 1H, Ar-H), 4.40 (q, J = 14.25 Hz, 7.16 Hz, 2H, CH_2), 1.40 (t, J = 7.17 Hz, J = 14.33 Hz, 3H, CH_3).

Ethyl 3,4-dimethoxybenzoate (58m): Colorless crystals; Yield = 71%; m.p. 42-44 °C (lit. m.p. 43-44°C);[111] ^{1}H NMR ($CDCl_3$): δ 7.69 (dd, J = 8.42 Hz, 1.75 Hz, 1H, Ar-H), 7.55 (d, J = 1.63 Hz, 1H, Ar-H), 6.88 (d, J = 8.46 Hz, 1H, Ar-H),4.36 (q, J = 14.28 Hz, 7.19 Hz, 2H, $CH_{2,}$), 3.94 (s, 6H, 2x$OCH_{3,}$), 1.39 (t, J = 7.13 Hz, J = 14.27 Hz, 3H, CH_3).

Table 3.1 : Physical and chemical properties of **58a-m**

Compounds	Substituents	Appearance	m.p. (°C)	Lit. m.p (°C)	Yield (%)
58a	H	Colorless liquid	--	--	83
58b	4-F	Slightly yellow liquid	--	--	76
58c	4-Br	Slightly yellow liquid	--	--	52
58d	4-Cl	Colorless liquid	--	--	78
58e	2-Cl	Slightly yellow liquid	--	--	78
58f	3-Cl	Slightly yellow liquid	--	--	85
58g	3,4-Cl_2	Colorless solid crystals	37-39	35-37[110]	76
58h	2,5-Cl_2	Slightly red brown liquid	--	--	75
58i	3-CH_3	Yellow liquid	--	--	73
58j	2-CH_3	Yellow liquid	--	--	81
58k	4-CH_3	Colorless liquid	--	--	89
58l	4-OCH_3	Slightly yellow liquid	--	--	86
58m	3,4-$(OCH_3)_2$	Colorless solid crystals	42-44	43-44[111]	71

3.2.2 Synthesis of the hydrazides 59a-m

Solutions of hydrazine hydrate (33.3 mmoles, 1.67 ml, 50-60% w/v aqueous) and ethyl benzoate (6.66 mmoles, 1 g) in ethanol (85.7 mmoles, 5 ml) were heated under reflux for 8-12 h.[112] The reaction was monitored by TLC using chloroform and methanol (9.5:0.5) as the solvent system. After completion of the reaction, the solvent was removed in vacuo and recrystallized from 95% ethanol. For all the hydrazides synthesized, ^{1}H NMR spectra obtained are consistent with their proposed structure. Data for three representative compounds **59a**, **59g** and **59m** are as follows:

Benzohydrazide (59a): Colourless crystals; Yield = 75%; m.p.110°C (lit. m.p. 112°C);[109] ^{1}H NMR (DMSO-d_6): δ 9.76 (s, 1H, CONH), 7.81 (d, J = 7.87 Hz, 2H, Ar-H), 7.51 (t, J = 6.9 Hz, J = 13.78 Hz, 1H, Ar-H), 7.44 (t, J = 7.6 Hz, J = 15.17 Hz, 2H, Ar-H), 4.48 (s, 2H, NH_2).

3,4-Dicholorbenzohydrazide (59g): Colourless crystals; Yield = 93%; m.p. 167-170°C (lit. m.p. 154-166°C);[110] ^{1}H NMR (DMSO-d_6): δ 9.96 (s, 1H, CONH), 8.04 (d, J = 1.94, 1H, Ar-H), 7.80 (dd, J = 8.37 Hz, 1.98 Hz, 1H), 7.74 (d, J = 8.36 Hz, 1H, Ar-H), 4.55 (s, 2H, Ar-H).

3,4-Dimethoxybenzohydrazide (59m): Colourless crystals; Yield = 91%; m.p. 148-150°C (lit. m.p. 151-152°C);[113] ^{1}H NMR (DMSO-d_6): δ 9.63 (s, 1H, CONH), 7.43 (td, 2H, Ar-H), 7.00 (d, J = 8.38 Hz, 1H, Ar-H), 4.47 (s, 2H, Ar-H), 3.79 (d, J = 1.85 Hz, 6H, 2xOCH_3).

Table 3.2 : Physical and chemical properties of **59a-m**

Compounds	Substituents	Appearance	m.p. (°C)	Lit. m.p (°C)	Yield (%)
59a	H	Colorless crystals	110-112	112[109]	95
59b	4-F	Slightly yellow crystals	160-162	162[109]	69
59c	4-Br	Colorless crystals	166-168	164[109]	42
59d	4-Cl	Colorless crystals	159-162	163[109]	66
59e	2-Cl	Colorless crystals	118-121	118-120[114]	74
59f	3-Cl	Colorless crystals	154-157	158[109]	93
59g	3,4-Cl_2	Colorless crystals	167-170	154-166[110]	73
59h	2,5-Cl_2	Colorless crystals	167-172	168-170[110]	35
59i	3-CH_3	Colorless crystals	99-102	97[109]	88
59j	2-CH_3	Colorless crystals	118-120	124[109]	83
59k	4-CH_3	Yellow crystals	115-118	117[109]	90
59l	4-OCH_3	Slightly yellow crystals	134-136	136-140[114]	88
59m	3,4-$(OCH_3)_2$	Colorless crystals	148-150	151-152[113]	91

3.2.3 Synthesis of the N^1-aroyl-N^2-acryloylhydrazine derivatives 60a-m

The benzohydrazide (7.34 mmoles, 1g) was added to a solution of sodium bicarbonate (8.07 mmoles, 0.678 g) in water (7.5 ml) and the reaction vessel was placed in an ice bath for 15 min. Acryloyl chloride (7.70 mmoles, 0.70 g) in chloroform (7.5 ml) was added dropwise with constant stirring to the suspension of the acid hydrazide and stirred at ice-bath temperature for 1 h. The reaction was monitored by TLC using a solvent system of chloroform and methanol (9.5:0.5). After the reaction was complete, the residues were collected, washed with ice cold water and dried.[115] For purification, these residues were dissolved in ethyl acetate (20 ml) and washed twice with 2N HCl solution (2 x 10 ml). The aqueous solution was discarded and the ethyl acetate solution containing the compound was washed with the brine solution (10 ml) and dried over

sodium sulphate. The solvent was removed by evaporation and the solid was recrystallized from 95% ethanol.

N^1-Acryloylbenzohydrazide 60a: Yield = 86%; m.p. 177-179°C (lit. m.p. 175-178°C);[115] ^{1}H NMR (DMSO-d_6): δ 10.34 (d, J = 109.3 Hz, 2H, CONH), 7.88 (m, 2H, Ar-H),7.59 (m, 1H, Ar-H), 7.50 (m, 2H, Ar-H), 6.35 (q, J = 17.17 Hz, 10.2 Hz, 1H, =CH), 6.23 (dd, J = 17.17 Hz, 2.05 Hz, 1H, =CH), 5.76 (dd, J = 10.2 Hz, 2.06 Hz, 1H, =CH). ^{13}C NMR (DMSO-d_6): 165.40, 163.87, 132.42, 131.84, 129.36, 128.47, 127.43, 126.93. MS (ESI): m/z 191.08 $[M+H]^+$.

N^1-Acryloyl-4-fluorobenzohydrazide 60b: Yield = 79%; m.p.176-179°C ; ^{1}H NMR (DMSO-d_6): δ 10.51 (d, J = 1.185 Hz, 1H, CONH), 10.22 (d, J = 1.206 Hz, 1H, CONH), 7.96 (m, 2H, Ar-H), 7.35 (m, 2H, Ar-H), 6.34 (q, J = 17.11 Hz,10.2 Hz, 1H, =CH),6.23 (dd, J = 17.17 Hz, 2.04 Hz, 1H, =CH), 5.76 (dd, J = 10.2 Hz, 2.07 Hz, 1H, =CH). The principal peak $[M+H]^+$ was not found in the mass spectra however the fragment peak was found. MS (ESI): m/z 105.95 $[M+H]^+$.

N^1-Acryloyl-4-bromobenzohydrazide 60c: Yield = 70%; m.p. 256-259°C; ^{1}H NMR (DMSO-d_6): δ 10.58 (d, J = 1.46 Hz, 1H, CONH), 10.25 (d, J = 1.45 Hz, 1H, CONH), 7.81 (m, 2H, Ar-H), 7.74 (m, 2H, Ar-H), 6.34 (q, J = 17.3 Hz, 10.16 Hz, 1H, =CH), 6.23 (dd, J = 17.07 Hz, 2.10 Hz, 1H, =CH), 5.76 (dd, J = 10.21 Hz, 2.06 Hz, 1H, =CH). MS (ESI): m/z 290.97 $[M+Na]^+$, 268.99 $[M+H]^+$.

N^1-Acryloyl-4-chlorobenzohydrazide 60d: Yield = 73%; m.p. 233-235°C; ^{1}H NMR (DMSO-d_6): δ 10.58 (d, J = 1.45 Hz, 1H, CONH), 10.25 (d, J = 1.49 Hz, 1H, CONH), 7.90 (m, 2H, Ar-H), 7.6 (m, 2H, Ar-H), 6.34 (q, J = 17.15 Hz, 10.22 Hz, 1H, =CH), 6.23 (dd, J = 17.15 Hz, 2.09 Hz, 1H, =CH), 5.76 (dd, J = 10.18 Hz, 2.06 Hz, 1H, =CH). MS (ESI): m/z 247.02 $[M+Na]^+$, 225.04 $[M+H]^+$.

N^1-Acryloyl-2-chlorobenzohydrazide 60e: Yield = 67%; m.p. 165-167°C; ^{1}H NMR (DMSO-d_6): δ 10.41 (brs, 2H, CONH), 7.52 (m, 3H, Ar-H), 7.44 (m, 1H, Ar-H), 6.33 (q, J = 17.15 Hz, 10.07 Hz, 1H, =CH), 6.23 (dd, J = 17.13 Hz, 2.13 Hz, 1H, =CH), 5.76 (dd, J =10.09 Hz, 2.13 Hz, 1H, =CH). MS (ESI): m/z 262.85 $[M+K]^+$, 247.02 $[M+Na]^+$, 225.04 $[M+H]^+$.

N^1-Acryloyl-3-chlorobenzohydrazide 60f: Yield = 86%; m.p. 155-158°C; ^{1}H NMR (DMSO-d_6): δ 10.62 (brs, 1H, CONH), 10.28 (s, 1H, CONH),7.91 (t, 1H, Ar-H), 7.84 (m, 1H, Ar-H), 7.67 (m, 1H, Ar-H), 7.56 (t, 1H, Ar-H), 6.34 (q, J = 17.15 Hz, 10.20 Hz, 1H, =CH), 6.23 (dd, J = 17.16 Hz,

2.06 Hz, 1H, =CH), 5.76 (dd, J = 10.21 Hz, 2.06 Hz, 1H, =CH). MS (ESI): m/z 247.02 $[M+Na]^+$, 225.04 $[M+H]^+$.

N^1-Acryloyl-3,4-dichlorobenzohydrazide 60g: Yield = 78%; m.p. 172-175°C; ^{1}H NMR (DMSO-d_6): δ 10.71 (s, 1H, CONH), 10.32 (s, 1H, CONH), 8.11 (d, J = 1.91 Hz, 1H, Ar-H), 7.87 (dd, J = 8.39 Hz, 2.00 Hz, 1H, Ar-H), 7.81 (d, J = 8.37 Hz, 1H, Ar-H), 6.35 (q, J = 17.18 Hz, 10.24 Hz, 1H, =CH), 6.23 (dd, J = 17.16 Hz, 2.06 Hz, 1H, =CH), 5.76 (dd, J = 10.16 Hz, 2.04 Hz, 1H, =CH). MS (ESI): m/z 280.98 $[M+Na]^+$, 259.00 $[M+H]^+$.

N^1-Acryloyl-2,5-dichlorobenzohydrazide 60h: Yield = 69%; m.p. 207-210°C; ^{1}H NMR (DMSO-d_6): δ 10.60 (d, J = 1.93 Hz, 1H, CONH), 10.45 (d, J = 1.93 Hz, 1H, CONH), 7.60 (m, 2H, Ar-H), 7.53 (m, 1H, Ar-H), 6.33 (q, J = 17.11 Hz, 10.09 Hz, 1H, =CH), 6.24 (dd, J = 17.14 Hz, 2.14 Hz, 1H, =CH), 5.76 (dd, J = 10.06 Hz, 2.16 Hz, 1H, =CH). MS (ESI): m/z 259.00 $[M+H]^+$.

N^1-Acryloyl-3-methylbenzohydrazide 60i: Yield = 87%; m.p. 138-140°C; ^{1}H NMR (DMSO-d_6): δ 10.41 (d, J = 1.41 Hz, 1H, CONH), 10.20 (d, J = 1.77 Hz, 1H, CONH), 7.67 (m, 2H, Ar-H), 7.39 (m, 1H, Ar-H), 6.34 (q, J=17.13 Hz, 10.19 Hz, 1H, =CH), 6.22 (dd, J=17.12 Hz, 2.09 Hz, 1H, =CH), 5.75 (dd, J = 10.21 Hz, 2.09 Hz, 1H, =CH), 2.37 (s, 3H, CH_3). MS (ESI): m/z 227.08 $[M+Na]^+$, 205.09 $[M+H]^+$.

N^1-Acryloyl-2-methylbenzohydrazide 60j: Yield = 82%; m.p. 151-153°C; ^{1}H NMR (DMSO-d_6): δ 10.18 (s, 2H, CONH), 7.38 (m, 2H, Ar-H), 7.27 (m, 2H, Ar-H), 6.33 (q, J = 17.14 Hz, 10.08 Hz, 1H, =CH), 6.23 (dd, J = 17.15 Hz, 2.16 Hz, 1H, =CH), 5.75 (dd, J = 10.09 Hz, 2.16 Hz, 1H, =CH), 2.39 (s, 3H, CH_3). MS (ESI): m/z 227.08 $[M+Na]^+$, 205.09 $[M+H]^+$.

N^1-Acryloyl-4-methylbenzohydrazide 60k: Yield = 79%; m.p. 157-160°C; ^{1}H NMR (DMSO-d_6): δ 10.29 (d, J = 85.67, 2H, CONH), 7.79 (d, J = 8.17 Hz, 2H, Ar-H), 7.30 (d, J = 8.00 Hz, 2H, Ar-H), 6.34 (q, J = 17.16 Hz, 10.20 Hz, 1H, =CH), 6.21 (dd, J = 17.13 Hz, 2.07 Hz, 1H, =CH), 5.75 (dd, J = 10.16 Hz, 2.10 Hz, 1H, =CH), 2.37 (s, 3H, CH_3). MS (ESI): m/z 205.09 $[M+H]^+$.

N^1-Acryloyl-4-methoxylbenzohydrazide 60l: Yield = 85%; m.p. 165-166°C; ^{1}H NMR (DMSO-d_6): δ 10.24 (d, J = 83.79 Hz, 2H, CONH), 7.87 (dd, J = 8.85 Hz, J = 4.95, 2H, Ar-H), 7.03 (dd, J = 8.85, J = 5.04 Hz, 2H, Ar-H), 6.34 (q, J = 17.16 Hz, 10.22 Hz, 1H, =CH), 6.22 (dd, J = 17.13

Hz, 2.10 Hz, 1H, =CH), 5.74 (dd, J = 10.22 Hz, 2.05 Hz, 1H, =CH), 3.82 (s, 3H, OCH_3). MS (ESI): m/z 243.07 $[M+Na]^+$, 221.09 $[M+H]^+$.

N^1-Acryloyl-3,4-dimethoxylbenzohydrazide 60m: Yield = 75%; m.p. 163-165°C; ^{1}H NMR (DMSO-d_6): δ 10.25 (brs, 2H, CONH), 7.53 (dd, J = 8.38 Hz, 1H, Ar-H), 7.47 (d, J = 2.00 Hz, 1H, Ar-H), 7.06 (d, J = 8.53 Hz, 1H, Ar-H), 6.35 (q, J = 17.13 Hz, 10.24 Hz, 1H, =CH), 6.22 (dd, J = 17.12 Hz, 2.08 Hz, 1H, =CH), 5.75 (dd, J = 10.22 Hz, 2.07 Hz, 1H, =CH), 3.81 (d, J = 5.26 Hz, 6H, 2xOCH_3). MS (ESI): m/z 273.08 $[M+Na]^+$, 251.10 $[M+H]^+$.

3.3 Scheme for the synthesis of N^2-[3-(benzoylaminoamino)-1-oxopropyl]-N^1-benzoylhydrazine 61a

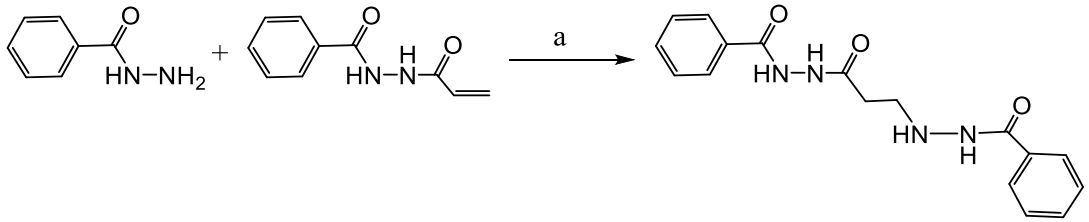

Benzohydrazide **59a** | N^1-phenyl-N^2-acryloyl hydrazine **60a** | N^2-[3-(benzoylaminoamino)-1-oxopropyl]-N^1-benzoylhydrazine **61a**

Scheme 3.2 : Scheme for the synthesis of N^2-[3-(benzoylaminoamino)-1-oxopropyl]-N^1-benzoylhydrazine **61a**.

The reaction conditions are as follows: a: ethanol, ~70-80°C, 24 h.

3.3.1 Synthesis of N^2-[3-(benzyoylaminoamino)-1-oxopropyl]-N^1-benzoylhydrazine 61a

Benzohydrazide (0.005 moles, 0.72 g) and N^1-acryloylbenzohydrazide (0.005 moles, 1 g) were dissolved in ethanol (0.17 moles, 10 ml) and refluxed for 24 h. The reaction was monitored using chloroform: methanol (9.5:0.5) and the solvent was evaporated *in vacuo* after the completion of the reaction. The residues were then recrystallised from 95% ethanol.

Yield = 69%; m.p. 193-195°C; ^{1}H NMR (DMSO-d_6): δ 10.36 (s, 1H, CONH), 10.05 (d, J = 6.23 Hz, 1H, CONH), 9.99 (s, 1H, CONH), 7.85 (q, J = 17.95 Hz, 7.45 Hz, 4H-Ar), 7.50 (m, 6H, Ar-H), 5.39 (q, 1H, NH), 3.06 (q, 2H, CH_2), 2.42 (t, 2H, CH_2). MS (ESI): m/z 327.14 $[M+H]^+$.

3.4 General scheme for the synthesis of the N^1-acylbenzohydrazide derivatives 62a-b

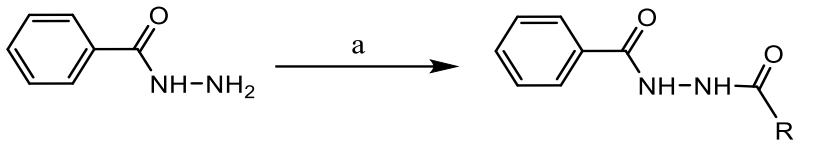

Benzohydrazide **59a** — N^1-aroyl-N^2-acylhydrazides **62a-b**

Scheme 3.3 : General scheme for the synthesis of N^1-aroyl-N^2-acylhydrazines **62a-b**.

The reaction conditions are as follows: a: acetyl anhydride/propionic anhydride, RT, 15 min. **62a:** R = CH_3 and **62b**: R = CH_2CH_3.

3.4.1 Synthesis of N^1-acetylbenzohydrazide 62a

Acetic anhydride (7.34 mmoles, 0.70 ml) was added dropwise to benzohydrazide (7.34 mmoles, 1g) dissolved in ethanol (85.63 mmoles, 5 ml) and stirred at room temperature for 15 min. The mixture was diluted with diethyl ether, filtered and rinsed with diethyl ether. The residues were then recrystallised from 95% ethanol.

Yield = 83% ; m.p.171-172°C (lit. m.p. 174°C);[116] ^{1}H NMR (DMSO-d_6): δ 10.28 (s, 1H, CONH), 9.88 (s, 1H, CONH), 7.86 (m, 2H, Ar-H), 7.58 (m, 1H, Ar-H), 7.50 (m, 2H, Ar-H), 1.91 (s, 3H, CH_3). ^{13}C NMR (DMSO-d_6): 168.84, 165.74, 132.60, 131.96, 128.60, 127.54, 20.72. MS (ESI): m/z 217.04 $[M+K]^+$, 179.07 $[M+H]^+$.

3.4.2 Synthesis of N^1-propionylbenzohydrazide 62b

Propionic anhydride (7.34 mmoles, 0.95 ml) was added dropwise to benzohydrazide (7.34 mmoles, 1g) dissolved in ethanol (85.63 mmoles, 5 ml) and stirred at room temperature for 15 min. The mixture was diluted with diethyl ether, filtered and rinsed with diethyl ether. The residues were then recrystallised from 95% ethanol.

Yield = 87%; m.p.106-107°C (lit. m.p.110°C);[116] ^{1}H NMR (DMSO-d_6): δ 10.29 (s, 1H, CONH), 9.84 (s, 1H, CONH), 7.86 (m, 2H, Ar-H), 7.58 (m, 1H, Ar-H), 7.50 (t, 2H, Ar-H), 2.19 (q, 2H, CH_2), 1.06 (t, 3H, CH_3). ^{13}C NMR (DMSO-d_6): 172.68, 165.77, 132.67, 131.92, 128.46, 127.54, 26.70, 9.80. MS (ESI): m/z 215.07 $[M+Na]^+$, 193.09 $[M+H]^+$.

3.5 General scheme for the synthesis of 3,5-bis(arylidene)-4-piperidone derivatives 63a-f

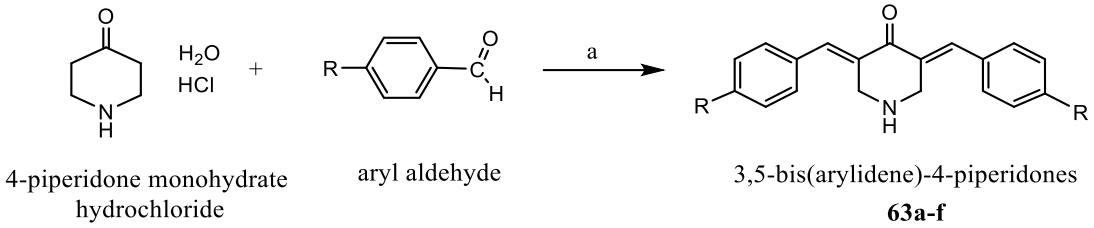

Scheme 3.4 : General scheme for the synthesis of 3,5-bis(arylidene)-4-piperidones **63a-f**.

The following reaction conditions were used: a: HCl/CH_3COOH, RT, followed by treatment with K_2CO_3 (25% w/v). **63a:** R = H, **63b:** R = Cl, **63c:** R = F, **63d:** R = NO_2, **63e:** R = OCH_3, **63f:** R = CH_3.

3.5.1 Synthesis of 3,5-bis(benzylidene)-4-piperidone derivatives 63a-f

The synthesis of **63a-f** was carried out as previously described in the literature.[64] Briefly, the appropriate aryl aldehyde (26.71 mmoles, 2.72 ml) was added to a suspension of 4-piperidone hydrochloride monohydrate (13.03 mmoles, 2 g) in acetic acid (35 ml) and dry hydrogen chloride was passed through it for 0.5 h until a clear solution was obtained. It was stirred at room temperature for 24 h. The precipitate was collected, added to a mixture of saturated aqueous potassium carbonate solution (25% w/v, 25 ml) and acetone (25 ml) and stirred for 0.5 h. The free base obtained was washed with water (50 ml), dried and further used without purification except **63a** was recrystallized from 95% ethanol and used for biological experiments.

3,5-Bis(benzylidene)-4-piperidone 63a: Yield = 86%; m.p. 175-177°C (lit. m.p.177-178°C);[64] ^{1}H NMR (DMSO-d_6): δ 7.82 (brs, 2H, =CH), 7.40 (m, 10H, Ar-H), 4.16 (d, J= 1.73 Hz, 4H, piperidyl H). The NH peak was not observed.

3,5-Bis(4-Chlorobenzylidene)-4-piperidone 63b: Crude yield = 64%; ^{1}H NMR (DMSO-d_6): δ 7.55 (brs, 2H, =CH), 7.52 (s, 8H, Ar-H), 3.96 (d, J = 1.33, 4H, piperidyl H). The NH peak was not observed.

3,5-Bis(4-Fluorobenzylidene)-4-piperidone 63c: Crude yield = 40%; ^{1}H NMR (DMSO-d_6): δ 7.56 {d, J = 8.94 Hz, 6H (4H, Ar-H; 2H, =CH)}, 7.30 (m, 4H, Ar-H), 3.96 (s, 4H, piperidyl H). The NH peak was not observed.

3,5-Bis(4-Nitrobenzylidene)-4-piperidone 63d: Crude yield = 94%; ^{1}H NMR (DMSO-d_6): δ 8.28 (d, J = 7.48 Hz, 4H, Ar-H), 7.76 (d, J = 7.57 Hz, 4H, Ar-H), 7.66 (s, 2H, =CH), 4.02 (s, 4H, piperidyl H). The NH peak was not observed.

3,5-Bis(4-Methyoxybenzylidene)-4-piperidone 63e: Crude yield = 73%; ^{1}H NMR (DMSO-d_6): δ 7.53 (s, 2H, =CH), 7.44 (s, 4H, Ar-H), 7.02 (s, 4H, Ar-H), 3.96 (s, 4H, piperidyl H), 3.8 (s, 6H, 2xOCH_3). The NH peak was not observed.

3,5-Bis(4-Methylbenzylidene)-4-piperidone 63f: Crude yield = 72%; ^{1}H NMR (DMSO-d_6): δ 7.66 (brs, 2H, =CH), 7.40 (d, 4H, J = 7.85 Hz, Ar-H), 7.30 (d, 4H, J = 7.77 Hz, Ar-H), 4.15 (s, 4H, piperidyl H), 2.35 (s, 3H, CH_3). The NH peak was not observed.

3.6 Scheme for the attempted synthesis of 3,5-bis(benzylidene)-1-[3-(arylcarbonylaminoamino)-3-oxo-1-propyl]-4-piperidone 64a

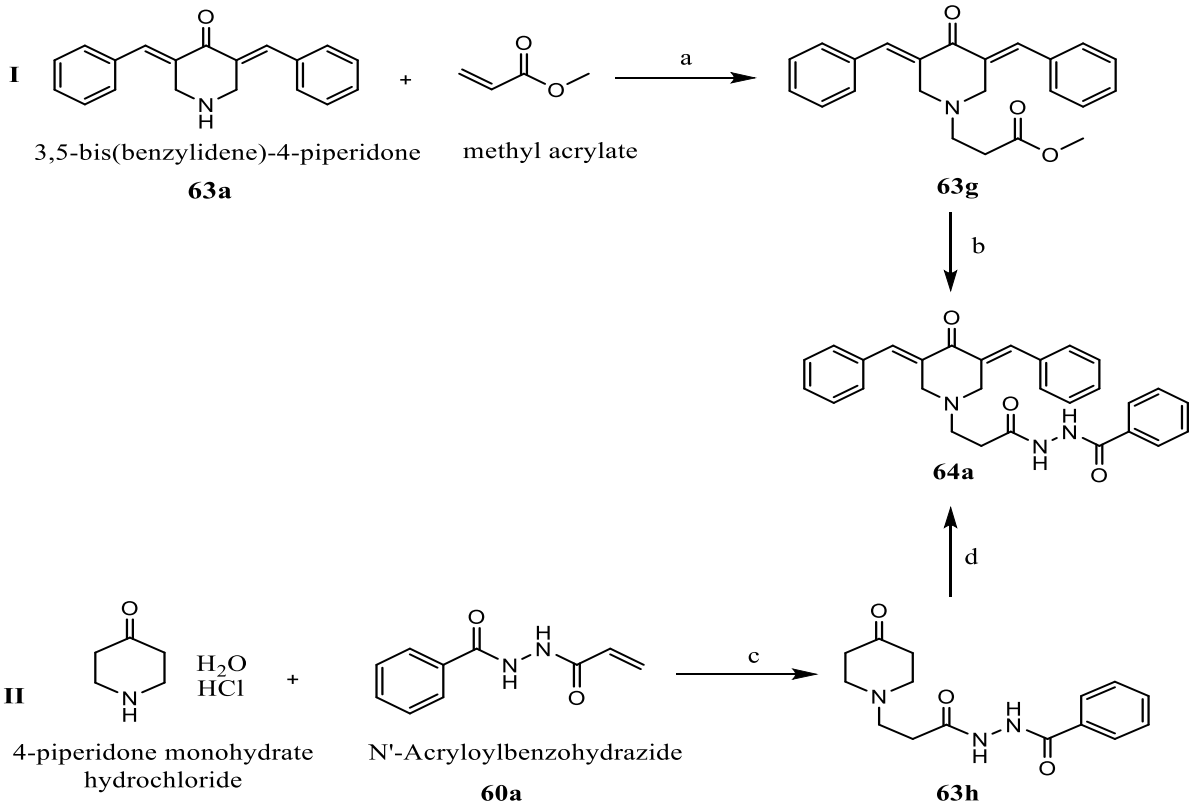

Scheme 3.5 : Scheme for the attempted synthesis of 3,5-bis(benzylidene)-1-[3-(arylcarbonylaminoamino)-3-oxo-1-propyl]-4-piperidone **64a**.

The reaction conditions are as follows: a: dichloromethane (CH_2Cl_2,) ~80°C, 24 h; b: ethanol, benzohydrazide, ~80°C, 24 h; c: triethylamine (TEA), CH_2Cl_2, RT, 24 h; d: benzaldehyde, HCl/CH_3COOH, RT, 24 h.

3.6.1 Synthesis of methyl-3-[3,5-bis(benzylidene)-4-oxo-1-piperidinyl]-propanoate 63g

Compound **63a** (5.45 mmoles, 1.5 g) was dissolved in chloroform and methanol (40 ml: 10 ml). Methyl acrylate (5.45 mmoles, 0.58 ml + 10% excess) was added dropwise to this solution and was stirred at 80°C for 17 h. Chloroform and methanol (9.5:0.5) was used as the TLC solvent system to monitor the reaction. The solvent was evaporated after completion of the reaction and yellow residues were obtained.

Yield = 60%; ^{1}H NMR ($CDCl_3$): δ 7.83 (s, 2H, =CH), 7.41(m, 10H, Ar-H), 3.87 (d, J = 1.51 Hz, 4H, piperidyl H), 3.61 (s, 3H, OCH_3), 2.90 (t, J = 7.26 Hz, 14.52 Hz, 2H, CH_2), 2.46 (t, J = 7.24 Hz, 14.48 Hz, 2H, CH_2).

3.6.2 Synthesis of N^2-benzoyl-N^1-3-[4-oxo-1-piperidinyl]-1-oxopropyl-hydrazine 63h

The 4-piperidone monohydrate hydrochloride (7.89 mmoles, 1.21 g) was condensed with N^1-acryloyl benzohydrazide (5.25 mmoles, 1 g) in the presence of triethylamine (36.4 mmoles, 3.64 g) in dichloromethane (10 ml) at room temperature for 24 h. Chloroform and methanol (9.5:0.5) were used as solvent to monitor the completion of the reaction using TLC. The solvent was evaporated *in vacuo* and the product was obtained.

Yield = 53%; ^{1}H NMR (DMSO-d_6): δ 7.84 (m, 2H, Ar-H), 7.56 (m, 1H, Ar-H), 7.49 (m, 2H, Ar-H), 2.93 (t, J = 6.06 Hz, 12.11 Hz, 4H, piperidyl H), 2.73 (t, J = 5.75 Hz, J = 11.51 Hz, 2H, CH_2), 2.35 (t, J = 6.14 Hz, 12.18 Hz, 4H, piperidyl H), 2.23 (t, J = 6.11 Hz, J = 12.21 Hz, 2H, CH_2).The NH peak was not observed.

The attempt was made to synthesize compound **64a** from **63g** and **63h** intermediates following the reaction conditions as indicated in scheme **3.5**. However, despite many efforts, the synthesis of 3,5-bis(benzylidene)-1-[3-(arylcarbonylaminoamino)-3-oxo-1-propyl]-4-piperidone **64a** did not take place. Hence, compound **64a** was synthesized by alternative scheme **3.6**.

3.7 General scheme for the synthesis of 3,5-bis(benzylidene)-1-[3-(arylcarbonylaminoamino)-3-oxo-1-propyl]-4-piperidone derivatives 64a-g

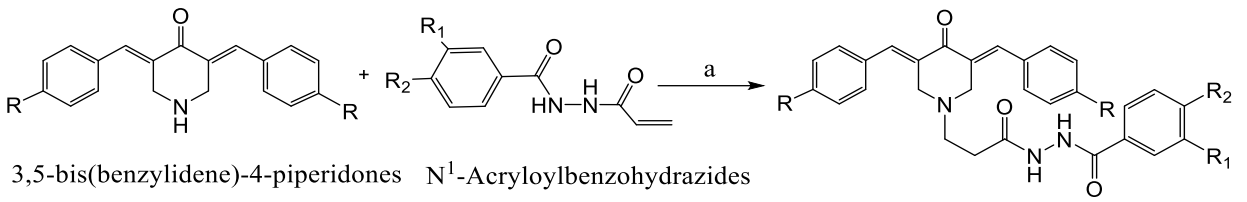

3,5-bis(benzylidene)-4-piperidones **63**

N^1-Acryloylbenzohydrazides **60**

3,5-bis(benzylidene)-1-[3-(arylcarbonylaminoamino)-3-oxo-1-propyl]-4-piperidones **64a-g**

Scheme 3.6 : General scheme for the synthesis of 3,5-bis(benzylidene)-1-[3-(arylcarbonylaminoamino)-3-oxo-1-propyl]-4-piperidones **64a-g**.

The following reaction conditions were used: a: Et_3N, CH_2Cl_2: methanol (2:1), ~80°C for 24 h.

64a: R = H, $R_1 = R_2$ = H, **64b:** R = H, $R_1 = R_2 = OCH_3$, **64c:** R = Cl, $R_1 = R_2 = OCH_3$, **64d:** R = NO_2, $R_1 = R_2 = OCH_3$, **64e:** R = F, $R_1 = R_2 = OCH_3$, **64f:** R = OCH_3, $R_1 = R_2 = OCH_3$, **64g:** R = CH_3, $R_1 = R_2 = OCH_3$.

3.7.1 Synthesis of 3,5-bis(benzylidene)-1-[3-(arylcarbonylaminoamino)-3-oxo-1-propyl]-4-piperidones 64a-g

3,5-Bis(benzylidene)-4-piperidone **63a** (0.0036 moles, 1 g) was condensed with N^1-acryloylbenzohydrazide **60a** (0.011 moles, 2.071 g) in the presence of triethylamine (0.018 moles, 1.84 g) in dichloromethane (10 ml) and methanol (5 ml) at ~80°C for 24 h. Chloroform and methanol (9.5:0.5) were used as the solvent to monitor the completion of the reaction using TLC. The solvent was evaporated *in vacuo* and the product was recrystallized from 95% ethanol.

3,5-Bis(benzylidene)-1-[3-(phenylcarbonylaminoamino)-3-oxo-1-propyl]-4-piperidone 64a

Yield = 81%; m.p. 154-156°C; ^{1}H NMR (DMSO-d_6): δ 10.34 (s, 1H, CONH), 9.92 (s, 1H, CONH), 7.83 (d, J = 7.82, 2H, Ar-H), 7.62 (s, 2H, =CH), 7.55 (d, J = 8.45 Hz, 5H, Ar-H), 7.48 (dd, J = 7.79, 5H, Ar-H), 7.44 (m, 3H, Ar-H), 3.88 (s, 4H, piperidyl H), 2.87 (t, J = 7.02 Hz, J = 14.05 Hz, 2H, CH_2), 2.39 (t, J = 7.03 Hz, J = 14.07 Hz, 2H, CH_2). MS (ESI): m/z 466.21 $[M+H]^+$.

3,5-Bis(benzylidene)-1-[3-(3,4-dimethoxylphenylcarbonylaminoamino)-3-oxo-1-propyl]-4-piperidone 64b

Yield = 86%; m.p. 151-154°C; ^{1}H NMR (DMSO-d_6): δ 10.20 (s, 1H, CONH), 9.86 (s, 1H, CONH), 7.62 (s, 2H, =CH), 7.55 (d, J = 7.31 Hz, 4H, Ar-H), 7.5 (m, 6H, Ar-H), 7.43 (m, 2H, Ar-H), 7.02 (d, J = 8.51 Hz, 1H, Ar-H), 3.88 (s, 4H, piperidyl H), 3.79 (d, J = 13.42 Hz, 6H, 2xOCH_3), 2.87 (t, J = 6.85 Hz, J = 13.70 Hz, 2H, CH_2), 2.39 (t, J = 6.94 Hz, J = 13.91 Hz, 2H, CH_2). MS (ESI): m/z 526.23 $[M+H]^+$.

3,5-Bis(4-chlorobenzylidene)-1-[3-(3,4-dimethoxyphenylcarbonylaminoamino)-3-oxo-1-propyl]-4-piperidone 64c

Yield = 76%; m.p. 200-202°C; ^{1}H NMR (DMSO-d_6): δ 10.21 (s, 1H, CONH), 9.86 (s, 1H, CONH), 7.59 (s, 2H, =CH), 7.55 (q, J = 21.20 Hz, 8H, Ar-H), 7.48 (dd, J = 8.47, 1H, Ar-H), 7.43 (d, J = 1.86 Hz, 1H, Ar-H), 7.03 (d, J = 8.52 Hz, 1H, Ar-H), 3.85 (s, 4H, piperidyl H), 3.79 (d, J = 12.07 Hz, 6H, 2xOCH_3), 2.87 (t, J = 6.88 Hz, 2H, CH_2), 2.34 (t, J = 6.83 Hz, 2H, CH_2). MS (ESI): m/z 594.15, 595.15 $[M+H]^+$, 596.15 $[M+2H]^+$.

3,5-Bis(4-fluorobenzylidene)-1-[3-(3,4-dimethoxyphenylcarbonylaminoamino)-3-oxo-1-propyl]-4-piperidone 64d

Yield = 80%; m.p.198-200°C; ^{1}H NMR (DMSO-d_6): δ 10.21 (s, 1H, CONH), 9.86 (s, 1H, CONH), {m, 6H (4H, Ar-H; 2H, =CH)}, 7.5 (dd, J = 8.42 Hz, 1H, Ar-H), 7.43 (d, J = 1.85 Hz, 1H, Ar-H), 7.31 (t, J = 8.81 Hz, 4H, Ar-H), 7.03 (d, J = 8.56 Hz, 1H, Ar-H), 3.85 (s, 4H, piperidyl H), 3.79 (d, J = 12.47 Hz, 6H, 2xOCH_3), 2.87 (t, J = 6.94 Hz, 2H, CH_2), 2.4 (t, J = 6.91 Hz, 2H, CH_2). MS (ESI): m/z 562.21 $[M+H]^+$.

3,5-Bis(4-nitrobenzylidene)-1-[3-(3,4-dimethoxyphenylcarbonylaminoamino)-3-oxo-1-propyl]-4-piperidone 64e

Yield = 71%; m.p. 153-158°C; ^{1}H NMR (DMSO-d_6): δ 10.22 (s, 1H, CONH), 9.87 (s, 1H, CONH), 8.29 (d, J = 8.76 Hz, 4H, Ar-H), 7.82 (d, J = 8.78 Hz, 2H, Ar-H), 7.77 (d, J = 8.78 Hz, 2H, Ar-H), 7.69 (d, J = 20.10 Hz, 2H, =CH), 7.48 (dd, J = 8.45 Hz, 10.38 Hz, 1H, Ar-H), 7.43 (d, J = 1.84 Hz, 1H, Ar-H), 7.02 (d, J = 8.55 Hz, 1H, Ar-H), 4.02 (s, 2H, piperidyl H), 3.92 (s, 2H, piperidyl H), 3.79 (d, J = 13.91 Hz, 6H, 2xOCH_3), 2.88 (t, J = 6.78 Hz, 13.56 Hz, 2H, CH_2), 2.39 (t, J = 6.78 Hz, 13.58 Hz, 2H, CH_2). MS (ESI): m/z 616.20 $[M+H]^+$.

3,5-Bis(4-methoxybenzylidene)-1-[3-(3,4-dimethoxyphenylcarbonylaminoamino)-3-oxo-1-propyl]-4-piperidone 64f

Yield = 75%; m.p. 175-178°C; ^{1}H NMR (DMSO-d_6): δ 10.21 (s, 1H, CONH), 9.88 (s, 1H, CONH), 7.56 (s, 2H, =CH), 7.50 (d, J = 8.88 Hz, 4H, Ar-H), 7.45 (m, 2H, Ar-H), 7.036 (m, 4H, Ar-H), 7.02 (s, 1H, Ar-H), 3.84 (s, 3H, OCH_3), 3.81 (s, 6H, 2xOCH_3), 3.80 (s, 4H, piperidyl H), 3.77 (s, 3H, OCH_3), 2.88 (t, J = 6.9 Hz, 13.80 Hz, 2H, CH_2), 2.41 (t, J = 6.88 Hz, 13.76 Hz, 2H, CH_2). MS (ESI): m/z 586.25 $[M+H]^+$.

3,5-Bis(4-methylbenzylidene)-1-[3-(3,4-dimethoxyphenylcarbonylaminoamino)-3-oxo-1-propyl]-4-piperidone 64g

Yield = 82%; m.p. 190-192°C; ^{1}H NMR (DMSO-d_6): δ 10.20 (s, 1H, CONH), 9.86 (s, 1H, CONH), 7.58 (s, 2H, =CH), 7.48 (dd, J = 8.37 Hz, 1H, Ar-H), 7.43 (m, 5H, Ar-H), 7.3 (d, J = 8.09 Hz, 4H, Ar-H), 7.02 (d, J = 8.54 Hz, 1H, Ar-H), 3.85 (s, 4H, piperidyl H), 3.79 (d, J = 13.07 Hz, 6H, 2xOCH_3), 2.86 (t, J = 7.04 Hz, 2H, CH_2), 2.38 (t, J = 7.14 Hz, 2H, CH_2), 2.35 (s, 6H, CH_3). MS (ESI): m/z 554.26 $[M+H]^+$.

CHAPTER 4 : BIOLOGICAL EVALUATIONS

4.1 Materials and Reagents

The human colon cancer cell line HCT 116 and human CRL-1790 normal colon cell line were purchased from the ATCC whereas the breast cancer cell lines MCF-7 and MDA-MB-231 were obtained from the Saskatchewan Cancer Agency. All the media and reagents were purchased from HyClone unless specified otherwise. HCT 116 cells were cultured in McCoy's 5A media, whereas minimum essential media (EMEM) obtained from the ATCC was used to culture CRL-1790 cells. For MCF-7 and MDA-MB-231 cells, DMEM media with a high concentration of glucose was used. Each of the culture media was supplemented with 10% fetal bovine serum (FBS) and 1% penicillin-streptomycin antibiotics. All the cell lines were grown in an atmosphere of 95% O_2 and 5% CO_2 at 37°C in an incubator.

All the chemicals were purchased from Sigma unless specified otherwise. Dimethyl sulfoxide (DMSO), 50% w/v trichloroacetic acid (TCA), 0.4% w/v sulforhodamine B (SRB) in 1% v/v acetic acid, 1% v/v acetic acid, 10 mM tris[hydroxymethyl]aminomethane buffer (TRIS base). 2′,7′-dichlorofluorescin diacetate (DCF-DA) was used for the ROS determination. The tetramethylrhodamine ethyl ester (TMRE) dye was purchased from Cayman Chemical which is used in the mitochondrial membrane potential study.

4.2 Antiproliferation assay using the sulforhodamine B dye

This assay was performed to determine the cytotoxicity of various compounds towards neoplastic (HCT 116, MCF-7 and MDA-MB-231) cells and non-malignant colon CRL-1790 cells. The SRB dye was used for quantitative measurement of cell numbers after treatment with the compounds. This assay was performed as previously described in the literature.[117] In brief, 5000 cells were plated per 100 µL of media at a concentration of 5 x 10^4 cells/mL in each well of a 96-well plate and kept in an incubator at 37°C and 5 % CO_2 for 24 h. On the next day, the control plate Tz, which is without the addition of any compound was treated with 25 µL of 50% w/v trichloroacetic acid (TCA) and incubated at 4°C for 1 h and the plate was washed with water four times and allowed to dry at room temperature. After 24 h, in the test plate Tc, the cytotoxic agents were added in different concentrations and incubated for 48 h. Each plate consisted of positive controls (5-FU and melphalan) and a negative control (only DMSO). After 48 h, 50 µL of 50% w/v trichloroacetic acid (TCA) was added to fix the cells which were incubated at 4°C for 1 h. After 1

h, the plates were washed with water four times and allowed to dry at room temperature for 24 h. 100 µL of sulforhodamine B solution was added to each well and stained at room temperature for 15 min then washed with 1% acetic acid about 4-5 times and kept at room temperature to dry for 24 h. The SRB dye was solubilized by the addition of 200 µL of 10 mM Trizma base solution to each well and the plate was kept in a microplate shaker for 5 min (room temperature 25 °C, 100 rpm) and the absorbance measured at 515 nm using a microplate reader. The optical density (OD) of SRB in each well is directly proportional to the cell number and therefore cell growth can be calculated using the following formula:

$$\%\ Cell\ growth = \frac{OD_{test} - OD_{control}}{OD_{DMSO} - OD_{control}}$$

where, OD_{test} is the optical density of the test well after 48 h drug exposure.

OD_{DMSO} is the optical density of the negative control (DMSO).

$OD_{control}$ is the optical density of untreated well at day 0.

Each experiment was carried out in triplicate on three different occasions. Initial screening of the compounds towards HCT 116, MCF-7 and MDA-MB 231 cell lines was carried out at two different concentrations of 100 µM and 10 µM such that the final concentration of DMSO in each well is less than 1%. For IC_{50} determinations, the concentration ranged from 100 µM to 0.001 µM.

In another assay performed by our collaborators in Japan, compounds **60a-m**, **61a** and **62a-b** were also evaluated against HSC-2, HSC-3 and HSC-4 human squamous cell carcinomas as well as human promyelocytic leukemia HL-60 cells in addition to human non-malignant human gingival fibroblasts (HGF), human pulp cells (HPC) and human periodontal ligament fibroblasts (HPLF). The assay was undertaken using a literature method[118] except the incubation time was 48 h. Different concentrations (maximum of 400 µM) of each compound were added to the cultured cells and incubated for 48 h at 37°C. The cytotoxic concentration (CC_{50}) values were determined from dose-response curves.

Another cytotoxicity study was conducted by our collaborators in El Paso wherein compounds **60a-m**, **61a** and **62a-b** were evaluated against various leukemic cells (Ramos, NALM-60, CEM, HL-60, JURKAT and RAJI) and normal cells (Hs27 and MCF10A) as described previously in the literature.[78,119,120] Briefly, solution of compounds dissolved in DMSO were added to different

malignant and non-malignant cells grown in either DMEM or RPMI media, followed by incubation at 37℃ for 24 h. The average cytotoxic potencies of three independent experiments, expressed as the concentration required for 50% of cell death (CC_{50} values) were obtained.

4.3 Combinatorial approach using HCT 116 cells

In this experiment, N^1-acryloyl-3,4-dimethoxylbenzohydrazide **60m** was used as a potential chemosensitizer of HCT 116 cells to 3,5-bis(benzylidene)-4-piperidone **63a**. 5-FU (3.0 µM) was used as a positive control and only DMSO was used as a negative control. In this study, approximately 1.2 x 10^6 cells were cultured in T_{75} flasks and kept in an incubator at 37°C and 5 % CO_2 for 24 h. Different solutions were prepared in DMSO such that the final concentration of DMSO in each flask is less than 1%. These solutions consisted of **60m** (5 µM, 10 µM and 15 µM), 5-FU (3.0 µM), **63a** (0.1 µM, 0.2 µM and 0.4 µM) in each tube along with 7.5 ml media. After 24 h, the media was aspirated and fresh media containing different cytotoxic agents with varying concentrations were added to each of the T_{75} flasks and kept in an incubator for 48 h. In tandem with these compounds, other T_{75} flasks were treated with **60m** (5 µM, 10 µM and 15 µM) and kept in an incubator for next 24 h. After 24 h, each of these flasks were treated with different concentrations of **63a** (0.1 µM, 0.2 µM and 0.4 µM) and 5-FU (3.0 µM) and kept in an incubator for the next 24 h. The following day, the media was aspirated and trypsin was added to each flask and kept in an incubator for one minute. Fresh media was added to each flask which was centrifuged at 1000 rpm for 5 min at 4°C. Following centrifugation, the supernatant was removed and fresh media was added to the cell pellet, mixed thoroughly and then a solution was prepared consisting of 50 µL of cells in the media and 50 µL of trypan blue and live cells were counted using an automated cell counter.

Simultaneously, a cytotoxic assay was performed using SRB dye, as per the procedure mentioned previously. Herein, the addition of compounds at different times is the same as that carried out in the T_{75} flasks and % cell growth was calculated by measuring the absorbance at 515 nm using a microplate reader.

4.4 Studies on mechanisms of action

4.4.1 Mitochondrial membrane potential ($\Delta\psi_m$)

The main intention to conduct this assay was to measure the effect of cytotoxic agents (**60m**, **64a**, **64e** and **64g**) on mitochondrial membrane potential. In this study, TMRE (tetramethylrhodamine ethyl ester), a fluorescent lipophilic cationic dye, was used to monitor changes in $\Delta\psi_m$. HCT 116 cells ($5x10^3$ cells/well) were cultured in 96 well optical-bottom plates and kept in an incubator at 37 °C and 5 % CO_2 for 24 h for proper adherence. Compounds were dissolved in DMSO at a concentration of 10 mM while in the case of 5-FU, a concentration of 40 mM was used. Further dilutions were made in the media such that the final concentration does not exceed more than 1% DMSO. After 24 h, the cells were treated with the IC_{50} concentrations of **60m**, **64a**, **64e**, **64g** and 5-FU and incubated for 48 h. CCCP and 2,4-DNP were used as the positive controls with a final concentration of 50 µM. After 48 h, 20 µL of CCCP and 2,4-DNP were added to the cell plate and incubated for 30 min. The TMRE dye was prepared in DMSO as a stock solution at a concentration of 25 mM and the final concentration added to the cell plate was 500 nM. 20 µL of a solution of the TMRE dye was added to each well and the plate was incubated for another 30 min at 37°C and in an atmosphere of 5 % CO_2.

After incubation, the cells were centrifuged at 400 x g for 5 min at room temperature and then the media was removed. 200 µL of phosphate buffered saline (PBS) was added to each well and again the cells were centrifuged. The supernatant was aspirated and this process was repeated once for the complete removal of excess of the dye. 100 µL of phosphate buffered saline (PBS) was added to each well and the fluorescence was measured at excitation and emission wavelengths at 530 nm and 590 nm respectively. Fluorescence was measured using a BioTek plate reader. After the reading were taken, 25 µL of 50% w/v TCA was added to each well and kept in a refrigerator for 1 h. The plates were washed with water four times and allowed to air dry. Next day, 100 µL of 0.4 % SRB solution was added to each well, incubated at room temperature for 10 min and washed four times with 1% acetic acid and allowed to air dry for a day. 200 µL of 10 mM Trizma base solution was added to each well and the absorbance was noted using a BioTek plate reader at 515 nm.

4.4.2 Evaluation of reactive oxygen species (ROS) levels

The main purpose of this assay was to evaluate the effect of cytotoxic agents (**60m**, **64a**, **64e** and **64g**) on ROS levels. In this study, the 2′,7′-dichlorofluorescein diacetate (DCF-DA) dye was used to measure reactive oxygen species activity within the cells. HCT 116 cells were cultured in a 96 well optical-bottom plates with a seeding density of 5,000 cells/well and kept in an incubator at 37°C and 5 % CO_2 for 24 h for the proper attachment of the cells. Compounds were dissolved in DMSO using a concentration of 10 mM and 5-FU at 40 mM. Further dilutions were made in the media such that the final concentration does not exceed more than 1% DMSO. After 24 h, the cells were treated with the IC_{50} concentrations of **60m**, **64a**, **64e**, **64g** and 5-FU and incubated for 48 h. Hydrogen peroxide was used as a positive control with a final concentration of 10 µM. After 48 h, 30 µL of H_2O_2 was added and incubated at 37°C and 5 % CO_2 for 30 min. Then 60 µL of the DCF-DA dye was added to each well with a final concentration of 30 µM and kept in an incubator for 30 min at 37°C and 5 % CO_2. After incubation, the cells were centrifuged at 400 x g at room temperature for 5 min and the media was removed. The cells were then washed once with 100 µL of PBS and the supernatant was aspirated. Finally, 100 µL of PBS was added to each well and the fluorescence was measured at the excited and emission wavelengths of 485 nm and 530 nm, respectively. A BioTek spectrometer was used to measure the fluorescence intensity.

4.5 Statistical analysis

All the data points are represented as the mean ± SD wherein the standard deviation was used for replicates of three independent experiments. Statistical analysis was carried out using either one-way or two-way ANOVA. One-way ANOVA with Dunnett's multiple comparison post-hoc analysis was used to determine the significance between the control and test groups. For the combination approach experiments, a two-way ANOVA was carried out. A p value below 0.05 was considered to be significant.

CHAPTER 5 : RESULTS

5.1 Assessment of cytotoxicity using sulforhodamine B (SRB)

The purpose of this experiment is to determine the potency of cytotoxic agents towards carcinoma cells such as HCT 116, MCF-7 and MDA-MB-231 neoplasms and against normal cells such as colon CRL-1790 cells. This assay is based on the use of the SRB dye that binds under mild acidic conditions to the proteins present in the trichloroacetic acid-fixed cells in the plate and the dye is extracted and solubilized with Trizma base under mild basic conditions to measure the cell density quantitatively. The IC_{50} values were obtained by plotting a graph of the log concentrations against the percentage inhibition using Graph Pad Prism software. A sigmoidal graph was obtained and the IC_{50} values were determined at a concentration when there is 50% of growth inhibition. Three independent experiments were conducted with three replicates in each experiment.

5.1.1 Antiproliferation assay using HCT 116 colon cancer cells and CRL-1790 normal colon cells

The initial screening of the compounds **60a-m**, **61a** and **62a-b** was carried out using concentrations of 100 µM and 10 µM in HCT 116 cells. The results in Table 5.1 reveal that **60m** showed more than 47% inhibition at 10 µM concentration and therefore it's IC_{50} value was determined using different concentrations ranging from 100 µM to 0.01 µM. 5-FU and melphalan were used as the positive controls in each experiment and their IC_{50} values were measured using concentrations ranging from 0.01 µM to 100 µM. The IC_{50} value of **63a** was also obtained which is later used in a combinational approach with **60m**. To study the structure-activity relationships, the IC_{50} values of **59a**, **59m**, **60a** and **62b** were determined. For compounds **64a-g**, the cytotoxic assay was performed using a concentration range of 0.01 µM to 100 µM.

Based on the calculated IC_{50} values as seen in Table 5.2, the benzohydrazides **59a** and 3,4-dimethoxybenzohydrazide **59m** did not show any noticeable toxicity against HCT 116 cancer colon cells or CRL-1790 normal colon cells. N^1-Acryloylbenzohydrazide **60a** and N^1-acryloyl-3,4-dimethoxybenzohydrazide **60m** showed some potency against HCT 116 cells but had little or no effect on CRL-1790 cells. The saturated compound **62b** did not show any marked toxicity against both the cell lines.

Compound **63a** showed remarkable potency compared to the standard drugs 5-FU and melphalan. The results from Table 5.3, reveal that all of the compounds **64a-g** are potent cytotoxins against HCT 116 cells and showed inhibition against normal CRL-1790 cells. In particular, **64e** has a IC_{50} value of 0.283 µM towards HCT 116 cells which is approximately 15 times more potent than the standard drug 5-FU.

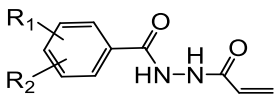

60a-m

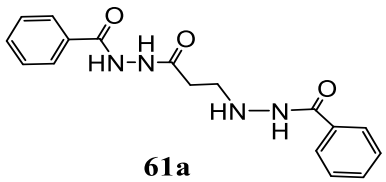

61a

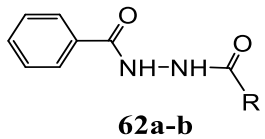

62a-b

Table 5.1 : Screening of **60a-m**, **61a**, **62a-b** against HCT 116 cells

Compound	Substituents	% inhibition at 100 µM	% inhibition at 10 µM
60a	H	94.13 ± 1.44	10.53 ± 1.70
60b	4-F	60.66 ± 3.22	-2.35 ± 2.24
60c	4-Br	87.90 ± 0.91	-3.28 ± 1.50
60d	4-Cl	82.31 ± 0.80	-5.05 ± 2.36
60e	2-Cl	75.73 ± 1.65	4.30 ± 1.38
60f	3-Cl	95.71 ± 1.71	13.45 ± 1.79
60g	3,4-Cl_2	>100	6.72 ± 1.97
60h	2,5-Cl_2	87.67 ± 1.62	7.12 ± 1.51
60i	3-CH_3	93.89 ± 3.35	15.43 ± 2.13
60j	2-CH_3	62.05 ± 2.48	10.36 ± 1.61
60k	4-CH_3	>100	11.52 ± 2.99
60l	4-OCH_3	85.07 ± 3.28	8.62 ± 2.79
60m	3,4-$(OCH_3)_2$	97.94 ± 1.92	46.89 ± 2.55
61a	--	96.99 ± 1.86	18.56 ± 3.98
62a	CH_3	13.64 ± 3.03	-4.89 ± 2.52
62b	CH_2CH_3	9.35 ± 2.53	-10.47 ± 2.93
5-FU	--	94.12 ± 0.96	84.76 ± 2.53
Melphalan	--	98.73 ± 1.12	33.94 ± 1.81

Further to confirm the functional group contributing towards cytotoxicity, it was decided that IC_{50} values should be determined for **59a**, **59m** and **62b**. Also compound **60m** showed higher growth inhibition as compared to other compounds in the series **60** at 10 µM concentration, and thus the decision was made to determine its IC_{50} value along with the unsubstituted compound **60a**.

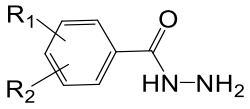

59a-m

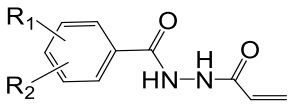

60a-m

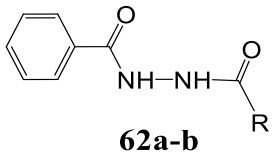

62a-b

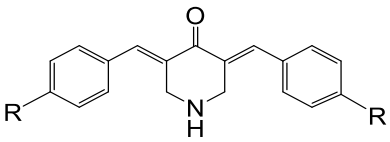

63a-f

Table 5.2 : Evaluation of **59a**, **59m**, **60a**, **60m**, **62b** and **63a** against HCT 116 cells and CRL-1790 cells

Compound	**Substituents**	**Mean IC_{50} (µM) ± *SD[a] against HCT 116 cancer cells**	**Mean IC_{50} (µM) ±*SD[a] against CRL-1790 non-malignant cells**	**Selectivity Index[b]**
59a	H	>100	>100	~1.00
59m	3,4 $(OCH_3)_2$	>100	>100	~1.00
60a	H	36.95 ± 2.84	>100	>2.70
60m	3,4 $(OCH_3)_2$	15.27 ± 0.42	>100	>6.55
62b	CH_2CH_3	>100	>100	~1.00
63a	H	0.37 ± 0.06	13.46 ± 1.99	36.38
5-FU	--	3.77 ± 0.48	10.99 ± 1.43	2.92
Melphalan	--	30.76 ± 2.73	>100	>3.25

[a] *SD = Standard deviation.

[b] The selectivity index is the ratio of IC_{50} of CRL-1790 normal cells and HCT 116 cancer cells.

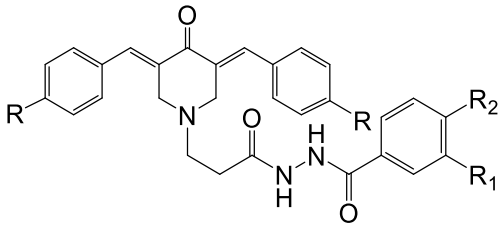

64a-g

Table 5.3 : Evaluation of **64a-g** against HCT 116 cells and CRL-1790 cells

Compound	Substituents		Mean IC_{50} (µM) ±*SD[a] against HCT 116 cancer cells	Mean IC_{50} (µM) ±*SD[a] against CRL-1790 non-malignant cells	Selectivity Index[b]
	R	$R_1 = R_2$			
64a	H	H	1.38 ± 0.25	12.31 ± 1.09	3.87
64b	H	OCH_3	3.15 ± 0.33	9.63 ± 1.62	3.06
64c	Cl	OCH_3	3.40 ± 0.01	12.23 ± 1.22	3.60
64d	F	OCH_3	3.82 ± 0.11	11.41 ± 2.22	2.99
64e	NO_2	OCH_3	0.28 ± 0.009	4.57 ± 0.53	16.32
64f	OCH_3	OCH_3	2.87 ± 0.23	11.07 ± 0.52	3.86
64g	CH_3	OCH_3	1.94 ± 0.18	9.24 ± 0.52	4.76
5-FU	--		4.11 ± 0.22	10.84 ± 1.64	2.64
Melphalan	--		33.16 ± 1.7	>100	3.02

[a] *SD = Standard deviation.

[b] The selectivity index is the ratio of IC_{50} of CRL-1790 normal cells and HCT 116 cancer cells.

a.

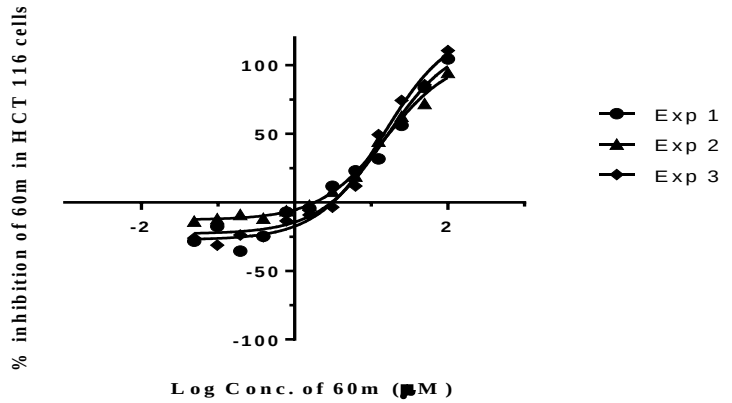
% inhibition of 60m in HCT 116 cells
100
50
-2
2
-50
-100
Log Conc. of 60m (μM)
Exp 1
Exp 2
Exp 3

b.

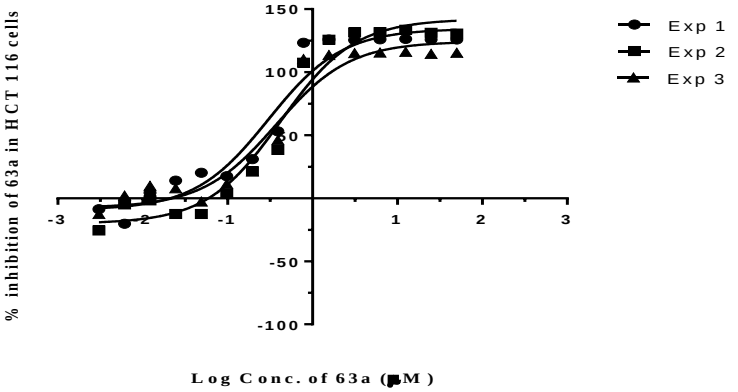
% inhibition of 63a in HCT 116 cells
150
100
-3
-2
-1
1
2
3
-50
-100
Log Conc. of 63a (μM)
Exp 1
Exp 2
Exp 3

c.

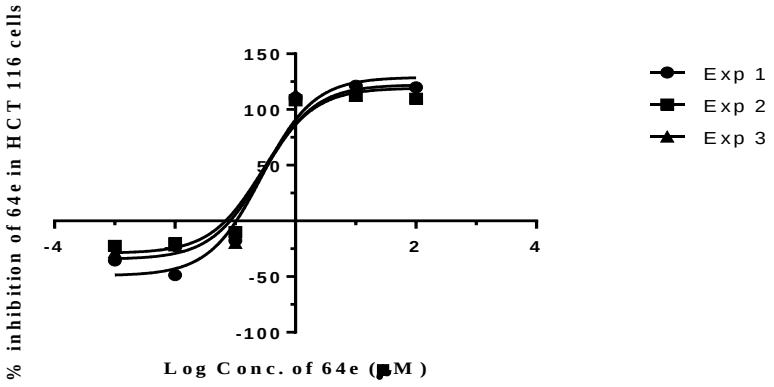
% inhibition of 64e in HCT 116 cells
150
100
50
-4
2
4
-50
-100
Log Conc. of 64e (μM)
Exp 1
Exp 2
Exp 3

d.

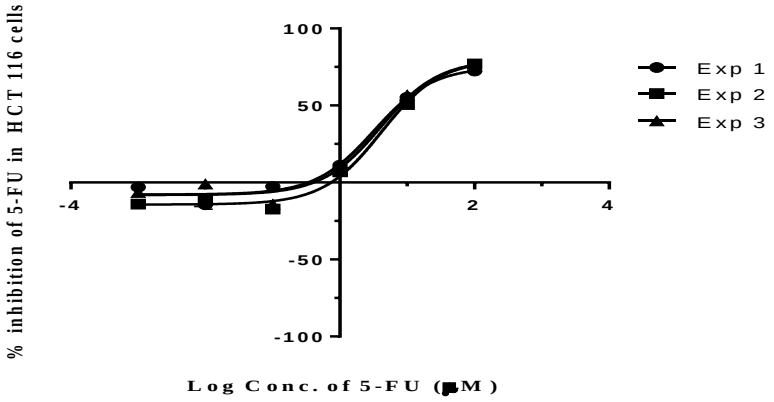

e.

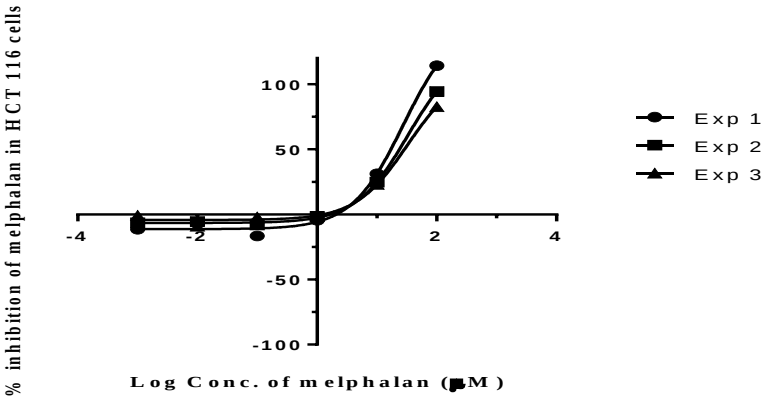

Figure 5.1 : a. Anti-proliferative assay of **60m** against HCT 116 cells. b. Anti-proliferative assay of **63a** against HCT 116 cells. c. Anti-proliferative assay of **64e** against HCT 116 cells. d. Anti-proliferative assay of 5-FU against HCT 116 cells. e. Anti-proliferative assay of melphalan against HCT 116 cells.

5.1.2 Antiproliferation assay using MCF-7 cells

MCF-7 cells are estrogen and progesterone receptors positive. The initial screening of the compounds (**60a-m**, **61a**, and **62a-b**) was carried out at 100 µM and 10 µM towards MCF-7 cells. Compounds **60j**, **60k**, **60l** displayed promising inhibition at 10 µM concentration and thus the IC_{50} values of those selected compounds were obtained. 5-FU and melphalan were used as the reference drugs.

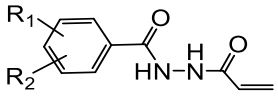

60a-m

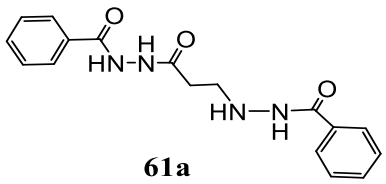

61a

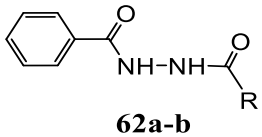

62a-b

Table 5.4 : Screening of **60a-m**, **61a**, **62a-b** against MCF-7 malignant cells

Compound	Substituents	% inhibition at 100 µM	% inhibition at 10 µM
60a	H	51.11 ± 2.87	5.47 ± 3.52
60b	4-F	33.21 ± 3.13	-40.14 ± 3.34
60c	4-Br	46.64 ± 3.35	-4.68 ± 3.17
60d	4-Cl	55.90 ± 2.82	3.59 ± 2.08
60e	2-Cl	75.83 ± 2.76	8.66 ± 1.81
60f	3-Cl	85.85 ± 2.70	-15.50 ± 3.38
60g	3,4-Cl_2	97.39 ± 2.60	-50.47 ± 3.27
60h	2,5-Cl_2	54.16 ± 3.42	14.74 ± 3.68
60i	3-CH_3	44.19 ± 2.96	-82.81 ± 3.48
60j	2-CH_3	100.84 ± 1.39	53.25 ± 3.07
60k	4-CH_3	>100	55.31 ± 3.05
60l	4-OCH_3	99.41 ± 2.34	60.61 ± 3.29
60m	3,4-$(OCH_3)_2$	100.99 ± 2.49	-16.10 ± 3.51
61a	---	97.99 ± 2.68	16.05 ± 3.55
62a	CH_3	-58.68 ± 3.24	-93.81 ± 4.15
62b	CH_2CH_3	-5.69 ± 2.54	-19.63 ± 3.66
5-FU	--	99.32 ± 2.87	91.23 ± 3.03
Melphalan	--	>100	>100

Table 5.5 indicates the cytotoxicity of **60j**, **60k** and **60l** against MCF-7 and CRL-1790 cells. All three compounds are cytotoxic against MCF-7 cells. These compounds are selectively toxic to MCF-7 cells and showed weak growth inhibition against non-malignant CRL-1790 cells.

Table 5.5 : Evaluation of **60j**, **60k**, **60l** against MCF-7 malignant cells and CRL-1790 non-malignant cells

Compound	**Mean IC_{50} (µM) ±*SD[a] against MCF-7 cancer cells**	**Mean IC_{50} (µM) ±*SD[a] against CRL-1790 non-malignant cells**	**Selectivity Index[b]**
60j	9.14 ± 1.31	>100	>10.94
60k	5.54 ± 0.51	>100	>18.05
60l	3.18 ± 0.53	>100	>31.45
5-FU	2.00 ± 0.25	10.84 ± 1.64	5.42
Melphalan	12.02 ± 1.43	>100	>8.32

[a] *SD = Standard deviation.

[b] The selectivity index is the ratio of IC_{50} of CRL-1790 normal cells and HCT 116 cancer cells.

5.1.3 Antiproliferation assay using MDA-MB-231 cells

MDA-MB-231 cells are triple negative (estrogen, progesterone and HER2 negative). Since a few compounds showed promising activity against MCF-7 cells, we conducted the screening of the **60a-m**, **61a**, **62a-b** at 100 µM and 10 µM towards MDA-MB-231 cells. The data are expressed as the percentage growth inhibition in Table 5.6. 5-FU and melphalan were used as the reference drugs.

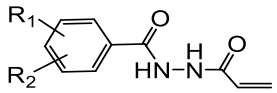

60a-m

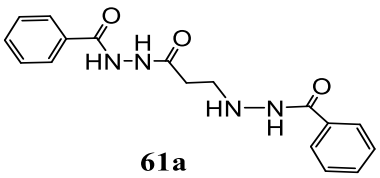

61a

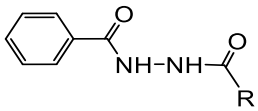

62a-b

Table 5.6 : Screening of **60a-m**, **61a**, **62a-b** against MDA-MB-231 malignant cells

Compound	Substituents	% inhibition at 100 µM	% inhibition at 10 µM
60a	H	52.08 ± 2.04	-12.13 ± 1.50
60b	4-F	39.88 ± 2.51	-7.37 ± 1.52
60c	4-Br	88.76 ± 1.26	-16.52 ± 1.45
60d	4-Cl	49.12 ± 2.04	-12.17 ± 4.05
60e	2-Cl	91.89 ± 4.53	-7.15 ± 2.29
60f	3-Cl	98.72 ± 0.92	15.58 ± 3.14
60g	3,4-Cl_2	>100	-19.37 ± 3.01
60h	2,5-Cl_2	>100	-5.95 ± 4.21
60i	3-CH_3	53.23 ± 2.89	-5.91 ± 3.86
60j	2-CH_3	46.79 ± 3.63	-2.64 ± 2.37
60k	4-CH_3	74.63 ± 2.96	-8.78 ± 1.52
60l	4-OCH_3	47.76 ± 3.19	-4.95 ± 3.12
60m	3,4-$(OCH_3)_2$	50.50 ± 1.42	-15.89 ± 1.96
61a	---	95.66 ± 4.22	-16.00 ± 2.91
62a	CH_3	-15.30 ± 3.46	-22.65 ± 2.65
62b	CH_2CH_3	-11.53 ± 2.52	-25.27 ± 1.82
5-FU	--	>100	17.43 ± 2.97
Melphalan	--	>100	28.53 ± 2.48

Table 5.7, indicates the cytotoxicity of reference compounds against MDA-MB-231 and CRL-1790 cells. Both compounds showed weak potency against MDA-MB-231 cells at 10 µM. These reference compounds are not selective as they showed little or no inhibition of the growth of MDA-MB-231 cells. The IC_{50} values of **60a-m** were not determined.

Table 5.7 : Evaluation of reference drugs 5-FU and melphalan against MDA-MB-231 cancer cells and non-malignant CRL-1790 cells

Compound	**Mean IC_{50} (µM) ± *SD[a] against MDA-MB-231 malignant cells**	**Mean IC_{50} (µM) ±*SD[a] against CRL-1790 non-malignant cells**	**Selectivity Index[b]**
5-FU	15.94 ± 1.65	10.84 ± 1.64	0.68
Melphalan	52.85 ± 2.32	>100	>1.90

[a] *SD = Standard deviation.

[b] The selectivity index is the ratio of IC_{50} of CRL-1790 normal cells and HCT 116 cancer cells.

5.2 Combinatorial approach in HCT 116 cells

The objective of this study was to determine whether N^1-acryloylbenzohydrazide derivatives act as chemosensitizers and show synergism with 3,5-bis(benzylidene)-4-piperidone or not. For this experiment N^1-acryloyl-3,4-dimethoxybenzohydrazide **60m** was used as a potential chemosensitizer.

As indicated in Table 5.8, the total and live cell count as well as the percentage of live cells were measured by an automated cell counter using trypan blue dye. The percentage of live cells is the ratio of the live cell count to the total cell count. The time t_0 is the reading taken 24 h after seeding of HCT 116 cells in T_{75} flasks and it is considered as control because no solvent vehicle such as DMSO was added to the cells. As seen in Table 5.8, the percentage of live cells of different concentrations of **60m** and **63a** were measured either alone or in combination with the reference drug 5-FU (3.0 µM) and the negative control (only DMSO). Three independent experiments were conducted with three replicates in each experiment.

Table 5.8 : The combinatorial effects of **60m**, **63a** and **5-FU** towards HCT 116 cells after 24 h and 48 h

Compounds	24 h			48 h		
	Total count (cells/ml)	**Live count (cells/ml)**	**% Live cells**[a]	**Total count (cells/ml)**	**Live count (cells/ml)**	**% Live cells**[a]
t_0	1.18×10^6	1.10×10^6	92	--	--	--
DMSO	1.01×10^6	9.20×10^5	91	1.02×10^6	8.75×10^5	86
Control	--	--	--	2.36×10^6	2.25×10^6	95
5-FU 3 µM	2.83×10^5	2.21×10^5	78	1.6×10^5	8.77×10^4	55
60m 5 µM	6.67×10^5	5.87×10^5	88	3.36×10^5	2.52×10^5	75
60m 10 µM	5.56×10^5	3.73×10^5	67	2.51×10^5	1.43×10^5	57
60m 15 µM	2.95×10^5	1.8×10^5	61	2.14×10^5	6.83×10^4	32
63a 0.1µM	4.45×10^5	3.7×10^5	83	2.42×10^5	1.88×10^5	78
63a 0.2 µM	1.32×10^5	9.10×10^4	69	1.78×10^5	9.25×10^4	52
63a 0.4 µM	1.5×10^5	7.2×10^4	48	1.28×10^5	4.15×10^4	32
60m 5 µM + **63a** 0.1µM	7.78×10^4	5.45×10^4	70	4.39×10^4	2.76×10^4	63
60m 10 µM + **63a** 0.1µM	6.75×10^4	4.59×10^4	68	5.67×10^4	3.34×10^4	59
60m 15 µM + **63a** 0.1µM	5.56×10^4	3.06×10^4	55	2.43×10^4	1.1×10^4	45
60m 5 µM + **63a** 0.2 µM	5.56×10^4	2.15×10^4	39	6.75×10^4	8.34×10^3	12
60m 10 µM + **63a** 0.2 µM	1.85×10^5	5×10^4	27	1.67×10^4	1.72×10^3	10
60m 15 µM + **63a** 0.2 µM	2.78×10^4	4.7×10^3	17	1.11×10^3	--	0
60m 5 µM + **63a** 0.4 µM	3.89×10^4	7.3×10^3	19	2.56×10^3	--	0
60m 10 µM + **63a** 0.4 µM	2.22×10^4	2.4×10^3	11	1.67×10^3	--	0
60m 15 µM + **63a** 0.4 µM	2.78×10^4	1.39×10^3	5	1.07×10^3	--	0
60m 5 µM + **5-FU** 3 µM	2.06×10^4	1.1×10^4	53	1.48×10^4	5.4×10^3	37
60m 10 µM + **5-FU** 3 µM	1.1×10^3	5.5×10^2	50	1.74×10^3	5.56×10^2	32
60m 15 µM + **5-FU** 3 µM	1.28×10^3	4×10^2	32	1.92×10^3	3.84×10^3	20

[a] The percentage live cells is calculated by the ratio of the live count (cells/ml) and the total cell count (cells/ml) obtained from an automated cell counter.

Compounds **60a-m**, **61a**, **62a-b** and **63a** were evaluated towards human oral squamous cell carcinomas (Ca9-22, HSC-2, HSC-3 and HSC-4). In addition, these compounds were evaluated against human non-malignant HGF, HPC and HPLF cells to study the possible selectivity of the compounds towards cancer cells. Table 5.9 indicates the CC_{50} values expressed in μM range. Two independent experiments were conducted with three replicates in each experiment.

Table 5.9 : Evaluation of **60a-m**, **61a**, **62a-b** and **63a** against various human carcinoma and normal cell lines

Compound	Human oral squamous carcinoma cells (CC_{50})[a]					Human normal oral cells (CC_{50})[a]				Selectivity Index (SI)[b]
	Ca9-22	HSC-2	HSC-3	HSC-4	Mean	HGF	HPLF	HPC	Mean	
60a	33.4 ± 4.0	40.4 ± 4.0	39.2 ± 10.3	70.3 ± 21.7	45.8 ± 16.6	32.1 ± 4.8	37.4 ± 2.0	72.8 ± 0.8	47.4 ± 22.1	1.0
60b	>400 ± 0.0	>400 ± 4.0	385.3 ± 13.7	>400 ± 0.0	>396.3 ± 7.3	222.0 ± 71.9	274.3 ± 154.6	176.7 ± 79.5	224.3 ± 48.9	<0.6
60c	130.0 ± 2.6	190.0 ± 4.0	237.0 ± 7.9	209.7 ± 18.2	191.7 ± 45.4	257.7 ± 22.6	287.0 ± 16.4	312.3 ± 18.1	285.7 ± 27.4	1.5
60d	42.4 ± 7.0	45.0 ± 4.0	52.0 ± 6.9	46.6 ± 1.9	46.5 ± 4.0	33.0 ± 1.6	38.5 ± 4.8	72.4 ± 2.0	48.0 ± 21.3	1.0
60e	53.5 ± 9.2	68.0 ± 4.0	35.7 ± 3.9	87.5 ± 9.1	61.2 ± 22.0	35.4 ± 3.6	57.0 ± 4.5	51.2 ± 63.1	47.9 ± 11.2	0.8
60f	238.3 ± 39.3	359.7 ± 4.0	>392 ± 13.9	>400 ± 0.0	>347.5 ± 74.8	>379.3 ± 35.8	>400.0 ± 0.0	158.7 ± 73.9	>312.7 ± 113.8	><0.9
60g	295.3 ± 24.7	>400 ± 4.0	374.0 ± 25.2	>400 ± 0.0	>367.3 ± 49.5	>400.0 ± 0.0	>391.0 ± 15.6	>400 ± 0.0	397 ± 5.2	><1.1
60h	99.4 ± 12	87.4 ± 4.0	73.1 ± 48.5	83.3 ± 10.7	85.8 ± 10.9	76.3 ± 80.8	223.3 ± 21.4	36.6 ± 4.8	112.1 ± 98.4	1.3
60i	90.1 ± 4.9	136.4 ± 4.0	59.7 ± 20.5	153.7 ± 19.8	110.0 ± 42.9	204.3 ± 169.8	132.8 ± 40.4	20.8 ± 3.3	119.3 ± 92.5	1.1
60j	247.3 ± 132.7	66.1 ± 4.0	>400.0 ± 0.0	168.0 ± 90.7	>220.4 ± 140.9	44.8 ± 28.9	74.9 ± 58.2	20.8 ± 4.7	46.8 ± 27.1	<0.2
60k	63.5 ± 4.8	151.7 ± 4.0	114.8 ± 16.8	116.6 ± 22.1	111.7 ± 36.3	92.7 ± 61.4	118.8 ± 51.1	108.8 ± 33.9	106.8 ± 13.2	1.0
60l	32.2 ± 2.4	46.0 ± 4.0	61.1 ± 6.6	47.2 ± 4.4	46.6 ± 11.8	31.8 ± 4.4	50.3 ± 10.5	67.8 ± 0.3	50.0 ± 18.0	1.1
60m	310.7 ± 79.9	>400 ± 0.0	>396 ± 6.9	>400 ± 0.0	>376.7 ± 44.0	273.0 ± 33.9	325.7 ± 65.4	206.3 ± 96.7	268.3 ± 59.8	<0.7
61a	>400 ± 0.0	>400 ± 0.0	>400 ± 0.0	>400 ± 0.0	>400 ± 0.0	328.3 ± 67.1	>377.7 ± 38.7	194.3 ± 113.3	>300.1 ± 94.9	><0.8
62a	>400 ± 0.0	>400 ± 0.0	>400 ± 0.0	>400 ± 0.0	>400 ± 0.0	330.3 ± 60.4	>391.3 ± 15.0	160.8 ± 107.2	>294.1 ± 119.5	><0.7
62b	>400 ± 0.0	>400 ± 0.0	>400 ± 0.0	>400 ± 0.0	>400 ± 0.0	>400 ± 0.0	>396.0 ± 6.9	273.1 ± 159.3	>356.4 ± 72.1	0.9
63a	<0.31 ± 0.0	0.45 ± 0.03	0.58 ± 0.01	0.50 ± 0.04	<0.46 ± 0.11	2.87 ± 0.56	2.21 ± 0.03	4.21 ± 0.22	3.10 ± 1.02	>6.8

[a] The CC_{50} values are the concentrations of the compounds required to kill 50% of the cells. The values are expressed in µM. Two independent experiments were conducted with three replicates in each experiment.

[b] The selectivity index (SI) is the ratio of the average CC_{50} value of the compound towards human normal oral cells to the average CC_{50} value for human oral squamous cancer cells.

Table 5.10 : Evaluation of **60a**, **60d**, **60h** and **60l** against various cancer cell lines (Ramos, NALM-60, CEM, HL-60, JURKAT and RAJI) and normal cell lines Hs27 and MCF10A

Compound	**Cancer cell lines (CC_{50}) [a]**												**Normal cell lines (CC_{50}) [a]**		
	Ramos	**SI[b]**	**NALM-60**	**SI[b]**	**CEM**	**SI[b]**	**HL-60**	**SI[b]**	**JURKAT**	**SI[b]**	**RAJI**	**SI[b]**	**Hs27**	**MCF10A**	**Avg[c]**
60a	0.19±0.01	67.63	2.74±0.59	4.69	0.91±0.48	14.12	3.32±0.26	3.87	3.52±0.36	3.65	5.18±0.35	2.48	12.05±0.91	13.65±1.10	12.85
60d	0.29±0.05	47.10	3.34±0.43	4.09	3.37±0.18	4.05	5.62±0.29	2.43	2.50±0.24	5.46	5.50±1.10	2.48	14.41±0.24	12.89±0.95	13.65
60h	0.15±0.02	57.74	2.86±0.55	3.03	0.86±0.07	10.07	2.90±0.76	2.99	1.07±0.09	8.09	2.71±0.09	3.20	10.45±0.05	6.87±0.48	8.66
60l	0.19±0.01	94.21	3.25±0.99	5.51	1.42±0.25	12.60	1.86±0.66	9.62	2.17±0.45	8.25	2.93±0.43	6.11	17.70±0.62	18.10±0.84	17.90

[a] The CC_{50} values are the concentrations of the compounds required to kill 50% of the cells. The values are expressed in µM.
[b] SI is the selectivity index, and represents the ratio of the average CC_{50} value of the compound towards normal cells and the CC_{50} value for each cancer cell line.
[c] These values are the average CC_{50} values of the compounds towards Hs27 and MCF10A cell lines.

Compounds **60a**, **60d**, **60h** and **60l** were evaluated against six malignant cell lines namely Ramos, NALM-60, CEM, HL-60, JURKAT and RAJI and normal cell lines Hs27 and MCF10A (Table 5.10). All the compounds are cytotoxic towards both the cancer and non-malignant cells. The selectivity index was measured by calculating the ratio of the average CC_{50} value of the compound towards normal skin Hs27 cells and normal breast MCF10A cells by the CC_{50} value of each compound towatds a particular cell line. It can be noted from the Figure 5.2, that all of the compounds showed high selectivity towards Ramos lymphocytes. Compound **60l** showed more than 90% selectivity toxicity towards Ramos lymphocytes.

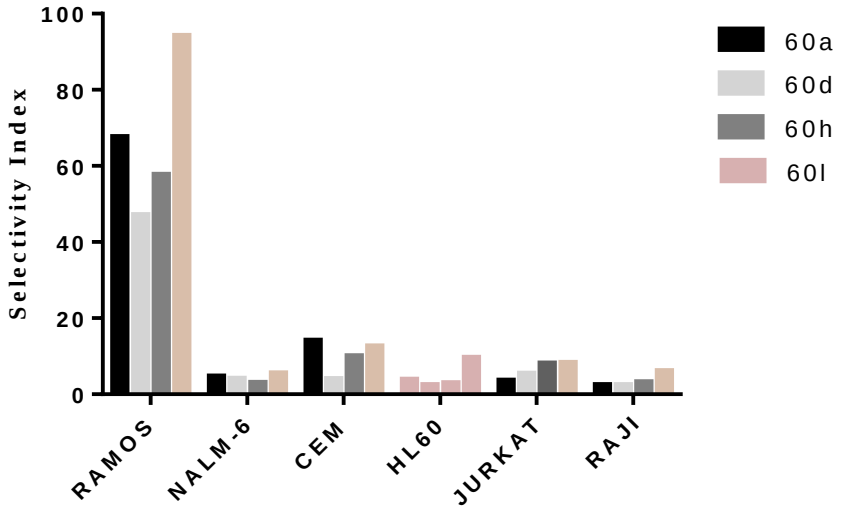

Figure 5.2 : The selectivity index figures of **60a**, **60d**, **60h** and **60l** against various malignant cells are presented.

5.3 Studies on mechanisms of action

5.3.1 Mitochondrial membrane potential

5.3.1.1 Mitochondrial membrane potential in HCT 116 cells using the TMRE dye

The TMRE dye accumulates in the mitochondria based on the mitochondrial membrane potential ($\Delta\psi_m$). In healthy cells, the TMRE dye remains intact within the mitochondria having a normal electrochemical gradient which gives rise to fluorescence upon excitation whereas in apoptotic cells, because of the changes in $\Delta\psi_m$, the TMRE dye moves out of the mitochondria into the cytosol resulting in a decrease in the fluorescence signal. CCCP acts as an uncoupling agent resulting in intracellular mitochondrial depolarization which remarkably reduces the electrochemical potential and thus significantly decreases the fluorescence signal as seen in Figure 5.3. CCCP and 2,4-DNP were used as positive controls whereas only DMSO was used as a negative control. It can be seen from Figure 5.3, that compound **64e** has a significant effect in reducing the MMP as compared to the negative control. Both **64a** and **64g** resulted in a decrease in the MMP with same intensity as the standard drug 5-FU. Compound **60m** does not show any effect on the MMP.

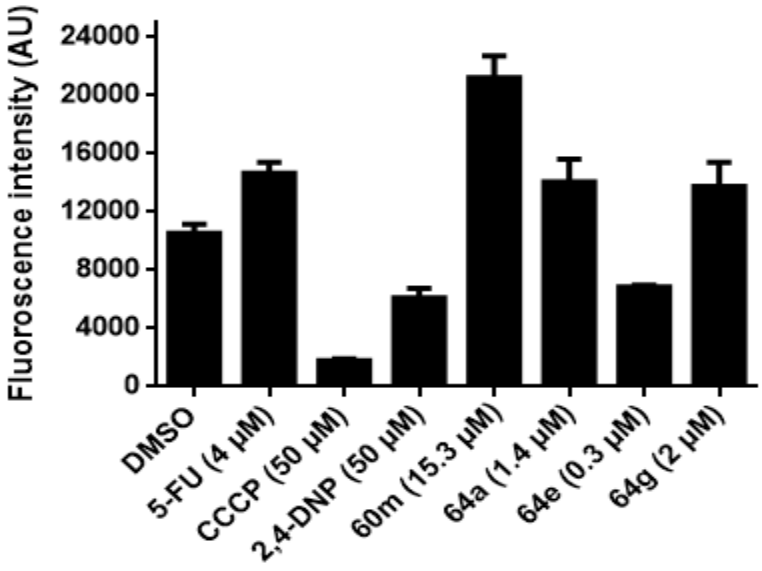

Figure 5.3 : The effects of cytotoxic agents **60m**, **64a**, **64e** and **64g** on the mitochondrial membrane potential in HCT 116 cells using the TMRE dye.

The bar represents means ± SD of three independent experiments with three replicates in each experiment. All the results are significantly different from the control (DMSO) based on one-way ANOVA with Dunnett post-hoc analysis and a p value < 0.05 as indicated in Appendix A.

5.3.1.2 Mitochondrial membrane potential in Ramos cells using the JC-1 dye

Our collaborators evaluated the effect of **60l** on the mitochondrial membrane potential of Ramos cells using the JC-1 dye as previously described in the literature.[78,121] JC-1 tends to form complexes such as J-aggregates in the healthy cells having high $\Delta\psi_m$ resulting in red fluorescence measured at 590 nm whereas the apoptotic cells having lower $\Delta\psi_m$ form monomers producing a green fluorescence at 530 nm. The ratio of the JC-1 aggregate to the JC-1 monomers is an indicator of overall health of the cells. Thus a decrease in the JC-1 aggregate signifies membrane depolarization.

DMSO was used as the negative control whereas H_2O_2 was used as the positive control. It was observed that H_2O_2 significantly depolarizes the mitochondrial membrane as compared to the untreated cells and DMSO. In this assay, the CC_{50} concentration of **60l** was used**.** It can be noticed from Figure 5.4, that there is nearly 35% of depolarization of **60l** at the CC_{50} concentration whereas at twice the CC_{50} concentration, there is almost a 2-fold increase in the mitochondrial depolarization.

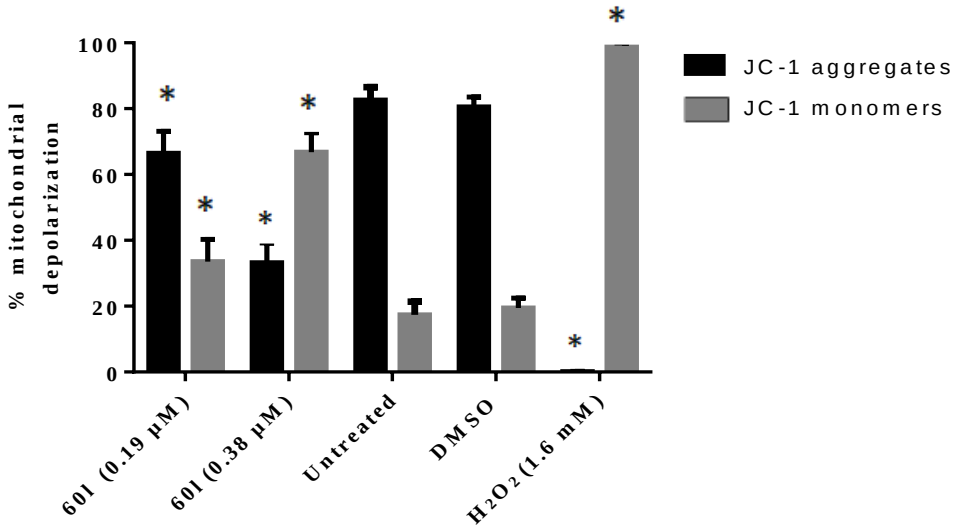

Figure 5.4 : The effects of the cytotoxic agent **60l** on mitochondrial membrane potential in Ramos cells using the JC-1 dye.

The bar represents means ± SD of three independent experiments with three replicates in each experiment. * indicates that the data points are significantly different ($p < 0.05$) from the control based on one-way ANOVA with Dunnett post-hoc analysis as indicated in Appendices B and C.

5.3.2 Evaluation of reactive oxygen species (ROS) levels in HCT 116 cells

In this assay, the DCF-DA (2′,7′–dichlorofluorescin diacetate) dye was used to measure ROS levels within the cells. DCF-DA is a fluorogenic dye which undergoes deacetylation by esterases present in the cells and is converted into a non-fluorescent compound. This non-fluorescent compound is oxidized by reactive oxygen species to DCF (2′,7′–dichlorofluorescin). DCF is a fluorescent compound which can be detected at excitation at 485 nm and emission at 530 nm.

DMSO was used as a negative control whereas H_2O_2 was used as a positive control. An increase in the average fluorescence intensity reveals an increase in ROS levels. It can be observed from Figure 5.5, that all the compounds caused a 2-4 fold increase in the fluorescence intensity resulting in increased ROS levels. All the compounds showed a greater increase in the ROS levels as compared to the standard drug 5-FU. HCT 116 cells were treated with the IC_{50} concentrations of the compounds and thus after 48 h incubation, their cell number was reduced to half and therefore their fluorescence signal was increased twice as compared to the number of cells treated with DMSO.

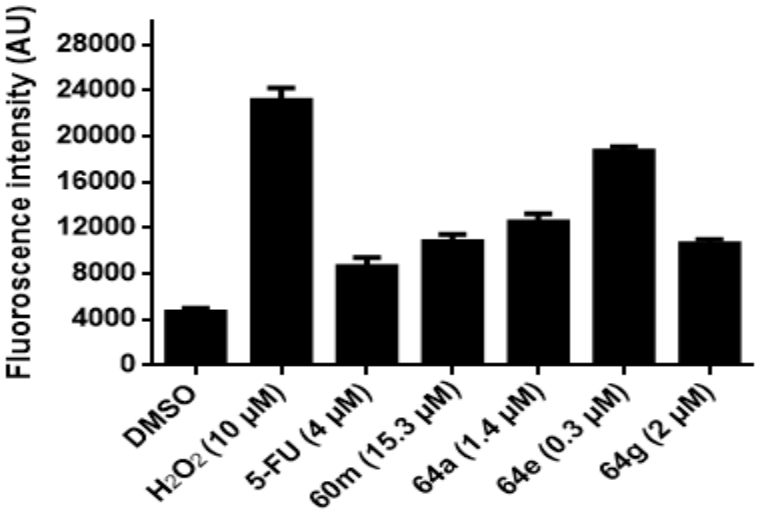

Figure 5.5 : The effects of cytotoxic agents **60m**, **64a**, **64e** and **64g** on ROS levels in HCT 116 cells using the DCF-DA dye.

The bar represents means ± SD of three independent experiments were conducted with three replicates in each experiment. All the results are significantly different from the control (DMSO) based on one-way ANOVA with Dunnett post-hoc analysis and a p value < 0.05 as indicated in Appendix D.

CHAPTER 6 : DISCUSSION

6.1 Design and development of novel cytotoxic agents

Over the years, our laboratory has mainly focused on the design and development of conjugated arylidene ketones as potential cytotoxic agents. These α,β-unsaturated compounds not only have various pharmacological properties but they also show a preferential affinity towards thiols rather than amino or hydroxyl groups which are present in nucleic acids, resulting in decreased genotoxic side effects.[80] Many different compounds possessing α,β-unsaturated keto moieties display biological activities; however a major interest is based on one or more of the constituents of a well-known herbaceous plant called turmeric. Curcumin, isolated from turmeric, is an important lead compound exhibiting various biological activities including anticancer properties. Although curcumin is safe and effective *in vivo*, it has emerged as a poor lead compound because of its low solubility, metabolic instability and rapid elimination.[47] Researchers have made several structural modifications of the curcumin moiety such as the 1,5-bis(arylidene)-pentan-2,4-diones which have been superceded by compounds containing the 1,5-diaryl-3-oxo-1,4-pentadienyl pharmacophore which resulted in the development of a number of curcuminoids as novel cytotoxic agents with improved pharmacological activity.

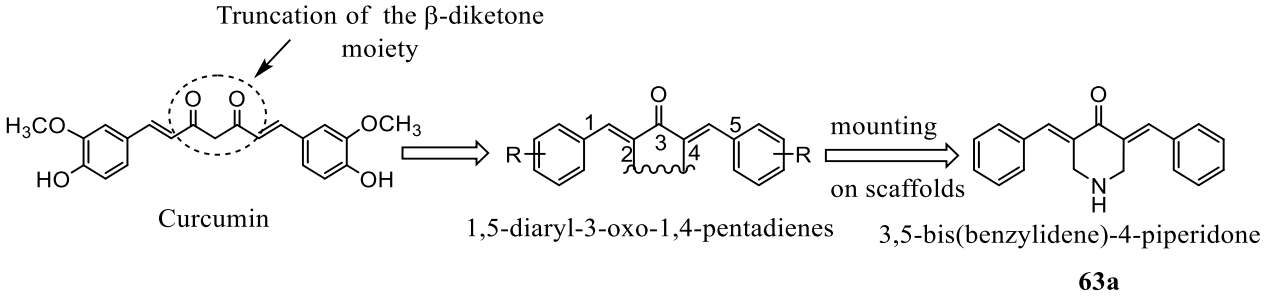

Figure 6.1 : Development of the 3,5-bis(benzylidene)-4-piperidone **63a**.

One such effort was led by Dr. Dimmock and his coworkers to incorporate the 1,5-diaryl-3-oxo-4-pentadienyl pharmacophore onto various scaffolds. This resulted in the development of 3,5-bis(benzylidene)-4-piperidone **63a** as a lead molecule in our laboratory by mounting the 1,5-diaryl-3-oxo-1,4-pentadienyl pharmacophore onto a piperidine ring.[63]

One of the major drawbacks associated with the use of chemotherapeutic agents is the toxic effect towards normal cells. This problem was addressed by designing novel cytotoxic agents using the

hypothesis of sequential cytotoxicity postulated by Dimmock *et al*. This theory states that an initial "chemical insult" may cause greater damage to neoplasms than non-malignant cells. Consequently a second interaction with cellular constituents could result in significant tumor-selective toxicity. The likelihood exists that the greater the number of alkylating sites that are present, the greater the possibility of increased selective toxicity towards tumors.[122] In light of this concept, the first hypothesis of this project is that attachment of the N^1-acyl hydrazides to the piperidyl atom of 3,5-bis-4-piperidones may increase cytotoxicity.

In line with the first objective of this project, a series of N^1-acyl hydrazides **60a-m** were synthesized from the esters **58a-m** and the hydrazide intermediates **59a-m**. Various substituents were placed in the aryl ring which have different electronic, hydrophobic and steric properties since one objective is to search for correlations between one or more of these parameters and cytotoxic properties. The auxiliary binders **60a-m** were designed so that they might be able to react with different cellular constituents such as thiols (reacting with the α,β-unsaturated keto group), amino and hydroxyl groups (interacting with amidic features of **60a-m**) as well as aryl and alkyl groups (reacting with aryl and alkyl groups of **60a-m**).

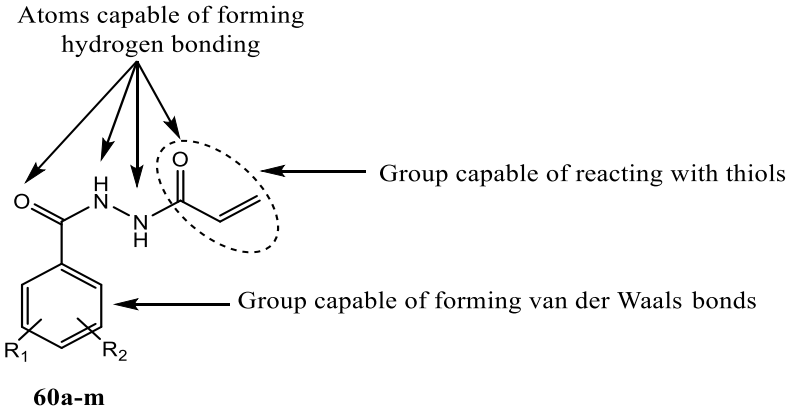

60a-m

Figure 6.2 : Possible interactions of **60a-m** at auxiliary binding sites.

3,5-bis(Benzylidene)-4-piperidone **63a** is a lead molecule developed in our laboratory as an anti-neoplastic agent which is cytotoxic towards various types of malignancies including leukemia, colon, breast, skin and ovarian tumors. The cytotoxicity displayed towards various neoplasms is due to the 1,5-diaryl-3-oxo-1,4-pentadienyl pharmacophore acting at the primary binding site. In order to prepare the target compounds **64a-g**, the auxiliary binders **60a-m** were reacted with **63a** and related compounds. These concepts are presented in Figure 6.3. One may also speculate that

the interaction of primary and auxiliary binding sites with the malignant and healthy cells might be different which may result in greater selectivity and toxicity towards neoplasms.

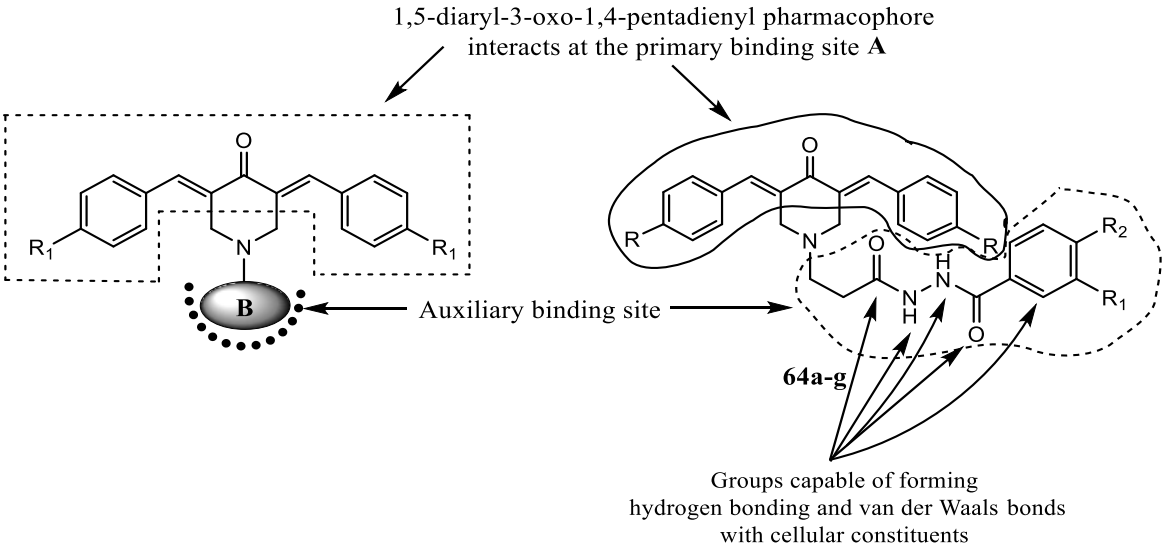

Figure 6.3 : Design of cytotoxins **64a-g** to interact at binding sites A and B.

6.2 Assessment of the cytotoxicity of novel cytotoxic agents

After the synthesis of the compounds, the sulforhodamine B assay was used to measure the cytotoxic potencies of some of the compounds **60a-m**, **61a**, **62a-b** and **64a-g** against malignant HCT 116, MCF-7 and MDA-MB-231 cells and non-malignant CRL-1790 cells. The sulforhodamine B dye is used for the quantitative measurement of the protein content. Its main principle is that it binds stoichiometrically to the basic amino acids of the cellular proteins under acidic conditions such as trichloroacetic acid fixed cells. The exposure to basic conditions such as Trizma base results in the solubilization of the dye and the colorimetric end point reflects the total protein mass which is proportional to the cell number. Here, the cytotoxic potencies are described in terms of IC_{50} values, namely the concentration at which cell growth is inhibited by 50%.

Using the colon cancer cell line HCT 116, all the auxiliary binders **60a-m** showed more than 60% inhibition at 100 µM concentration. However, only compound **60m** showed nearly 47% inhibition at 10 µM concentration. The IC_{50} value of the 3,4-dimethoxy derivative **60m** towards HCT 116 cells was found to be 15.27 µM which is almost 2.4-fold more potent than the unsubstituted analog **60a** (Table 5.2). A noteworthy feature of the results presented in Table 5.1 is the higher potencies associated with meta substitution. For example, in terms of the chloro analogs, **60f** (3-Cl) > **60e**

(2-Cl) > **60d** (4-Cl). The addition of a 3-chloro group to **60d** to give **60g** (3, 4-Cl_2) was accompanied by an increase in potency. In addition, **60i** (3-CH_3) > **60j** (2-CH_3) > **60k** (4-CH_3). In the case of the compounds containing aryl methoxy groups, **60m** [3,4(OCH_3)$_2$] is 5.4 times more potent than **60l** (4-OCH_3). Hence in the future the 3-methoxy and 3,4,5-trimethoxy analogs should be prepared.

The cytotoxic evaluation of **61a** is important for two reasons at least. First, cytotoxicity is displayed in the absence of a thiol alkylating group which is present in **60a**. Second, the symmetrical molecule **61a**, which is 1.76 times more potent than **60a**, reveals the contribution to cytotoxicity of the hydrogen bonding capacity of different groups in **61a** as well as the increased potential of van der Waals bonding. In the future, a variety of aryl substituents should be placed in one or both aryl rings with a view to producing novel potent cytotoxins.

The data in Table 5.1 reveal that removal of the olefinic double bond of **60a** to give **62a** and **62b** was accompanied by a substantial drop in potencies. Thus considering the data obtained using a concentration of 100 μM, **62a** and **62b** have an average of 12.2% of the potency of **60a**. This result reveals the importance of the α,β-unsaturated keto group in **60a** suggesting that interaction of this compound with cellular thiols likely contributes significantly to its cytotoxic potency.

Another observation that may be made on the results portrayed in the Table 5.1 is in regard to comparing the cytotoxic potencies of the compounds in series **60** with two established anticancer drugs. 5-Fluorouracil was chosen as an agent used in treating colon cancer while melphalan is an alkylating agent. Thus the lead compound in the series **60**, namely **60m**, is more potent than melphalan but less cytotoxic than 5-FU.

The biodata generated in Table 5.2 highlights the IC_{50} values of the hydrazide analogs **59a** and **59m**, as well as the saturated compound **62b**, is greater than 100 μM suggesting that their corresponding functional groups do not contribute much to cytotoxicity but the acryloyl group in series **60** mainly accounts for the cytotoxic potency. For the 3,5-bis(arylidene)-4-piperidones derivatives **63**, only the unsubstituted compound **63a** was examined for its biological activities. The other derivatives **63b-f** were used for the synthesis of the target compounds **64b-g**. The IC_{50} value of 3,5-bis (benzylidene)-4-piperidone **63a** was found to be 0.365 μM towards HCT 116 cells as indicated in Table 5.2.

All the target compounds **64a-g**, have IC_{50} values below 4 μM which means at least 50% of HCT 116 cancer cell growth was inhibited below that concentration (Table 5.3). The "terminal" aryl ring is at the end of the side chain on the piperidinyl nitrogen atom. It was found that the compound **64a** which is unsubstituted at the terminal ring was more potent than the **64b** which has 3,4-dimethoxy groups. Overall, **64e** possessing a nitro substituent at the para position of the benzylidene ring attached directly to the piperidine ring was the most potent compound of series **64** with the IC_{50} value of 0.28 μM. The order of potencies for the substituent at the para position of the benzylidene ring attached directly to piperidine ring is as follows: **64e** (NO_2) > **64g** (CH_3) > **64f** (OCH_3) > **64b** (H) > **64c** (Cl) > **64d** (F). In the case of the reference drugs 5-FU and melphalan, the IC_{50} values were 4.11 μM and 33.2 μM respectively which are similar to the reported values by the NCI of 4.55 μM and 30.2 μM, respectively.[123] **64a-f** are in range of 9-117-fold more potent than the reference drug melphalan in HCT 116 cells. The IC_{50} values of **64a-f** are 1.1 to 15 times lower than the figure for 5-FU.

As mentioned earlier, in order to overcome the inherent toxic effects associated with current chemotherapeutic agents, it is important to ascertain if the compounds in series **60** and **64** exert a greater cytotoxicity towards neoplasms than normal cells and therefore these agents were screened against the non-malignant colon CRL-1790 cell line. The selectivity index (SI) was calculated by dividing the average IC_{50} values of the compounds towards normal cell lines by the IC_{50} values of the compounds against a specific cancer cell line. All the compounds showed SI figures >1 which indicates that they are selectively toxic towards malignant cells. The order of the SI figures presented in Table 5.2 is as indicated: **63a** (37) > **60m** (>6.6) > **60a** (>2.70). The order of the SI figures in series **64** (Table 5.3) is as follows: **64e** (16.15) > **64g** (4.8) > **64a** (3.87) > **64f** (3.86) > **64c** (3.6) > **64b** (3.06) > **64d** (2.99).

Further to understand the relationship between various physicochemical parameters and the cytotoxic potencies of target compounds **64b-g**, multilinear regression analysis was performed using SPSS analysis software.[124] Various structural descriptors such as Hansch π, Hammett σ, molecular refractivity (MR) and partition coefficient (logP) were used as dependent variables and $\log_{10}IC_{50}$ was considered as the independent variable.

The Hansch π value represents the nature of a substituent towards hydrophilicity and hydrophobicity of a compound, i.e., the contribution of various group for the transportation of a

drug from its site of administration to its site of action. A positive π value indicates that the substituent increases lipophilicity whereas a negative π value means that the aqueous solubility will be increased. The Hammett σ values represent the electronic effects of aryl substituents on the chemical reactivity of the side chain. The Hammett σ values are calculated for the substituents in the meta and para positions of the aryl ring. The molecular refractivity (MR) indicates the sizes of different atoms or groups. The logP values refer to the distribution of a solute between hydrophilic and hydrophobic solvents. Higher logP values indicates lipophilic nature of a compound whereas lower logP values represents its hydrophilicity.[125]

The σ, π and MR constants were obtained from the literature.[126,127] LogP values of the compounds were estimated using Chemdraw Prime 15.0 software.[128] Excellent correlations were observed between various descriptors and the IC_{50} values of **64b-g** in malignant HCT 116 cells and non-malignant CRL-170 cells as indicated in equations 1 and 2, respectively. Omitting some descriptors did not improve the correlation.

$$\mathrm{Log}_{10}(IC_{50\,HCT116}) = 4.79\sum\pi + 1.73\sum\sigma + 0.07\sum MR - 3.33logP - 17.93,$$

$r = 0.986$, $n = 6$ (1)

$$\mathrm{Log}_{10}(IC_{50\,CRL-1790}) = -22.07\sum\pi - 7.66\sum\sigma - 0.23\sum MR + 16.03logP + 50.56,$$

$r = 0.955$, $n = 6$ (2)

In these equations, r is the correlation coefficient and n is the number of determinations. Thus in future, different analogs with various physicochemical constants can be inserted into equations 1 and 2 and their cytotoxic potency may be predicted.

In order to discern whether these compounds showed toxicity towards other malignant cells, the auxiliary binders **60a-m** were screened against two breast cancer cell lines. MCF-7 cells are epithelial estrogen and progesterone positive breast neoplasms whereas MDA-MB-231 is a triple negative breast cancer cell line (TNBC), i.e., it is estrogen, progesterone and HER-2 negative. The initial screening of **60a-m** at 100 μM and 10 μM concentration revealed that only three compounds **60j**, **60k** and **60l** displayed strong growth inhibiting properties (>50%) at 10 μM towards MCF-7 cells. Thus the decision was made further to determine their IC_{50} values and their order of potencies are as follows: **60l** (3.18 μM) > **60k** (5.54 μM) > **60j** (9.14 μM). The SI figures of **60l** is more than 31 which is noteworthy and it is 4.5-fold more potent than the reference drug 5-FU. Results showed that all the three compounds displayed more selectivity towards MCF-7 cells rather than normal

colon CRL-1790 cells. The possible explanation of why only three agents showed inhibition and the remaining compounds did not could be that these compounds might be experiencing biphasic response, i.e., a compound can stimulate cell growth at lower concentrations but inhibits at higher concentration and such expressions are called hormetic responses. Another possible reason can be that since the SRB assay is based on quantitative measurement of cellular protein which is directly proportional to the cell number, the exact number of healthy cells is difficult to determine. This is because the proteins which might be undergoing apoptosis or any other cellular processes, might be detected which shows a false high number of living cells.

The screening of series **60**, **61a** and **62a-b** against MDA-MB-231 cells at 100 µM and 10 µM reported in Table 5.6 displayed poor growth-inhibiting properties suggesting that compounds were more vulnerable towards estrogen and progesterone positive MCF-7 cell lines than triple negative cells. Table 5.7 represents the IC_{50} values of 5-FU and melphalan which are 15.94 µM and 52.85 respectively and it was noticed that 5-FU has a greater than 2.8-fold weaker selectivity towards malignant cells in comparison to melphalan.

The hybrid compound **61a** formed by condensation of benzohydrazide **59a** and N^1-acryloyl-benzohydraizde **60a** showed weak inhibition towards all three cancer cell lines (HCT 116, MCF-7 and MDA-MB-231) at 10 µM concentration and thus further evaluations were not carried out. In regard to the saturated compounds **62a-b**, as hypothesized, they showed no inhibition at 10 µM towards cancer cells HCT 116, MCF-7, MDA-MB-231 as well as to normal cells CRL-1790. The probable explanation is that there is no alkylating group in the molecule.

There is a marked difference between the IC_{50} values and CC_{50} values. CC_{50} values represent the cytotoxic concentrations required to kill 50% of the cells whereas IC_{50} values represent the concentration required to inhibit the growth of cells by 50%. Our collaborators in Japan performed a cytotoxicity study to examine the effects of **60a-m**, **61a**, **62a-b** and **63a** against four human oral squamous carcinomas namely Ca9-22, HSC-2, HSC-3 and HSC-4 cells. In addition, they were also screened against three human normal cells namely HGF gingival fibroblasts, HPC pulp cells and HPLF periodontal ligament fibroblasts. This biodata are presented in Table 5.9.

The biodata in Table 5.9 indicates that many of the compounds **60b-c**, **60f-g**, **60i-k**, **60m**, **61a**, **62a-b**, display cytotoxicity towards the carcinomas at CC_{50} values higher than 100 µM. However, some of the compounds in series **60** displayed cytotoxicity towards four human carcinoma cells at

CC_{50} values between 46-86 µM (average CC_{50} values in µM parenthesis) namely **60a** (46), **60d** (46), **60e** (61), **60h** (86) and **60l** (47). Further, the 3,5-bis(benzylidene)-4-piperidone **63a** displayed an average CC_{50} value of <0.46 µM with a selective index of more than 6.8 which is noteworthy. Overall, compounds **60a**, **60d**, **60e**, **60h**, **60l** and **63a** exhibited CC_{50} values less than 100 µM and selectivity greater or equal to 1 which indicates that their toxicity towards normal cells is in general lower than for the neoplasms. For compounds in series **64**, the bioevaluations are yet to be performed.

Further biological evaluation of the auxiliary binders **60a**, **60d**, **60h** and **60l** was undertaken to investigate their cytotoxic potencies to non-adherent malignant cells. Many leukemic cells are spherical and are non-adherent. Our collaborators in El Paso performed the screening of **60a**, **60d**, **60h** and **60l** against six different leukemic cell lines such as Ramos, NALM-60, CEM, HL-60, JURKAT and RAJI cells. Moreover, normal human foreskin Hs27 cells and breast cells MCF10A were also used to investigate whether these compounds have greater selectivity towards malignant cells instead of the non-malignant cells.

The biodata presented in the Table 5.10 indicates that the auxiliary binders **60a**, **60d**, **60h** and **60l** displayed high cytotoxic potency towards all the leukemic cells with CC_{50} values of 5.6 µM or less. All four compounds displayed high potency towards Ramos cells in the range of 0.15-0.19 µM (average CC_{50} values in µM parenthesis) namely **60h** (0.15), **60a** (0.18), **60l** (0.19) and **60d** (0.29). It can be clearly observed that all auxiliary binders are highly selective towards Ramos cells as compared to other five leukemic cells. The SI figures were obtained by taking the ratio of the average CC_{50} value of the compound towards normal cells and the CC_{50} value for each cancer cell line. Compound **60l** has more than 90% selectivity towards Ramos leukemic cells as compared to the normal Hs27 and MCF10A cells. The order of selectivity towards Ramos cells are as follows: **60l > 60a > 60h > 60d**.

A study was conducted to examine if any of the target compounds **64a-g** have drug-like properties. Thus these compounds were examined in terms of physicochemical parameters which govern intestinal absorption and also predicts their ability to induce toxicity. The results in Table 6.1, reveal that the most desirable ratings appear are **64a**, **64b** and **64d**. Although **64e** is the most potent compound but because of the presence of a nitro group, there is a possibility that it may form toxic

metabolites like imines, hydroxylamines, amines *in vivo* and therefore **64a** is the lead molecule with the IC_{50} values of 1.38 µM and SI figure of 3.87.

Table 6.1 : Evaluation of **63a**, **64a-g** for drug like properties

Compound	Physicochemical properties[a]						Toxicity[b]				
	LogP	MW	HBA	HBD	RB	TPSA	M	T	I	R	Ratings[c]
63a	3.36	275.35	2	1	2	29.10	-	-	-	-	10
64a	4.12	465.55	6	2	7	78.50	-	-	-	-	10
64b	3.77	525.61	8	2	9	96.97	-	-	-	-	9
64c	5.12	594.50	8	2	9	96.97	-	-	-	-	8
64d	4.09	561.59	8	2	9	96.97	-	-	-	-	9
64e	3.69	615.60	14	2	11	188.62	-	-	-	-	6
64f	3.88	585.66	10	2	11	115.44	-	-	-	+	6
64g	4.67	553.66	8	2	9	96.97	-	-	-	-	9
Drug like compound	<5	<500	<10	<5	<10	<140	-	-	-	-	10

[a] The physicochemical properties considered as the logarithm of the partition coefficient (logP), molecular weight (MW), the number of hydrogen bond acceptors (HBA), the number of hydrogen bond donors (HBD), RB (rotatable bonds) and the total polar surface area (TPSA). These values were obtained using the molinspiration Web browser.[129]

[b] The assessment of toxicity was indicated in terms of mutagenicity (M), tumor-indication (T), irritant effects (I) and impairment of reproduction (R) using the Osiris Property Explorer tool. The toxic effects are indicated as + sign whereas – indicated no possible toxic effects.[130]

[c] A scale of 10 points was used for rating. One point was allocated for each positive result that is favourable physical property or the absence of the toxic effects.

6.3 Combinatorial approach in HCT 116 cells

A study of whether a representative compound in series **60** is capable of sensitizing HCT 116 colon cancer cells to antineoplastic agents was undertaken. The lead compound in series **60** is **60m** and the cytotoxin chosen is **63a** as well as a reference drug 5-FU. The approach taken is to incubate the potential chemosensitizer **60m** with HCT 116 cells for 24 hours and after this time, the cytotoxin is added and the mixture incubated for a further 24 hours. This effect is quantified by observing the percentage of live cells at the end of 24 and 48 hours time periods. This raw data is portrayed in Table 5.8 (page 74).

The calculations for evaluating whether chemosensitization has occurred or not are undertaken as follows.

1. The percentage of dead cells was obtained for individual compounds from which is deducted the percentage lethality of the solvent DMSO. For example, at the end of 48 hours, the percentage of dead cells after incubation of 5 µM of **60m** is 86 – 75 or 11 % (Table 5.8, entries 2 and 5) and portrayed in Table 6.2, entry 2.

For example, in the case of **63a** (0.1 µM), after 24 hours incubation, the percentage of dead cells is 91-83 or 8% (Table 5.8, entries 2 and 8) and presented in Table 6.2, entry 5.

Table 6.2: The percentage of dead HCT 116 cells after treatment with 5-FU, **60m** and **63a** for 24 h and 48 h

Compound	**Percentage of dead HCT 116 cells** [a]	
	24 h	48 h
5-FU 3 µM	13	31
60m 5 µM	3	11
60m 10 µM	24	29
60m 15 µM	30	54
63a 0.1 µM	8	8
63a 0.2 µM	22	34
63a 0.4 µM	43	54

[a] The figures of the percentages of the dead cells were calculated by subtracting the percentage of live cells of compound from the percentage of DMSO live cells.

2. The question which now requires resolution is whether chemosensitization takes place with the combination of a potential sensitizer (**60m**) and the cytotoxins **63a** and 5-FU. The calculations are based on the following biodata generated.

First consider if the effect was additive, i.e., both **60m** and **63a** contribute to overall toxicity but no chemosensitization has occurred. For example, at the end of 48 h the percentage of dead cells after treatment with **60m** (5 µM) is 11 (Table 6.2, entry 2). After 24 hours the percentage of dead cells treated with **63a** (0.1 µM) is 8 (Table 6.2, entry 5). Hence if the cytotoxicity effects are additive, the percentage of dead cells should be 11+ 8 or 19.

However the percentage of dead cells using a combination of **60m** (5 µM) and **63a** (0.1 µM) is 23 (86-63, entries 2 and 11, Table 5.8). In this case the difference in percentage of dead cells is not significant (Table 6.3, entry 1). On the other hand, when the biodata for a combination of **60m** (5 µM) and **63a** (0.2 µM) are considered, sensitization has taken place (Table 6.3, entry 4).

Table 6.3: Evaluation of the cytotoxic potencies of combinations of **60m** with **63a** and 5-FU

Combination	**Percentage of dead HCT 116 cells**[a]					
	60m (48 h)	**63a** (24 h)	**5-FU** (24 h)	**Calculated**[b]	**Found**[c]	**Significant p value**[d]
60m 5 µM + **63a** 0.1 µM	11	8	--	19	23	No
60m 10 µM + **63a** 0.1 µM	29	8	--	37	27	No
60m 15 µM + **63a** 0.1 µM	54	8	--	62	42	Yes
60m 5 µM + **63a** 0.2 µM	11	22	--	33	74	Yes
60m 10 µM + **63a** 0.2 µM	29	22	--	52	76	Yes
60m 15 µM + **63a** 0.2 µM	54	22	--	77	100	Yes
60m 5 µM + **63a** 0.4 µM	11	44	--	55	100	Yes
60m 10 µM + **63a** 0.4 µM	29	44	--	73	100	Yes
60m 15 µM + **63a** 0.4 µM	54	44	--	98	100	No
60m 5 µM + **5-FU** 0.3 µM	11	--	13	24	50	Yes
60m 10 µM + **5-FU** 0.3 µM	29	--	13	42	54	No
60m 15 µM + **5-FU** 0.3 µM	54	--	13	67	66	No

[a] The figures of the percentages of the dead cells were calculated by subtracting the percentage of live cells after treatment of the compounds from the percentage of DMSO live cells.

[b] The calculated values are the sum of either **60m** (48 h) and **63a** (24 h) or **60m** (48 h) and 5-FU (24 h).

[c] Actual experimental values.

[d] Paired t-test was performed using GraphPad Prism software at p value < 0.05.

Thus these experiments have demonstrated a proof of principle that the hydrazide **60m** (and probably related analogs) under certain conditions sensitizes HCT 116 cells to **63a** and 5-FU. In the future, this concept of chemosensitization should be developed using other cell lines (including non- malignant ones) and changing the times of incubations prior to the addition of the cytotoxin.

6.4 Mechanisms of action

6.4.1 Mitochondrial membrane potential in HCT 116 cells using the TMRE dye and in Ramos cells using JC-1 dye

During oxidative phosphorylation, transfer of protons occurs via complexes in mitochondria resulting in electrochemical gradient across the membrane which generates the mitochondrial membrane potential. MMP is directly associated with ATP formation and any alterations is an early indicator for the oxidative stress. As mentioned earlier, the changes in MMP occurs due to various factors resulting in mitochondrial dysfunction and consequently undesired cell death. High $\Delta\psi_m$ significantly generates ROS. Elevation in the ROS levels leads to alterations in mitochondrial membrane permeability which in turn initiates degenerative processes. [105]

Diverse fluorescent lipophilic cationic dyes such as tetramethylrhodamine methyl (TMRM) and ethyl (TMRE) ester, Rhodamine 123, DiOC6(3) (3,3′-dihexyloxacarbocyanine iodide), and JC-1 are used for the determination of the MMP.[131] In this project, initial attempt was made to measure MMP using JC-1 dye because of its more selectivity than cellular membrane potential but JC-1 dye precipitated in McCoy's media (used for HCT 116 cells) after incubation resulting in false-positive results. Hence, we have used TMRE dye for **60m**, **64a**, **64e** and **64g** cytotoxins to monitor MMP changes towards HCT 116 cells. The potent cytotoxic agents **60m**, **64a**, **64e** and **64g** at its IC_{50} values were examined to determine whether interference with the MMP was one of the ways in which bioactivity was achieved. CCCP and 2,4-dinitrophenol depolarizes mitochondria by increasing the permeability of protons[132] exhibited lowest $\Delta\psi_m$. The three target compounds **64a**, **64e** and **64g** along with 5-FU lowered the MMP.

Our collaborators have used JC-1 dye for **60l** compound. The healthy cells having higher $\Delta\psi_m$ forms J-aggregates and a drop in $\Delta\psi_m$ results in formation of J-monomers. The collapse of $\Delta\psi_m$ may be due to early stage of apoptosis. The ratio of J-aggregates to J-monomers signals cell health or injury. Mitochondrial depolarisation leads to conversion of J-aggregates (healthy cells) to J-monomers (unhealthy cells). Compound **60l** causes 35% of depolarisation at its CC_{50} value of 0.19 µM towards Ramos cells and at its doubled CC_{50} value more than 65% of depolarisation was observed which is noteworthy. It will be interesting to investigate the effect of cytotoxins on mitochondrial functions and perform assays such as measuring ATP/ADP levels, oxygen

consumption determination, mitochondrial swelling assay, GST inhibition and activities of the electron transport chain complexes.

6.4.2 Evaluation of reactive oxygen species (ROS) levels in HCT 116 cells

Reactive oxygen species (ROS) such as hydrogen peroxide (H_2O_2), hydroxyl ion (OH^-) and superoxide anion (O_2^-) originate either from intracellular electron transport process in mitochondria during aerobic respiration or exogenously by interaction with xenobiotics.[133] In normal conditions, ROS acts as messengers and plays a crucial role in cell homeostasis via regulation of signaling pathways at lower concentrations.[134] The supply of nutrients and oxygen via angiogenesis allows cancer cells to proliferate resulting in hypermetabolism and higher ROS generation in cancer cells as compared to the healthy cells. In cancer cells, mitochondria, endoplasmic reticulum and enzymes such as NADPH oxidases contribute to high levels of ROS.[135] To counteract such levels, cancer cells increase their antioxidants activities by several mechanisms to maintain the redox levels and incapability to do so leads to oxidative stress inducing cell death.

Several mechanisms may be responsible for increase in the ROS levels. Any imbalance in intracellular ratio of GSSG/GSH or NADPH/NADP+ levels, mitochondrial mutations, electron transport dysfunction,[135] posttranslational changes of proteins,[136] release of cytochrome c and Ca^{+2} causing impaired permeability of mitochondrial membranes can damage the cellular constituents.[137] Excessive production of ROS during oxidative phosphorylation leads to oxidative stress which leads to alteration of mitochondrial proteins, damage to DNA and lipid peroxidation.[135,136] Consequently, the mitochondrial dysfunction results in imbalanced redox reactions leading to changes in mitochondrial membrane potential, less ATP formation[137], cell arrest[138] and apoptosis.[137] Their alterations can exacerbate neurogenerative disorders such as Alzheimer's and Parkinson diseases as well as musclar dystrophy and brain injury.[134]

DCF-DA (2′,7′–dichlorofluorescin diacetate) dye was used to measure ROS levels however this study did not detect different types of ROS (H_2O_2, OH^-) species. The main purpose was to study the effects of cytotoxins on ROS. About a 2-4 fold increase in ROS was measured after treatment of HCT 116 cells with IC_{50} concentrations of **60m**, **64a**, **64e**, and **64g** along with reference drug 5-FU. The order of intensities inducing elevation of ROS levels is as follows: **64e** > **64a** > **64g** > **60m** > 5-FU. This finding suggests that these cytotoxins impaired HCT 116 malignant cells growth

by increasing ROS levels. It would be also interesting to determine the antioxidant activity of these cytotoxins.

6.5 Future work

The first step in expanding the project is to determine structure-activity relationships of the target compounds and correlate the sizes of the atoms and nature of functional groups for better alignment with the cellular constituents. Moreover, *ex vitro* stability studies which mimic the *in vivo* environment should be carried out to examine any degradation of the target compounds, if any. If the compounds are degraded, then the possible metabolites should be identified by such techniques as LC-MS. It will be also interesting to investigate their mechanisms of actions and their effect on signaling pathways.

The next step can be the design and synthesis of varied analogs of lead molecule **64a** by incorporating various substituents with different electronic parameters onto the benzylidene ring attached to the piperidone ring. Additionally, a strong structure-activity relationship may be established. Further, it may be important to know whether these analogs act by the same mechanisms. The results showed that the target compounds have some effect on mitochondria; however, the exact mechanisms are yet to be addressed. Different mechanisms may be responsible for apoptosis such as mitochondrial swelling, regulation of GST/GSH levels, changes in an electron respiratory complex, damaging mitochondrial DNA and increase in intracellular ROS levels. Thus, it will be interesting to investigate the mode of action studies for these compounds.

Later after confirming the activity of the lead cytotoxin **64a** *in vitro*, further evaluation can be carried out *in vivo* because of its likelihood for drug-like properties (Table 6.1).

CHAPTER 7 : CONCLUSIONS

A series of novel N^1-acylhydrazides **64a-g** as potential cytotoxic agents having 1,5-diaryl-3-oxo-1,4-pentadienyl and N^1-acylhydrazides pharmacophores were developed. The auxiliary binder N^1-acryloyl-3,4-dimethoxylbenzohydrazide **60m** is the lead compound in series **60** which inhibits the proliferation of HCT 116 cells with an IC_{50} value of 15.3 µM. Moreover, **60m** is highly selective towards some colon cancer cells with a SI value of more than 6.55. The combinatorial study revealed that the auxiliary binder **60m** acts as a chemosensitizer to 3,5-bis(benzylidene)-4-piperidone **63a** as well as the reference drug 5-FU towards colon HCT 116 cancer cells.

The auxiliary binders **60j**, **60k** and **60l** inhibited the proliferation of MCF-7 breast cells and **60l** was found to be the most potent compound with an IC_{50} value of 3.18 µM and a SI value > 31. These auxiliary binders showed weak growth inhibition at 10 µM concentration towards MDA-MB-231 cells. This means that these compounds are more susceptible in the presence of estrogen and progesterone environments of MCF-7 cancer cells than in triple negative MDA-MB-231 breast malignant cells. The selectivity of these cytotoxic agents towards MCF-7 is quite interesting and further investigations in regard to its mode of action should be carried out.

The auxiliary binders **60a-m**, **61a**, **62a-b** and **63a** were evaluated against a number of oral carcinomas as well as normal cell lines by our collaborators in Japan. Although only a few agents show some activity, compound **63a** displayed noticeable results with good selectivity towards oral malignant cells than non-malignant cells. Another study was conducted by our collaborators in El Paso who found some remarkable results when these auxiliary binders were screened against various leukemic cell lines as well as normal cell lines. The auxiliary binders **60a**, **60d**, **60h** and **60l** not only killed 50 % of cancer cells at the average CC_{50} values less than 0.3 µM but were also highly selective towards Ramos leukemic cells. In particular, compound **60l** showed more than 90 % selectivity. Thus compound **60l** was further investigated for its mode of action of causing cell death and a mitochondrial membrane potential (MMP) study was conducted by our collaborators using the JC-1 dye. The results showed that by employing twice the CC_{50} concentration, there is 2-fold increase in the mitochondrial depolarization.

A series of novel cytotoxins were developed and compound **64e** possessing a nitro substitution at the para position of the arylidene ring of 4-piperidone and having a 3,4-dimethoxy group in the

terminal ring was the most potent compound (IC_{50} = 0.28 μM) against HCT 116 cancer cells; however compound **64a** emerged as the lead cytotoxin as there is a possibility that nitro groups may form toxic metabolites like imines, hydroxylamines and amines *in vivo*. In general, all the target compounds were selectively toxic towards colon HCT 116 malignant cells than CRL-1790 non-malignant cells. The collapse of the mitochondrial membrane potential in HCT 116 cells by **64a**, **64e** and **64g** confirmed that mitochondria are an important target involved in cell death. Compounds **60m**, **64a**, **64e** and **64g** resulted in a 2-4 fold increase of ROS levels, however, the exact mechanism for the higher induction of ROS levels should be further examined.

APPENDIX

Appendix A

Table 1 indicates one-way ANOVA with Dunnett's multiple comparison post-hoc analysis of each compound when compared to DMSO to study the effect on MMP in HCT 116 cells using the TMRE dye.

Dunnett's multiple comparisons test	**Mean Diff.**	**95% CI of diff.**	**Significant p <0.05**
DMSO vs. 5-FU	-4136	-6645 to -1626	Yes
DMSO vs. CCCP	8734	6224 to 11243	Yes
DMSO vs. 2,4-DNP	4417	1908 to 6927	Yes
DMSO vs. **60m**	-10715	-13224 to -8205	Yes
DMSO vs. **64a**	-3530	-6040 to -1020	Yes
DMSO vs. **64e**	3682	1173 to 6192	Yes
DMSO vs. **64g**	-3225	-5734 to -715.2	Yes

All the values were significantly different with a *p* value < 0.05. The GraphPad Prism program was used for the statistical analysis.[139]

Appendix B

Table 2 indicates one-way ANOVA with Dunnett's multiple comparison post-hoc analysis of **60l** when compared to DMSO to study the effect on MMP in Ramos cells for JC-1 aggregates.

Dunnett's multiple comparisons test	**Mean Diff.**	**95% CI of diff.**	**Significant p <0.05**
DMSO vs. **60l** CC_{50}	14.10	3.267 to 24.93	Yes
DMSO vs. **60l** $2xCC_{50}$	47.30	36.47 to 58.13	Yes
DMSO vs. untreated cells	-2.067	-12.90 to 8.766	No
DMSO vs. H_2O_2	80.40	69.57 to 91.23	Yes

All the values were significantly different with a *p* value < 0.05 except for the values of DMSO and the untreated cells. The GraphPad Prism program was used for the statistical analysis.[139]

Appendix C

Table 3 indicates one-way ANOVA with Dunnett's multiple comparison post-hoc analysis of **60l** when compared to DMSO to study the effect on MMP in Ramos cells for JC-1 monomers.

Dunnett's multiple comparisons test	**Mean Diff.**	**95% CI of diff.**	**Significant p <0.05**
DMSO vs. **60l** CC_{50}	-14.10	-24.93 to -3.267	Yes
DMSO vs. **60l** $2xCC_{50}$	-47.30	-58.13 to -36.47	Yes
DMSO vs. untreated cells	2.067	- 8.766 to 12.90	No
DMSO vs. H_2O_2	-80.40	-91.23 to -69.57	Yes

All the values were significantly different with a *p* value < 0.05 except for the values of DMSO and the untreated cells. The GraphPad Prism program was used for the statistical analysis.[139]

Appendix D

Table 4 indicates one-way ANOVA with Dunnett's multiple comparison post-hoc analysis of each compound when compared to DMSO to study the effect of ROS levels in HCT 116 cells.

Dunnett's multiple comparisons test	**Mean Diff.**	**95% CI of diff.**	**Significant p <0.05**
DMSO vs. H_2O_2	-18500	-20099 to -16901	Yes
DMSO vs. 5-FU	-3977	-5576 to -2378	Yes
DMSO vs. **60m**	-6148	-7747 to -4549	Yes
DMSO vs. **64a**	-7863	-9461 to -6264	Yes
DMSO vs. **64e**	-14071	-15670 to -12472	Yes
DMSO vs. **64g**	-5940	-7539 to -4341	Yes

All the values were significantly different with a *p* value < 0.05. The GraphPad Prism program was used for the statistical analysis.[139]

REFERENCES

(1) *WHO. Cancer Factsheet*; World Health Organization, 2018.

(2) Aitken, M.; Kleinrock, M.; Kumar, S. Global Oncology Trends 2017. Advances, Complexity and Cost. *QuintilesIMS Institute* **2017**, *June*, 1–40.

(3) Canadian Cancer Society's Advisory Committee on Cancer Statistics. Canadian Cancer Statistics 2017. *Canadian Cancer Society*. Toronto ON: Canadian Cancer Society 2017.

(4) Johnstone, R. W.; Ruefli, A. A.; Lowe, S. W. Apoptosis: A Link between Cancer Genetics and Chemotherapy. *Cell* **2002**, *108* (2), 153–164.

(5) Harris, A. L. Angiogenesis as a New Target for Cancer Control. *European Journal of Cancer Supplements* **2003**, *1* (2), 1–12.

(6) Pecorino, L. The Cell Cycle; Growth Inhibition and Tumor Suppressor Genes. In *Molecular Biology of Cancer : Mechanisms, Targets, and Therapeutics*; Oxford University Press, 2016; pp 109–154.

(7) Khleif, S., Rixe, O., Skeel, R. T. Biologic and Pharmacologic Basis of Cancer Chemotherapy. In *Skeel's Handbook of Cancer Therapy*; Philadelphia : Wolters Kluwer Health, 2016; pp 1–16.

(8) Bland, J. S.; Minich, D. M.; Eck, B. M. A Systems Medicine Approach: Translating Emerging Science into Individualized Wellness. *Advances in Medicine* **2017**, *2017*, 1–5.

(9) Mordente, A.; Meucci, E.; Martorana, G. E.; Silvestrini, A. Cancer Biomarkers Discovery and Validation: State of the Art, Problems and Future Perspectives. In *Advances in Cancer Biomarkers*; Advances in Experimental Medicine and Biology; Springer Netherlands, 2015; Vol. 867, pp 9–26.

(10) Chinen, L. T. D.; Abdallah, E. A.; Braun, A. C.; Flores, B. de C. T. de C.; Corassa, M.; Sanches, S. M.; Fanelli, M. F. Circulating Tumor Cells as Cancer Biomarkers in the Clinic. In *Isolation and Molecular Characterization of Circulating Tumor Cells*; Advances in Experimental Medicine and Biology, 2017; pp 1–41.

(11) Krebs, M. G.; Hou, J.-M.; Ward, T. H.; Blackhall, F. H.; Dive, C. Circulating Tumour Cells: Their Utility in Cancer Management and Predicting Outcomes. *Therapeutic Advances in Medical Oncology* **2010**, *2* (6), 351–365.

(12) Satelli, A.; Batth, I. S.; Brownlee, Z.; Rojas, C.; Meng, Q. H.; Kopetz, S.; Li, S. Potential Role of Nuclear PD-L1 Expression in Cell-Surface Vimentin Positive Circulating Tumor Cells as a Prognostic Marker in Cancer Patients. *Scientific Reports* **2016**, *6*, 28910.

(13) Faivre, S.; Djelloul, S.; Raymond, E. New Paradigms in Anticancer Therapy: Targeting Multiple Signaling Pathways With Kinase Inhibitors. *Seminars in Oncology* **2006**, *33* (4), 407–420.

(14) George, D. J.; Moore, C. Angiogenesis Inhibitors in Clinical Oncology. *Update on Cancer Therapeutics* **2006**, *1* (4), 429–434.

(15) Pandya, N. M.; Dhalla, N. S.; Santani, D. D. Angiogenesis—a New Target for Future Therapy. *Vascular Pharmacology* **2006**, *44* (5), 265–274.

(16) Ribatti, D.; Vacca, A.; Nico, B.; Sansonno, D.; Dammacco, F. Angiogenesis and Anti-Angiogenesis in Hepatocellular Carcinoma. *Cancer Treatment Reviews* **2006**, *32* (6), 437–444.

(17) Zhong, H.; Bowen, J. P. Antiangiogenesis Drug Design: Multiple Pathways Targeting Tumor Vasculature. *Current Medicinal Chemistry* **2006**, *13* (8), 849–862.

(18) Burke, P. A.; DeNardo, S. J. Antiangiogenic Agents and Their Promising Potential in Combined Therapy. *Critical Reviews in Oncology/Hematology* **2001**, *39*, 155–171.

(19) Sakurai, K.; Yamada, N.; Yashiro, M.; Matsuzaki, T.; Komatsu, M.; Ohira, M.; Miwa, A.; Hirakawa, K. A Novel Angiogenesis Inhibitor, Ki23057, Is Useful for Preventing the Progression of Colon Cancer and the Spreading of Cancer Cells to the Liver. *European Journal of Cancer* **2007**, *43* (17), 2612–2620.

(20) Zhang, S. Antibody Therapies in Cancer. In *Progress in Cancer Immunotherapy*; Advances in Experimental Medicine and Biology; Springer Netherlands, 2016; Vol. 909, pp 1–67.

(21) Bardelli, A.; Siena, S. Molecular Mechanisms of Resistance to Cetuximab and Panitumumab in Colorectal Cancer. *Journal of Clinical Oncology* **2010**, *28* (7), 1254–1261.

(22) Davey, P., Wilcox, M., Irving, W., Thwaites, G. Mechanisms of Action and Resistance to Modern Antibacterials, with a History of Their Development. In *Antimicrobial Chemotherapy*; Oxford University Press, 2015; pp 3–9.

(23) Muhammad, Y; Kerr, S. Comparative Effects of Cinnamaldehyde and Cinnamyl-Containing Compounds on the Viability of Two Human Melanoma Cell Lines, SK-MEL19 and SK-MEL23 (LB611). *Experimental Biology Conference* **2014**, AN: 714229.

(24) Deshmukh, R. R.; Kim, S.; Elghoul, Y.; Dou, Q. P. P-Glycoprotein Inhibition Sensitizes Human Breast Cancer Cells to Proteasome Inhibitors. *Journal of Cellular Biochemistry* **2017**, *118* (5), 1239–1248.

(25) Jia, H.; Yang, Q.; Wang, T.; Cao, Y.; Jiang, Q. Y.; Ma, H. Da; Sun, H. W.; Hou, M. X.; Yang, Y. P.; Feng, F. Rhamnetin Induces Sensitization of Hepatocellular Carcinoma Cells to a Small Molecular Kinase Inhibitor or Chemotherapeutic Agents. *Biochimica et Biophysica Acta - General Subjects* **2016**, *1860* (7), 1417–1430.

(26) Wang, H. Y.; Zhang, Y.; Zhou, Y.; Lu, Y. Y.; Wang, W. F.; Xin, M.; Guo, X. L. Rosiglitazone Elevates Sensitization of Drug-Resistant Oral Epidermoid Carcinoma Cells to Vincristine by G2/M-Phase Arrest, Independent of PPAR-γ Pathway. *Biomedicine and Pharmacotherapy* **2016**, *83*, 349–361.

(27) Hajjaji, N.; Bougnoux, P. Selective Sensitization of Tumors to Chemotherapy by Marine-Derived Lipids: A Review. *Cancer Treatment Reviews* **2013**, *39* (5), 473–488.

(28) Shi, L.; Fei, X.; Wang, Z. Demethoxycurcumin Was Prior to Temozolomide on Inhibiting Proliferation and Induced Apoptosis of Glioblastoma Stem Cells. *Tumor Biology* **2015**, *36* (9), 7107–7119.

(29) Chen, L.; Wang, L.; Shen, H.; Lin, H.; Li, D. Anthelminthic Drug Niclosamide Sensitizes the Responsiveness of Cervical Cancer Cells to Paclitaxel via Oxidative Stress-Mediated MTOR Inhibition. *Biochemical and Biophysical Research Communications* **2017**, *484* (2), 416–421.

(30) Meade, G. Chemical Modulation of Chemotherapy Resistance in Cultured Oesophageal Carcinoma Cells. *Biochemical Society Transactions* **2000**, *28* (2), 27–32.

(31) Amslinger, S. The Tunable Functionality of α,β-Unsaturated Carbonyl Compounds Enables Their Differential Application in Biological Systems. *ChemMedChem* **2010**, *5* (3), 351–356.

(32) Jha, A.; Mukherjee, C.; Rolle, A. J.; De Clercq, E.; Balzarini, J.; Stables, J. P. Cytostatic Activity of Novel 4′-Aminochalcone-Based Imides. *Bioorganic and Medicinal Chemistry Letters* **2007**, *17* (16), 4545–4550.

(33) K. Sahu, N.; S. Balbhadra, S.; Choudhary, J.; V. Kohli, D. Exploring Pharmacological Significance of Chalcone Scaffold: A Review. *Current Medicinal Chemistry* **2012**, *19* (2), 209–225.

(34) Sun, J.; Hou, G.; Zhao, F.; Cong, W.; Li, H.; Liu, W.; Wang, C. Synthesis, Antiproliferative, and Multidrug Resistance Reversal Activities of Heterocyclic α,β-Unsaturated Carbonyl Compounds. *Chemical Biology and Drug Design* **2016**, *88* (4), 534–541.

(35) Pati, H. H. N.; Das, U.; Sharma, R. K.; Dimmock, J. R. Cytotoxic Thiol Alkylators. *Mini Reviews in Medicinal Chemistry* **2007**, *7*, 131–139.

(36) Britten, R. A.; Green, J. A.; Warenius, H. M. Cellular Glutathione (GSH) and Glutathione S-Transferase (GST) Activity in Human Ovarian Tumor Biopsies Following Exposure to Alkylating Agents. *International Journal of Radiation Oncology, Biology, Physics* **1992**, *24* (3), 527–531.

(37) Ferrari, E.; Pignedoli, F.; Imbriano, C.; Marverti, G.; Basile, V.; Venturi, E.; Saladini, M. Newly Synthesized Curcumin Derivatives: Crosstalk between Chemico-Physical Properties and Biological Activity. *Journal of Medicinal Chemistry* **2011**, *54* (23), 8066–8077.

(38) Liu, G. Y.; Zhai, Q.; Chen, J. Z.; Zhang, Z. Q.; Yang, J. 2,2′-Fluorine Mono-Carbonyl Curcumin Induce Reactive Oxygen Species-Mediated Apoptosis in Human Lung Cancer NCI-H460 Cells. *European Journal of Pharmacology* **2016**, *786*, 161–168.

(39) Liang, B.; Liu, Z.; Cao, Y.; Zhu, C.; Zuo, Y.; Huang, L.; Wen, G.; Shang, N.; Chen, Y.; Yue, X.; et al. MC37, A New Mono-Carbonyl Curcumin Analog, Induces G2/M Cell Cycle Arrest and Mitochondria-Mediated Apoptosis in Human Colorectal Cancer Cells. *European Journal of Pharmacology* **2017**, *796*, 139–148.

(40) Jin, T.; Song, Z.; Weng, J.; Fantus, I. G. Curcumin and Other Dietary Polyphenols: Potential Mechanisms of Metabolic Actions and Therapy for Diabetes and Obesity. *American Journal of Physiology-Endocrinology and Metabolism* **2018**, *314* (3), E201–E205.

(41) Qureshi, M.; Al-Suhaimi, E. A.; Wahid, F.; Shehzad, O.; Shehzad, A. Therapeutic Potential of Curcumin for Multiple Sclerosis. *Neurological Sciences* **2017**, 1–8.

(42) Momtazi-Borojeni, A. A.; Haftcheshmeh, S. M.; Esmaeili, S. A.; Johnston, T. P.; Abdollahi, E.; Sahebkar, A. Curcumin: A Natural Modulator of Immune Cells in Systemic Lupus Erythematosus. *Autoimmunity Reviews* **2017**, *17* (2), 125–135.

(43) Mounce, B. C.; Cesaro, T.; Carrau, L.; Vallet, T.; Vignuzzi, M. Curcumin Inhibits Zika and Chikungunya Virus Infection by Inhibiting Cell Binding. *Antiviral Research* **2017**, *142*, 148–157.

(44) Holder, G. M.; Plummer, J. L.; Ryan, A. J. The Metabolism and Excretion of Curcumin (1,7-Bis-(4-Hydroxy-3-Methoxyphenyl)-1,6-Heptadiene-3,5-Dione) in the Rat. *Xenobiotica* **1978**, *8* (12), 761–768.

(45) Dinkova-Kostova, T.; Talalay, P. Relation of Structure of Curcumin Analogs to Their Potencies as Inducers of Phase 2 Detoxification Enzymes. *Carcinogenesis* **1999**, *20* (5), 911–914.

(46) Sharma, R. A.; Steward, W. P.; Gescher, A. J. Pharmacokinetics and Pharmacodynamics of Curcumin. In *The Molecular Targets and Therapeutic Uses of Curcumin in Health and Disease*; Springer US, 2007; Vol. 595, pp 453–470.

(47) Jäger, R.; Lowery, R. P.; Calvanese, A. V.; Joy, J. M.; Purpura, M.; Wilson, J. M. Comparative Absorption of Curcumin Formulations. *Nutrition Journal* **2014**, *13* (1), 1–8.

(48) Nelson, K. M.; Dahlin, J. L.; Bisson, J.; Graham, J.; Pauli, G. F.; Walters, M. A. The Essential Medicinal Chemistry of Curcumin. *Journal of Medicinal Chemistry* **2017**, *60* (5), 1620–1637.

(49) Singh, R. K.; Rai, D.; Yadav, D.; Bhargava, A.; Balzarini, J.; De Clercq, E. Synthesis, Antibacterial and Antiviral Properties of Curcumin Bioconjugates Bearing Dipeptide, Fatty Acids and Folic Acid. *European Journal of Medicinal Chemistry* **2010**, *45* (3), 1078–1086.

(50) Solano, L. N.; Nelson, G. L.; Ronayne, C. T.; Lueth, E. A.; Foxley, M. A.; Jonnalagadda, S. K.; Gurrapu, S.; Mereddy, V. R. Synthesis, in Vitro, and in Vivo Evaluation of Novel Functionalized Quaternary Ammonium Curcuminoids as Potential Anti-Cancer Agents. *Bioorganic and Medicinal Chemistry Letters* **2015**, *25* (24), 5777–5780.

(51) Weng, Q.; Fu, L.; Chen, G.; Hui, J.; Song, J.; Feng, J.; Shi, D.; Cai, Y.; Ji, J.; Liang, G. Design, Synthesis, and Anticancer Evaluation of Long-Chain Alkoxylated Mono-Carbonyl Analogues of Curcumin. *European Journal of Medicinal Chemistry* **2015**, *103*, 44–55.

(52) Hsieh, M. T.; Chang, L. C.; Hung, H. Y.; Lin, H. Y.; Shih, M. H.; Tsai, C. H.; Kuo, S. C.; Lee, K. H. New Bis(Hydroxymethyl) Alkanoate Curcuminoid Derivatives Exhibit Activity against Triple-Negative Breast Cancer in Vitro and in Vivo. *European Journal of Medicinal Chemistry* **2017**, *131*, 141–151.

(53) Sanabria-Ríos, D. J.; Rivera-Torres, Y.; Rosario, J.; Ríos, C.; Gutierrez, R.; Carballeira, N. M.; Vélez, C.; Zayas, B.; Álvarez-Colón, F.; Ortiz-Soto, G.; et al. Synthesis of Novel C5-Curcuminoid-Fatty Acid Conjugates and Mechanistic Investigation of Their Anticancer Activity. *Bioorganic and Medicinal Chemistry Letters* **2015**, *25* (10), 2174–2180.

(54) Patil, V. S.; Gutierrez, A. M.; Sunkara, M.; Morris, A. J.; Hilt, J. Z.; Kalika, D. S.; Dziubla, T. D. Curcumin Acrylation for Biological and Environmental Applications. *Journal of*

Natural Products **2017**, *80* (7), 1964–1971.

(55) Wattamwar, P. P.; Biswal, D.; Cochran, D. B.; Lyvers, A. C.; Eitel, R. E.; Anderson, K. W.; Hilt, J. Z.; Dziubla, T. D. Synthesis and Characterization of Poly(Antioxidant β-Amino Esters) for Controlled Release of Polyphenolic Antioxidants. *Acta Biomaterialia* **2012**, *8* (7), 2529–2537.

(56) Cassano, R.; Trombino, S.; Ferrarelli, T.; Bilia, A. R.; Bergonzi, M. C.; Russo, A.; De Amicis, F.; Picci, N. Preparation, Characterization and in Vitro Activities Evaluation of Curcumin Based Microspheres for Azathioprine Oral Delivery. *Reactive and Functional Polymers* **2012**, *72* (7), 446–450.

(57) Das, U.; Sharma, R. K.; Dimmock, J. R. 1,5-Diaryl-3-Oxo-1,4-Pentadienes: A Case for Antineoplastics With Multiple Targets. *Current Medicinal Chemistry* **2009**, *16* (16), 2001–2020.

(58) Dimmock, J. R. ; Advikolanu, K. M. ; Scott, H. E. ; Duffy, M. J. ; Reid, R. S. ; Quail, J. W. ; Jia, Z. ; Hickie, R. A. ; Allen, T. M. ; Rutledge, J. M. ; Tempest, M. L. ; Oreski, A. B. Evaluation of Cytotoxicity of Some Mannich Bases of Various Aryl and Arylidene Ketones and Their Corresponding Arylhydrazones. *Journal of Pharmaceutical Sciences* **1992**, *81*, 1142–1152.

(59) Dimmock, J. R.; Wonko, S. L.; Hickie, R. A.; Ambrose, S. J.; Reid, R. S.; Mutus, B.; Talpas, C. J.; Tuer, R. G. Evaluation of Some Mannich Bases of Conjugated Styryl Ketones and Related Compounds versus the WiDr Colon Cancer in Vitro. *European Journal of Medicinal Chemistry* **1989**, *24*, 217–226.

(60) Sexton, D. J.; Dimmock, J. R.; Mutus, B. A Spectrophotometric Glutathione S-Transferase Assay Displaying Alpha-Class Selectivity Utilizing 1-*p*-Chlorophenyl-4,4-Dimethyl-5-Diethylamino-1-Penten-3- One Hydrobromide. *Biochemistry and Cell biology* **1993**, *71* (1–2).

(61) Pati, H. N.; Das, U.; Ramirez-Erosa, I. J.; Dunlop, D. M.; Hickie, R. A.; Dimmock, J. R. Alpha-Substituted 1-Aryl-3-Dimethylaminopropanone Hydrochlorides: Potent Cytotoxins towards Human WiDr Colon Cancer Cells. *Chemical and Pharmaceutical bulletin* **2007**, *55* (4), 511–515.

(62) Dimmock, J. R.; Kumar, P.; Quail, J. W.; Pugazhenthi, U.; Yang, J.; Chen, M.; Reid, R. S.; Allen, T. M.; Kao, G. Y.; Cole, S. P. C.; et al. Synthesis and Cytotoxic Evaluation of Some Styryl Ketones and Related Compounds. *European Journal of Medicinal Chemistry* **1995**, *30* (3), 209–217.

(63) Dimmock, J. R.; Arora, V. K.; Wonko, S. L.; Hamon, N. W.; Quail, J. W.; Jia, Z.; Warrington, R. C.; Fang, W. D.; Lee, J. S. 3,5-Bis-Benzylidene-4-Piperidones and Related Compounds with High Activity towards P388 Leukemia Cells. *Drug Design and Delivery* **1990**, *6* (3), 183–194.

(64) Dimmock, J. R.; Padmanilayam, M. P.; Puthucode, R. N.; Nazarali, A. J.; Motaganahalli, N. L.; Zello, G. A.; Quail, J. W.; Oloo, E. O.; Kraatz, H. B.; Prisciak, J. S.; et al. A Conformational and Structure-Activity Relationship Study of Cytotoxic 3,5-Bis(Arylidene)-4-Piperidones and Related N-Acryloyl Analogues. *Journal of Medicinal*

Chemistry **2001**, *44* (4), 586–593.

(65) Pati, H. N.; Das, U.; Quail, J. W.; Kawase, M.; Sakagami, H.; Dimmock, J. R. Cytotoxic 3,5-Bis(Benzylidene)Piperidin-4-Ones and N-Acyl Analogs Displaying Selective Toxicity for Malignant Cells. *European Journal of Medicinal Chemistry* **2008**, *43* (1), 1–7.

(66) Dimmock, J. R.; Arora, V. K.; Chen, M.; Allen, T. M.; Kao, G. Y. Cytotoxic Evaluation of Some N-Acyl and N-Acyloxy Analogues of 3,5-Bis(Arylidene)-4-Piperidones. *Drug Design and Discovery* **1994**, *12* (1), 19–28.

(67) Das, U.; Das, S.; Bandy, B.; Stables, J. P.; Dimmock, J. R. N-Aroyl-3,5-Bis(Benzylidene)-4-Piperidones: A Novel Class of Antimycobacterial Agents. *Bioorganic and Medicinal Chemistry* **2008**, *16* (7), 3602–3607.

(68) Das, U.; Singh, R. S. P.; Alcorn, J.; Hickman, M. R.; Sciotti, R. J.; Leed, S. E.; Lee, P. J.; Roncal, N.; Dimmock, J. R. 3,5-Bis(Benzylidene)-4-Piperidones and Related N-Acyl Analogs: A Novel Cluster of Antimalarials Targeting the Liver Stage of Plasmodium Falciparum. *Bioorganic and Medicinal Chemistry* **2013**, *21* (23), 7250–7256.

(69) Adams, B. K.; Ferstl, E. M.; Davis, M. C.; Herold, M.; Kurtkaya, S.; Camalier, R. F.; Hollingshead, M. G.; Kaur, G.; Sausville, E. A.; Rickles, F. R.; et al. Synthesis and Biological Evaluation of Novel Curcumin Analogs as Anti-Cancer and Anti-Angiogenesis Agents. *Bioorganic and Medicinal Chemistry* **2004**, *12* (14), 3871–3883.

(70) Adams, B. K.; Cai, J.; Armstrong, J.; Herold, M.; Lu, Y. J.; Sun, A.; Snyder, J. P.; Liotta, D. C.; Jones, D. P.; Shoji, M. EF24, a Novel Synthetic Curcumin Analog, Induces Apoptosis in Cancer Cells via a Redox-Dependent Mechanism. *Anti-Cancer Drugs* **2005**, *16* (3), 263–275.

(71) Thomas, S. L.; Zhong, D.; Zhou, W.; Malik, S.; Liotta, D.; Snyder, J. P.; Hamel, E.; Giannakakou, P. EF24, a Novel Curcumin Analog, Disrupts the Microtubule Cytoskeleton and Inhibits HIF-1. *Cell Cycle* **2008**, *7* (15), 2409–2417.

(72) Yin, D. L.; Liang, Y. J.; Zheng, T. Sen; Song, R. P.; Wang, J. B.; Sun, B. S.; Pan, S. H.; Qu, L. D.; Liu, J. R.; Jiang, H. C.; et al. EF24 Inhibits Tumor Growth and Metastasis via Suppressing NF-KappaB Dependent Pathways in Human Cholangiocarcinoma. *Scientific Reports* **2016**, *6* (March), 1–11.

(73) Vilekar, P.; King, C.; Lagisetty, P.; Awasthi, V.; Awasthi, S. Antibacterial Activity of Synthetic Curcumin Derivatives: 3,5-Bis(Benzylidene)-4-Piperidone (EF24) and EF24-Dimer Linked via Diethylenetriaminepentacetic Acid (EF2DTPA). *Applied Biochemistry and Biotechnology* **2014**, *172* (7), 3363–3373.

(74) Modzelewska, A.; Pettit, C.; Achanta, G.; Davidson, N. E.; Huang, P.; Khan, S. R. Anticancer Activities of Novel Chalcone and Bis-Chalcone Derivatives. *Bioorganic and Medicinal Chemistry* **2006**, *14* (10), 3491–3495.

(75) Li, N.; Xin, W. Y.; Yao, B. R.; Wang, C. H.; Cong, W.; Zhao, F.; Li, H. J.; Hou, Y.; Meng, Q. G.; Hou, G. G. Novel Dissymmetric 3,5-Bis(Arylidene)-4-Piperidones as Potential Antitumor Agents with Biological Evaluation in Vitro and in Vivo. *European Journal of Medicinal Chemistry* **2018**, *147*, 21–33.

(76) Karki, S. S.; Das, U.; Umemura, N.; Sakagami, H.; Iwamoto, S.; Kawase, M.; Balzarini, J.; De Clercq, E.; Dimmock, S. G.; Dimmock, J. R. 3,5-Bis(3-Alkylaminomethyl-4-Hydroxybenzylidene)-4-Piperidones: A Novel Class of Potent Tumor-Selective Cytotoxins. *Journal of Medicinal Chemistry* **2016**, *59* (2), 763–769.

(77) Abdullah Bar, A. O. Enhancement of the Cytotoxic Activity of Some α,β-Unsaturated Ketones through Auxiliary Binding, MSc. Thesis, University of Saskatchewan, 2012.

(78) Santiago-Vázquez, Y.; Das, U.; Varela-Ramirez, A.; Baca, S. T.; Ayala-Marin, Y.; Lema, C.; Das, S.; Baryyan, A.; Dimmock, J. R.; Aguilera, R. J. Tumor-Selective Cytotoxicity of a Novel Pentadiene Analogue on Human Leukemia/Lymphoma Cells. *Clinical Cancer Drugs* **2016**, *3* (2), 138–146.

(79) Chen, Q.; Hou, Y.; Hou, G.-G.; Sun, J.-F.; Li, N.; Cong, W.; Zhao, F.; Li, H. J.; Wang, C.-H. Design, Synthesis, Anticancer Activity and Cytotoxicity of Novel 4-Piperidone/Cyclohexanone Derivatives. *Research on Chemical Intermediates* **2016**, *42* (12), 8119–8130.

(80) Dimmock, J. R.; Arora, V. K.; Duffy, M. J.; Reid, R. S.; Allen, T. M.; Kao, G. Y. Evaluation of Some N-Acyl Analogues of 3,5-Bis(Arylidene)-4-Piperidones for Cytotoxic Activity. *Drug Design and Discovery* **1992**, *8* (4), 291–299.

(81) Das, U.; Alcorn, J.; Shrivastav, A.; Sharma, R. K.; De Clercq, E.; Balzarini, J.; Dimmock, J. R. Design, Synthesis and Cytotoxic Properties of Novel 1-[4-(2-Alkylaminoethoxy)Phenylcarbonyl]-3,5-Bis(Arylidene)-4-Piperidones and Related Compounds. *European Journal of Medicinal Chemistry* **2007**, *42* (1), 71–80.

(82) Das, U.; Sakagami, H.; Chu, Q.; Wang, Q.; Kawase, M.; Selvakumar, P.; Sharma, R. K.; Dimmock, J. R. 3,5-Bis(Benzylidene)-1-[4-2-(Morpholin-4-Yl)Ethoxyphenylcarbonyl]-4-Piperidone Hydrochloride: A Lead Tumor-Specific Cytotoxin which induces Apoptosis and Autophagy. *Bioorganic and Medicinal Chemistry Letters* **2010**, *20* (3), 912–917.

(83) Das, U.; Pati, H. N.; Sakagami, H.; Hashimoto, K.; Kawase, M.; Balzarini, J.; De Clercq, E.; Dimmock, J. R. 3,5-Bis(Benzylidene)-1-[3-(2-Hydroxyethylthio)Propanoyl]Piperidin-4-Ones: A Novel Cluster of Potent Tumor-Selective Cytotoxins. *Journal of Medicinal Chemistry* **2011**, *54* (9), 3445–3449.

(84) Hossain, M.; Das, U.; Umemura, N.; Sakagami, H.; Balzarini, J.; De Clercq, E.; Kawase, M.; Dimmock, J. R. Tumour-Specific Cytotoxicity and Structure–activity Relationships of Novel 1-[3-(2-Methoxyethylthio)Propionyl]-3,5-Bis(Benzylidene)-4-Piperidones. *Bioorganic and Medicinal Chemistry* **2016**, *24* (10), 2206–2214.

(85) Das, S.; Das, U.; Selvakumar, P.; Sharma, R. K.; Balzarini, J.; De Clercq, E.; Molnár, J.; Serly, J.; Baráth, Z.; Schatte, G.; et al. 3,5-Bis(Benzylidene)-4-Oxo-1-Phosphonopiperidines and Related Diethyl Esters: Potent Cytotoxins with Multi-Drug-Resistance Reverting Properties. *ChemMedChem* **2009**, *4* (11), 1831–1840.

(86) Das, S.; Das, U.; Sakagami, H.; Hashimoto, K.; Kawase, M.; Gorecki, D. K. J.; Dimmock, J. R. Sequential Cytotoxicity: A Theory Examined Using a Series of 3,5-Bis(Benzylidene)-1-Diethylphosphono-4-Oxopiperidines and Related Phosphonic Acids. *Bioorganic and Medicinal Chemistry Letters* **2010**, *20* (22), 6464–6468.

(87) Sun, J.; Wang, S.; Li, H.; Jiang, W.; Hou, G.; Zhao, F.; Cong, W. Synthesis, Antitumor Activity Evaluation of Some New N-Aroyl-α,β-Unsaturated Piperidones with Fluorescence. *Journal of Enzyme Inhibition and Medicinal Chemistry* **2016**, *31* (3), 495–502.

(88) Huber, I.; Zupkó, I.; Kovács, I. J.; Minorics, R.; Gulyás-Fekete, G.; Maász, G.; Perjési, P. Synthesis and Antiproliferative Activity of Cyclic Arylidene Ketones: A Direct Comparison of Monobenzylidene and Dibenzylidene Derivatives. *Monatshefte für Chemie - Chemical Monthly* **2015**, *146* (6), 973–981.

(89) Popiołek, Ł. Hydrazide–hydrazones as Potential Antimicrobial Agents: Overview of the Literature since 2010. *Medicinal Chemistry Research* **2017**, *26* (2), 287–301.

(90) Khan, M. S.; Siddiqui, S. P.; Tarannum, N. A Systematic Review on the Synthesis and Biological Activity of Hydrazide Derivatives. *Hygeia: Journal for Drugs and Medicines* **2017**, *9*, 61–79.

(91) Dimmock, J. R.; Vashishtha, S. C.; Stables, J. P. Anticonvulsant Properties of Various Acetylhydrazones, Oxamoylhydrazones and Semicarbazones Derived from Aromatic and Unsaturated Carbonyl Compounds. *European Journal of Medicinal Chemistry* **2000**, *35* (2), 241–248.

(92) Ke, S. Y.; Qian, X. H.; Liu, F. Y.; Wang, N.; Yang, Q.; Li, Z. Novel 4H-1,3,4-Oxadiazin-5(6H)-Ones with Hydrophobic and Long Alkyl Chains: Design, Synthesis, and Bioactive Diversity on Inhibition of Monoamine Oxidase, Chitin Biosynthesis and Tumor Cell. *European Journal of Medicinal Chemistry* **2009**, *44* (5), 2113–2121.

(93) Li, L. Y.; Peng, J. Di; Zhou, W.; Qiao, H.; Deng, X.; Li, Z. H.; Li, J. D.; Fu, Y. D.; Li, S.; Sun, K.; et al. Potent Hydrazone Derivatives Targeting Esophageal Cancer Cells. *European Journal of Medicinal Chemistry* **2018**, *148*, 359–371.

(94) Neera Raghav, M. S. Acyl Hydrazides and Triazoles as Novel Inhibitors of Mammalian Cathepsin B and Cathepsin H. *European Journal of Medicinal Chemistry* **2014**, *77*, 231–242.

(95) Das Mukherjee, D.; Kumar, N. M.; Tantak, M. P.; Das, A.; Ganguli, A.; Datta, S.; Kumar, D.; Chakrabarti, G. Development of Novel Bis(Indolyl)-Hydrazide–Hydrazone Derivatives as Potent Microtubule-Targeting Cytotoxic Agents against A549 Lung Cancer Cells. *Biochemistry* **2016**, *55* (21), 3020–3035.

(96) Mousavi, E.; Tavakolfar, S.; Almasirad, A.; Kooshafar, Z.; Dehghani, S.; Afsharinasab, A.; Amanzadeh, A.; Shafiee, S.; Salimi, M. In Vitro and in Vivo Assessments of Two Novel Hydrazide Compounds against Breast Cancer as Well as Mammary Tumor Cells. *Cancer Chemotherapy and Pharmacology* **2017**, *79* (6), 1195–1203.

(97) Li, F.-Y.; Wang, X.; Duan, W.-G.; Lin, G.-S. Synthesis and In Vitro Anticancer Activity of Novel Dehydroabietic Acid-Based Acylhydrazones. *Molecules* **2017**, *22* (7), 1087.

(98) Küçükgüzel, Ş. G.; Koç, D.; Çıkla-Süzgün, P.; Özsavcı, D.; Bingöl-Özakpınar, Ö.; Mega-Tiber, P.; Orun, O.; Erzincan, P.; Sağ-Erdem, S.; Şahin, F. Synthesis of Tolmetin Hydrazide-Hydrazones and Discovery of a Potent Apoptosis Inducer in Colon Cancer Cells. *Archiv der Pharmazie* **2015**, *348* (10), 730–742.

(99) O. Ozdemir, U.; İlbiz, F.; Balaban Gunduzalp, A.; Ozbek, N.; Karagoz Genç, Z.; Hamurcu, F.; Tekin, S. Alkyl Sulfonic Acide Hydrazides: Synthesis, Characterization, Computational Studies and Anticancer, Antibacterial, Anticarbonic Anhydrase II (HCA II) Activities. *Journal of Molecular Structure* **2015**, *1100*, 464–474.

(100) De, P.; Baltas, M.; Lamoral-Theys, D.; Bruyère, C.; Kiss, R.; Bedos-Belval, F.; Saffon, N. Synthesis and Anticancer Activity Evaluation of 2(4-Alkoxyphenyl)Cyclopropyl Hydrazides and Triazolo Phthalazines. *Bioorganic and Medicinal Chemistry* **2010**, *18* (7), 2537–2548.

(101) Bingul, M.; Tan, O.; Gardner, C.; Sutton, S.; Arndt, G.; Marshall, G.; Cheung, B.; Kumar, N.; Black, D. Synthesis, Characterization and Anti-Cancer Activity of Hydrazide Derivatives Incorporating a Quinoline Moiety. *Molecules* **2016**, *21* (7), 916.

(102) Jones, D. P.; Lash, L. H. Introduction: Criteria for Assessing Normal and Abnormal Mitochondrial Function. In *Mitochondrial Dysfunction*; Elsevier, 1993; Vol. 2, pp 1–7.

(103) Helal, M. Investigation of Some Molecular Mechansims of Cytotoxic 1, 5-Diaryl-3-Oxo-1,4-Pentadienes, MSc. Thesis, University of Saskatchewan, 2012.

(104) Forrest, M. D. Why Cancer Cells Have a More Hyperpolarised Mitochondrial Membrane Potential and Emergent Prospects for Therapy. *bioRxiv* **2015**.

(105) Zorova, L. D.; Popkov, V. A.; Plotnikov, E. Y.; Silachev, D. N.; Pevzner, I. B.; Jankauskas, S. S.; Babenko, V. A.; Zorov, S. D.; Balakireva, A. V.; Juhaszova, M.; et al. Mitochondrial Membrane Potential. *Analytical Biochemistry* **2018**, *552*, 50–59.

(106) Vakifahmetoglu-Norberg, H.; Ouchida, A. T.; Norberg, E. The Role of Mitochondria in Metabolism and Cell Death. *Biochemical and Biophysical Research Communications* **2017**, *482* (3), 426–431.

(107) Helal, M.; Das, U.; Bandy, B.; Islam, A.; Nazarali, A. J.; Dimmock, J. R. Mitochondrial Dysfunction Contributes to the Cytotoxicity of Some 3,5-Bis(Benzylidene)-4-Piperidone Derivatives in Colon HCT-116 Cells. *Bioorganic and Medicinal Chemistry Letters* **2013**, *23* (4), 1075–1078.

(108) Addala, E.; Rafiei, H.; Das, S.; Bandy, B.; Das, U.; Karki, S. S.; Dimmock, J. R. 3,5-Bis(3-Dimethylaminomethyl-4-Hydroxybenzylidene)-4-Piperidone and Related Compounds Induce Glutathione Oxidation and Mitochondria-Mediated Cell Death in HCT-116 Colon Cancer Cells. *Bioorganic and Medicinal Chemistry Letters* **2017**, *27* (16), 3669–3673.

(109) Furniss, B. S.; Hannaford, A. J.; Smith, P. W.; Tatchell, A. R. Vogel's Textbook of Practical Organic Chemistry; Longman Scientific and Technical, Essex England, 1989; pp 1077–1078.

(110) Blickenstaff, R. T.; Hanson, W. R.; Reddy, S.; Witt, R. Potential Radioprotective Agents—VI. Chalcones, Benzophenones, Acid Hydrazides, Nitro Amines and Chloro Compounds. Radioprotection of Murine Intestinal Stem Cells. *Bioorganic and Medicinal Chemistry* **1995**, *3* (7), 917–922.

(111) Available at : https://www.chemicalbook.com/ProductChemicalPropertiescb3406135_EN.htm.

(112) Yale, H. L.; Losee, K.; Martins, J.; Holsing, M.; Perry, F. M.; Bernstein, J. Chemotherapy of Experimental Tuberculosis. VIII. The Synthesis of Acid Hydrazides, Their Derivatives and Related Compounds. *Journal of the American Chemical Society* **1953**, *75* (8), 1933–1942.

(113) Saha, A.; Kumar, R.; Kumar, R.; Devakumar, C. Development and Assessment of Green Synthesis of Hydrazides. *Indian Journal of Chemistry* **2010**, *49*B (4), 526–531.

(114) Kaushik, D.; Khan, S. A.; Chawla, G.; Kumar, S. N'-[(5-Chloro-3-Methyl-1-Phenyl-1H-Pyrazol-4-Yl)Methylene] 2/4-Substituted Hydrazides: Synthesis and Anticonvulsant Activity. *European Journal of Medicinal Chemistry* **2010**, *45* (9), 3943–3949.

(115) Gad, A. .; El-Dissouky, A.; Mansour, E. .; El-Maghraby, A. Thermal Stability of Poly Acryloyl Benzoic Hydrazide and Its Complexes with Some Transition Metals. *Polymer Degradation and Stability* **2000**, *68* (2), 153–158.

(116) Clemence, F; Joliveau-Maushart, C; Meier, J; Cerede, J; Delevallee, F; Benzoni, J; Deraedt, R. Synthesis and Analgesic Activity in the 1,2,4-Triazole Series. *European Journal of Medicinal Chemistry* **1985**, *20* (3), 257–266.

(117) Vichai, V.; Kirtikara, K. Sulforhodamine B Colorimetric Assay for Cytotoxicity Screening. *Nature Protocols* **2006**, *1* (3), 1112–1116.

(118) Motohashi, N.; Wakabayashi, H.; Kurihara, T.; Fukushima, H.; Yamada, T.; Kawase, M.; Sohara, Y.; Tani, S.; Shirataki, Y.; Sakagami, H.; et al. Biological Activity of Barbados Cherry (Acerola Fruits, Fruit of Malpighia Emarginata DC) Extracts and Fractions. *Phytotherapy Research* **2004**, *18* (3), 212–223.

(119) Elie, B. T.; Levine, C.; Ubarretxena-Belandia, I.; Varela-Ramírez, A.; Aguilera, R. J.; Ovalle, R.; Contel, M. Water-Soluble (Phosphane)Gold(I) Complexes - Applications as Recyclable Catalysts in a Three-Component Coupling Reaction and as Antimicrobial and Anticancer Agents. *European Journal of Inorganic Chemistry* **2009**, *23*, 3421–3430.

(120) Lema, C.; Varela-Ramirez, A.; Aguilera, R. J. Differential Nuclear Staining Assay for High-Throughput Screening to Identify Cytotoxic Compounds. *Current Cellular Biochemistry* **2011**, *1* (1), 1–14.

(121) Robles-Escajeda, E.; Das, U.; Ortega, N. M.; Parra, K.; Francia, G.; Dimmock, J. R.; Varela-Ramirez, A.; Aguilera, R. J. A Novel Curcumin-like Dienone Induces Apoptosis in Triple-Negative Breast Cancer Cells. *Cellular Oncology* **2016**, *39* (3), 265–277.

(122) Dimmock JR, Sidhu KK, Chen M, Reid RS, Allen TM, Kao GY, T. G. Evaluation of Some Mannich Bases of Cycloalkanones and Related Compounds. *European Journal of Medicinal Chemistry* **1993**, *28*, 313–322.

(123) Available at: https://dtp.cancer.gov/dtpstandard/dwindex/index.jsp.

(124) IBM SPSS Statistics for Windows, Version 24.0. Armonk, NY: IBM Corp., 2016, https://www.ibm.com/ca-en/marketplace/spss-statistics.

(125) Pandeya SN; Dimmock, J. R. Physicochemical Parameters in Drug Design. In *An Introduction to Drug Design*; New Age International (P) limited, 1997; pp 119–121.

(126) Newman, M. S. Steric Effects in Organic Chemistry; John Wiley and Sons, New York, 1956; p 591.

(127) Hansch C; Leo AJ. Substituted Constants for Correlation Analogs in Chemistry and Biology; John Wiley and Sons, New York, 1979; p 49.

(128) Available at: http://www.perkinelmer.com/category/chemdraw.

(129) Molinspiration web explorer, http://www.molinspiration.com/.

(130) Osiris Property Explorer tool, https://www.organic-chemistry.org/prog/peo/.

(131) Sakamuru, S.; Attene-Ramos, M. S.; Xia, M. Mitochondrial Membrane Potential Assay. *Methods in Molecular Biology (Clifton, N.J.)* **2016**, *1473*, 17–22.

(132) Perry, S. W.; Norman, J. P.; Barbieri, J.; Brown, E. B.; Gelbard, H. A. Mitochondrial Membrane Potential Probes and the Proton Gradient: A Practical Usage Guide. *BioTechniques* **2011**, *50* (2), 98–115.

(133) Ray, P. D.; Huang, B.-W.; Tsuji, Y. Reactive Oxygen Species (ROS) Homeostasis and Redox Regulation in Cellular Signaling. *Cellular Signalling* **2012**, *24* (5), 981–990.

(134) Moreira, P. I.; Zhu, X.; Wang, X.; Lee, H.; Nunomura, A.; Petersen, R. B.; Perry, G.; Smith, M. A. Mitochondria: A Therapeutic Target in Neurodegeneration. *Biochimica et Biophysica Acta (BBA) - Molecular Basis of Disease* **2010**, *1802* (1), 212–220.

(135) Schieber, M.; Chandel, N. S. ROS Function in Redox Signaling and Oxidative Stress. *Current Biology* **2014**, *24* (10), R453–R462.

(136) Akbar, M.; Essa, M. M.; Daradkeh, G.; Abdelmegeed, M. A.; Choi, Y.; Mahmood, L.; Song, B.-J. Mitochondrial Dysfunction and Cell Death in Neurodegenerative Diseases through Nitroxidative Stress. *Brain Research* **2016**, *1637*, 34–55.

(137) Bhat, A. H.; Dar, K. B.; Anees, S.; Zargar, M. A.; Masood, A.; Sofi, M. A.; Ganie, S. A. Oxidative Stress, Mitochondrial Dysfunction and Neurodegenerative Diseases; a Mechanistic Insight. *Biomedicine and Pharmacotherapy* **2015**, *74*, 101–110.

(138) Masgras, I.; Carrera, S.; de Verdier, P. J.; Brennan, P.; Majid, A.; Makhtar, W.; Tulchinsky, E.; Jones, G. D. D.; Roninson, I. B.; Macip, S. Reactive Oxygen Species and Mitochondrial Sensitivity to Oxidative Stress Determine Induction of Cancer Cell Death by P21. *Journal of Biological Chemistry* **2012**, *287* (13), 9845–9854.

(139) Available at: https://www.graphpad.com/scientific-software/prism/.